

Co-adsorption of phenol and calcium from an industrial wastewater stream

K. van der Merwe



orcid.org/0000-0002-1483-1580

Dissertation accepted in fulfilment of the requirements for the degree *Master of Engineering in Chemical Engineering* at the North-West University

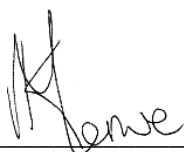
Supervisor: Prof S. Marx

Graduation: July 2020

Student number: 31551025

DECLARATION

I, **Karina van der Merwe**, hereby declare that the dissertation entitled: “Co-adsorption of phenol and calcium from an industrial wastewater stream” is my own work. This dissertation is being submitted for the degree in Masters of Engineering in Chemical Engineering to the North-West University, Potchefstroom.



K. VAN DER MERWE

2019/11/13

DATE

ABSTRACT

The pulp and paper industries are large producers of industrial wastewater that contain both organic and inorganic pollutants that influence water quality and availability. Conventional wastewater treatment methods such as chemical precipitation and membrane filtration are not economical and environmentally friendly. In comparison, adsorption is more cost-effective and easier to implement on an industrial scale. The use of activated carbon as adsorbent of choice is no longer viable due to the high manufacturing costs compared to the low levels of contaminants that need to be removed. Biochar adsorbents produced by hydrothermal liquefaction (HTL) from biomass waste such as paper sludge is a less expensive alternative to activated carbon. The utilisation of paper sludge, destined for landfilling, as feedstock for adsorbent production offers cost-effective waste management solutions that also contribute to the preservation of the environment. However, limited information is available on the application and success of HTL produced paper sludge-based biochar adsorbents for the removal of problematic pollutants such as phenol and calcium, especially with regards to industrial wastewater streams.

The aim of this study was to determine the effectiveness of paper sludge-based biochar as adsorbent for the co-removal of phenol and calcium from the wastewater stream of an industrial paper mill. The objectives of this study were to understand the behaviour of the paper sludge-based biochar when subjected to synthetic phenol and calcium environments, to understand how and why the affinity of the paper sludge-based biochar towards phenol changes in the presence of calcium and lastly, to understand the performance of paper sludge-based biochar in a real industrial wastewater stream, compared to that of commercial activated carbon.

The paper sludge-based biochar was produced through batch hydrothermal liquefaction at a temperature of 300°C by using paper sludge collected from a local paper mill as feedstock. The produced biochar was characterised and subjected to various adsorption scenarios. The performance of the characterised paper sludge-based biochar was firstly evaluated in synthetic single phenol (10 ppm – 150 ppm) and calcium (600 ppm – 1000 ppm) environments whereas the adsorbent dosage (2 g.L^{-1} – 12 g.L^{-1}) and the initial concentration of each adsorbate was varied. The performance of the biochar was then tested in a synthetic binary environment with both phenol (10 ppm) and calcium (600 ppm), containing concentrations similar to that found in the collected industrial wastewater. Lastly, the performance of the paper sludge-based biochar was tested in the collected industrial wastewater and compared to the performance of commercial activated carbon. The adsorption experiments were performed at a temperature of $25^\circ\text{C} \pm 2^\circ\text{C}$, rotary speed of 150 rpm and solution pH of 8. The phenol concentration was determined by high-performance liquid chromatography (HPLC) analysis, where inductively coupled plasma optical emission spectrometry (ICP-OES) analysis was used to determine the calcium concentration.

The chemical and structural characteristics of the biochar had a large influence on its adsorptive capabilities towards both phenol and calcium. Low phenol removal efficiencies of $12.30\% \pm 0.83\%$ were obtained with a maximum adsorbent dosage of 12 g.L^{-1} as only a limited number of active sites were available on the surface of the biochar due to the low surface area of the produced biochar. The low surface area was attributed to the blockage of pores by mineral-based species such as calcite which was majorly present in the produced biochar. The mineral-rich nature of the biochar also resulted in the biochar not being an appropriate adsorbent for the removal of calcium from both synthetic and real wastewater streams. This can be attributed to the biochar not consisting of exchangeable sites that can accommodate ion exchange mechanisms for calcium adsorption. Also, it was found that the calcium, in co-operation with the hydroxyl ions in the solution, rather attacked some of the surface functional groups present on the surface of the biochar, than adsorbing itself.

In the binary adsorption experiments, the addition of calcium had a negative effect on the adsorption of phenol. The phenol removal efficiency decreased with $15.76\% \pm 1.06\%$ when calcium was added to the adsorption medium. This can be attributed to the mass transfer limitations experienced in the medium due to the low concentration of phenol molecules that had to compete with the high concentration of calcium hydroxide molecules also diffusing to the surface of the biochar.

The produced biochar performed better in the collected industrial wastewater than the synthetic solutions, due to the presence of other less-soluble phenolics other than phenol. The biochar achieved a COD removal efficiency of $77.83\% \pm 5.22\%$, close to the COD removal efficiency of $92.72\% \pm 6.22\%$ obtained by commercial activated carbon. Therefore, biochar derived from paper sludge, a waste product produced by the pulp and paper industry, has the potential to replace expensive adsorbents such as activated carbon for the treatment of contaminated industrial wastewater streams.

The impact of the pulp and paper industry will also be reduced by the usage of paper sludge for adsorbent production and applications. Firstly, the direct processing of wet biomass such as paper sludge in HTL offers cost-effective waste management solutions that can be used as an alternative to the current disposal methods employed. And secondly, pulp and paper mills can now effectively utilise their own waste products such as paper sludge to clean the wastewater produced during the paper manufacturing activities. This will then result in the production of cleaner water, with a lower COD concentration, that can be re-circulated back into the system without adversely affecting the properties of the paper products produced in the process. Also, by re-circulating the water, the demand for freshwater resources by the pulp and paper industry can be reduced.

Since the characterisation results showed that the chemical and structural characteristics of the biochar had a large influence on the adsorption of phenol, it is recommended that most of the ash compounds are removed from the paper sludge before the biochar is produced. The removal of the ash compounds from the paper sludge beforehand will ensure that pore development is not limited during the HTL process, and therefore biochar can be produced with more attractive chemical and structural characteristics for adsorption applications.

Keywords: adsorption, biochar, calcium, hydrothermal liquefaction, paper sludge, phenol, wastewater

ACKNOWLEDGEMENTS

“For I know the plans I have for you,” declares the LORD, “plans to prosper you and not to harm you, plans to give you hope and a future” – Jeremiah 29:11

I would like to thank the following people/organisations for their contributions to the project:

- My Heavenly Father, who has blessed me with abilities beyond what I ever could have imagined and for reminding me each time of his amazing plan for me.
- My supervisor, Professor Sanette Marx for her advice, patience, and especially her help with the interpretation of the results.
- Dr Roelf Venter, Dr Frikkie Conradie and Prof Elvis Fosso-Kankeu for their advice and help when needed.
- The Biofuels lab manager, René, for creating a lab environment any student would want to be part of and for all her advice and assistance in the lab when needed.
- My dearest friend, Maans Marais for his constant advice, support, motivation and help throughout the project. Also for listening to my unique ideas and guiding me to the right path. I will try to remember not to re-invent the wheel each time!
- PAMSA and especially Mpact for their financial assistance.
- Antonie Brink, for answering all my mill-related questions and helping me understand the concepts behind them. Sonja Boshoff, for only being an email away and offering advice and motivation when needed. Lastly, Dr Valeska Cloete for granting me the opportunity to complete a master's degree, I will be forever grateful!
- My friends, Nya, Faan, TC and Christine for their constant motivation and support. Christine, thank you for helping me see the problem when I was not able to do so myself.
- Elsa and Willie, for everything they have done for me these past few years. I will be ever grateful for all the lessons I have learned!
- My mother, Karen, for teaching me from a young age what hard work and determination was about. Thank you for always listening and giving advice when needed. Lastly, thank you for seeing the potential in me even when others failed to do so.
- My best friend and loving husband, Frik, for always believing in me and being my rock, biggest fan and biggest supporter. Thank you for motivating and supporting me in all my endeavours and thank you for helping me realise that reaching beyond the stars is not impossible. Lastly, thank you for allowing me the opportunity to do my masters. I will forever be grateful for all the sacrifices you made for me!

TABLE OF CONTENTS

DECLARATION	III
ABSTRACT	IV
ACKNOWLEDGEMENTS	VII
CHAPTER 1 – INTRODUCTION	1
1.1 Background and motivation	1
1.2 Problem statement	4
1.3 Aim and objectives	4
1.4 Project scope	5
REFERENCES.....	7
CHAPTER 2 – LITERATURE REVIEW.....	10
2.1 Water usage in the pulp and paper industry.....	10
2.2 Characteristics of pulp and paper wastewater	11
2.3 Composition of pulp and paper wastewater	12
2.3.1 Organic pollutants.....	12
2.3.2 Inorganic pollutants	12
2.4 Impact of the pulp and paper industry	13
2.5 Conventional treatment methods	13
2.6 Post-treatment methods.....	14
2.6.1 Chemical precipitation	14
2.6.2 Membrane filtration	14
2.6.3 Chemical oxidation processes	15
2.6.4 Ion exchange	15

2.7	Adsorption	16
2.7.1	Adsorption capacity	16
2.7.2	Removal efficiency	17
2.8	Activated carbon	17
2.8.1	Physical activation	18
2.8.2	Chemical activation	18
2.9	Low-cost activated carbon.....	19
2.10	Paper sludge as feedstock.....	21
2.10.1	Conventional disposal methods	22
2.10.2	Alternative disposal methods	23
2.11	Biochar production from paper sludge.....	23
2.11.1	Pyrolysis	24
2.11.2	Hydrothermal liquefaction (HTL)	24
2.12	Paper sludge-based biochar	25
2.13	HTL produced biochar	27
2.14	Adsorption processing conditions.....	28
2.14.1	Solution pH.....	28
2.14.1.1	Point of zero charge of adsorbent.....	29
2.14.1.2	pKa value of adsorbate	29
2.14.2	Adsorbent dosage	30
2.14.3	Initial adsorbate concentration	30
2.15	Operating conditions: single-component systems	31
2.16	Adsorption isotherms	34

2.16.1	Langmuir isotherm	34
2.16.2	Freundlich isotherm	35
2.16.3	Henry's law	36
2.17	Adsorption mechanisms	37
2.17.1	Organic adsorption mechanisms.....	37
2.17.1.1	Electrostatic forces	37
2.17.1.2	Hydrogen bonding	38
2.17.1.3	π - π interaction.....	38
2.17.1.4	Hydrophobic interactions	38
2.17.1.5	Pore-filling	39
2.17.2	Inorganic adsorption mechanisms	39
2.17.2.1	Ion exchange.....	39
2.17.2.2	Surface complexation and precipitation	39
2.18	Adsorption kinetics	40
2.18.1	Pseudo-first-order model	40
2.18.2	Pseudo-second-order model.....	41
2.18.3	Intra-particle diffusion	41
2.18.4	Overall diffusion coefficient.....	43
2.19	Binary adsorption systems.....	44
2.20	Concluding remarks	46
REFERENCES.....		47
CHAPTER 3 – RESEARCH METHODOLOGY		61
3.1	Materials.....	61

3.1.1	Paper mill materials	61
3.1.2	Chemicals.....	62
3.2	Biochar preparation from paper sludge.....	62
3.2.1	Experimental setup.....	63
3.2.2	Experimental procedure.....	63
3.2.2.1	Autoclave start-up.....	63
3.2.2.2	Autoclave operation.....	65
3.2.2.3	Autoclave shutdown.....	65
3.2.2.4	Bio-oil and aqueous phase removal.....	66
3.2.2.5	Biochar drying.....	67
3.2.3	Washing of the biochar	67
3.2.4	Homogeneous sample preparation	67
3.3	Physicochemical characterisation of paper sludge, paper sludge-based biochar and activated carbon	68
3.3.1	Elemental analysis.....	69
3.3.2	Proximate analysis	69
3.3.3	Brunauer-Emmett-Teller (BET) analysis	69
3.3.4	Fibre analysis	69
3.3.5	Scanning electron microscope (SEM) analysis	69
3.3.6	X-ray powder diffraction (XRD)	70
3.3.7	X-ray fluorescence (XRF)	70
3.3.8	Fourier-transform infrared spectroscopy (FTIR)	70
3.3.9	Point of zero charge.....	70
3.3.10	Particle size diameter	70

3.4	Wastewater characterisation	71
3.5	Adsorption experiments.....	71
3.5.1	Experimental setup.....	71
3.5.2	Experimental planning	72
3.5.3	Experimental procedure.....	73
3.5.3.1	Preparation of glassware	73
3.5.3.2	Preparation of adsorption medium	73
3.5.3.3	Weighing of the adsorbent.....	74
3.5.3.4	Preparation of the adsorbate solution	74
3.5.3.5	The adsorption process	74
3.5.3.6	Sampling	74
3.6	Data analysis.....	75
3.7	Analytical methods: adsorption	75
3.7.1	Inductively coupled plasma optical emission spectrometry (ICP-OES).....	75
3.7.2	High-performance liquid chromatography (HPLC)	76
	REFERENCES.....	78
	CHAPTER 4 – RESULTS AND DISCUSSION	79
4.1	Yield of paper sludge-based biochar	79
4.2	Characterisation of paper sludge, biochar and activated carbon	79
4.2.1	Proximate and elemental analysis	79
4.2.2	Surface area and porosity.....	81
4.2.3	Organic composition of the paper sludge.....	82
4.2.4	Surface morphology.....	83

4.2.5	Crystalline constituents and major mineral composition of biochar	85
4.2.6	Functional group analysis	87
4.2.7	Point of zero charge.....	89
4.3	Phenol adsorption	90
4.3.1	Effect of biochar dosage	90
4.3.2	Effect of initial phenol concentration	91
4.4	Adsorption isotherms	93
4.4.1	Equilibrium isotherm	93
4.4.2	Adsorption isotherm models	94
4.4.3	Active sites responsible for phenol adsorption	98
4.5	Adsorption kinetics	99
4.5.1	Pseudo-second-order model.....	101
4.5.2	Intra-particle diffusion model.....	104
4.5.3	Rate-limiting mass transfer mechanism	107
4.6	Calcium adsorption	109
4.7	Binary adsorption studies.....	111
4.8	Wastewater adsorption studies	113
4.8.1	Characterisation of wastewater	114
4.8.2	COD removal results	115
4.8.3	Total phenolic adsorptive performance	116
4.9	Concluding remarks	118
REFERENCES.....		119
CHAPTER 5 – CONCLUSIONS AND RECOMMENDATIONS		128

5.1	Conclusions.....	128
5.2	Recommendations.....	129
APPENDIX A		130
A.1	Batch hydrothermal liquefaction: standard operating procedure	130
A.2	Phenol calibration curve	131
APPENDIX B		132
B.1	Preliminary adsorption experiments	132
B.2	Raw adsorption data.....	132
B.3	Experimental error calculations.....	136

LIST OF TABLES

Table 2-1:	Commercial activated carbon characteristics	18
Table 2-2:	Biomass generations.....	20
Table 2-3:	Low-cost activated carbon adsorbents	20
Table 2-4:	Paper sludge-based biochar adsorbents' characteristics and performance.....	26
Table 2-5:	Adsorption parameter ranges for the batch adsorption of organic and inorganic pollutants	33
Table 2-6:	Binary batch adsorption studies performed in literature.....	45
Table 3-1:	Chemicals required for biochar production and adsorption experiments.....	62
Table 3-2:	Reasoning behind manipulated variables.....	73
Table 4-1:	Proximate and elemental analysis of paper sludge, biochar and activated carbon (g.g ⁻¹ , dry basis)	80
Table 4-2:	Surface area and porosity of the biochar and activated carbon	81
Table 4-3:	Composition of the paper sludge (dry basis)	82
Table 4-4:	XRF analysis of the biochar produced.....	86
Table 4-5:	FTIR classification of bond vibrations in compounds	87
Table 4-6:	Isothermal parameters for phenol adsorption onto biochar at 25°C ± 2°C	97
Table 4-7:	Pseudo-second-order parameters for phenol adsorption onto biochar at 25°C ± 2°C.....	103
Table 4-8:	Intra-particle diffusion parameters for phenol adsorption onto biochar at 252°C ± 2°C.....	106
Table 4-9:	Film and intra-particle diffusion coefficients calculated at a temperature of 25°C ± 2°C.....	107
Table 4-10:	Overall diffusion coefficients for different initial phenol concentrations at 25°C ± 2°C.....	108

Table 4-11:	Characteristic properties of collected industrial wastewater.....	114
Table 4-12:	Total phenolic concentration comparison	116

LIST OF FIGURES

Figure 2-1:	Paper sludge production process (adapted from Likon and Trebše, 2012).....	21
Figure 3-1:	The paper sludge as collected on-site	61
Figure 3-2:	Schematic representation of the batch HTL reactor experimental setup	63
Figure 3-3:	Paper sludge loaded into the autoclave.....	64
Figure 3-4:	Reactor product mixture after cool down	66
Figure 3-5:	Reactor product mixture before filtration.....	66
Figure 3-6:	Biochar after drying	67
Figure 3-7:	Sample splitter	68
Figure 3-8:	Actual batch adsorption experimental setup	72
Figure 3-9:	ICP-OES	76
Figure 3-10:	Phenolic HPLC.....	77
Figure 4-1:	SEM micrograph of the dried paper sludge	83
Figure 4-2:	SEM micrographs of the produced biochar, showing the presence of irregularly sized pores (a) and volatiles (b) on the surface of the biochar	84
Figure 4-3:	SEM micrographs of the commercial activated carbon, showing its external (a) and internal (b) surfaces.....	85
Figure 4-4:	XRD spectra of the biochar produced.....	86
Figure 4-5:	FTIR spectra of paper sludge (-), biochar (-) and activated carbon (-)	88
Figure 4-6:	Determination of point of zero charge for the biochar (●) and activated carbon (■) samples	89
Figure 4-7:	Effect of the biochar dosage on phenol removal efficiency (■) and adsorption capacity (●) ($C_i = 150$ ppm, pH 8, contact time = 1440 min, $T = 25^\circ\text{C} \pm 2^\circ\text{C}$)	90

Figure 4-8:	Effect of initial concentration on phenol removal (dosage = 12 g.L ⁻¹ , pH 8, contact time = 1440 min, T= 25°C ± 2°C)	92
Figure 4-9:	Adsorption isotherm of phenol onto biochar (dosage = 12 g.L ⁻¹ , pH 8, T= 25°C ± 2°C).....	94
Figure 4-10:	Langmuir plot for phenol adsorption onto biochar (dosage = 12 g.L ⁻¹ , pH 8, T= 25°C ± 2°C).....	95
Figure 4-11:	Freundlich plot for phenol adsorption onto biochar (dosage = 12 g.L ⁻¹ , pH 8, T= 25°C ± 2°C)	95
Figure 4-12:	Henry's law plot for phenol adsorption onto biochar (dosage = 12 g.L ⁻¹ , pH 8, T= 25°C ± 2°C)	96
Figure 4-13:	FTIR spectra produced for unused biochar (-), biochar after 10 ppm phenol adsorption (-) and biochar after 150 ppm phenol adsorption (-).....	98
Figure 4-14:	Kinetics of phenol adsorption (dosage = 12 g.L ⁻¹ , pH 8, contact time = 1440 min, T= 25°C ± 2°C) (Phenol concentration: ■, 10 ppm; ✖, 30 ppm; ▲, 60 ppm; ◆, 90 ppm; ✕, 120 ppm; ●, 150 ppm).....	100
Figure 4-15:	t/q _t versus contact time fit for the pseudo second-order rate expression (dosage = 12 g.L ⁻¹ , pH 8, T= 25°C ± 2°C) (Phenol concentration: ■, 10 ppm; ✖, 30 ppm; ▲, 60 ppm; ◆, 90 ppm; ✕, 120 ppm; ●, 150 ppm) ...	102
Figure 4-16:	Effect of contact time on the intra-particle diffusion of phenol onto PSBC (dosage = 12 g.L ⁻¹ , pH 8, T= 25°C ± 2°C) (Phenol concentration: ■, 10 ppm; ✖, 30 ppm; ▲, 60 ppm; ◆, 90 ppm; ✕, 120 ppm; ●, 150 ppm) ...	105
Figure 4-17:	FTIR spectra produced for unused biochar (-) and biochar after being exposed to 600 ppm calcium (-)	110
Figure 4-18:	Phenol removal efficiency with (▲) and without (■) the presence of 600 ppm calcium (dosage = 12 g.L ⁻¹ , pH 8, contact time = 1440 min, T= 25°C ± 2°C).....	112
Figure 4-19:	FTIR spectra of biochar after 10 ppm phenol adsorption (-) and after binary adsorption with 10 ppm phenol and 600 ppm calcium (-)	113
Figure 4-20:	COD removal efficiency of biochar (●) compared with activated carbon (■) (dosage = 12 g.L ⁻¹ , pH 8, contact time = 1440 min, T= 25°C ± 2°C).....	115

CHAPTER 1 – INTRODUCTION

In this chapter, the motivation behind the project is discussed. Section 1.1 gives a brief discussion on the importance of water, conventional wastewater treatment methods and further insight into alternative methods for adsorbent production and application. Section 1.2 and Section 1.3 give the problem statement, aim and objectives of the study. The chapter concludes with a brief overview and scope of the project given in Section 1.4.

1.1 Background and motivation

Water is an important natural resource required, not only to sustain all life on earth but also to ensure the effective operation of various industrial processes. Therefore, the 0.6% of usable freshwater resources still available on earth are under constant pressure to cater to the world's growing freshwater requirements (Vikrant *et al.*, 2018). According to Mubarik *et al.* (2012), studies indicate that the demand for freshwater will increase with 55% within the next 30 years, whereas approximately 40% of the population will be living in water-scarce areas like South Africa. Thus, countries like South Africa cannot afford further water limitations due to the pollution of natural water resources by anthropogenic activities. One of the main anthropogenic activities that have led to the contaminant of freshwater resources is the discharge of industrial effluents, containing problematic organic and inorganic pollutants, into nearby rivers and lakes (Al-Malack & Dauda, 2017). According to a recent study by Wong *et al.* (2018), 70% of developing countries discard their industrial wastewater into nearby water sources without further treatment, whereas approximately 90% of the wastewater produced then enters the water cycle by flowing into adjacent rivers, lakes and oceans.

The pulp and paper industries are one of the largest producers of industrial wastewater worldwide. According to Rahman and Kabir (2010), the pulp and paper industry produces approximately 137 500 000 m³ of wastewater per year. The wastewater produced by the pulp and paper industry has been found to consist mainly of organic pollutants such as phenol and phenol derivatives, as well as various organic acids, depending on the manufacturing processes employed (Amat *et al.*, 2005).

Phenol and phenol derivatives are well-known for their toxicity to all forms of life. Characteristics of phenol derivatives include being non-biodegradable and bio-accumulative, especially in living organisms, when the adsorption rate of the specific pollutant exceeds the metabolic and excretion rate of the organism (Wong *et al.*, 2018; Zhou *et al.*, 2017). Bio-accumulation of phenolic compounds further result in biomagnification as species higher up in the ecological food chain then consume contaminated organisms, which magnifies the effect and concentration of the pollutant all the way up to the end consumer (Wong *et al.*, 2018). The presence of phenolic

compounds have also been found to result in undesirable tastes and odours in industrial effluents (Gholizadeh *et al.*, 2013). Therefore, the maximum allowable phenolic concentration has been fixed at 1 ppb in potable water sources and less than 1 ppm in industrial effluents (Tabassi *et al.*, 2017).

The wastewater produced by the pulp and paper industry has also been found to contain high concentrations of inorganic pollutants such as calcium, due to the chemicals used in the paper manufacturing process. Calcium is a mineral-based specie that is directly related to the hardness of water. According to Aragaw and Ayalew (2019), a considerable amount of capital is spent annually on the softening of hard water to avoid the negative impact it has on the efficiency of industrial processes and the well-being of various ecosystems which rely on a constant supply of calcium carbonate. Therefore, wastewater produced by the pulp and paper industry must be treated properly before discharged into nearby water resources.

Various methods have been developed to treat industrial wastewater. The most common methods used include adsorption, chemical precipitation, membrane filtration, solvent extraction, ion exchange, flotation and electrocoagulation (Ariffin *et al.*, 2017; Aziz *et al.*, 2008). Although methods such as chemical precipitation, membrane filtration and ion exchange have been proven to be efficient in removing both organic and inorganic pollutants, the disadvantages associated with these methods outweigh their operational feasibility. Disadvantages include high operational costs, high maintenance costs, toxic sludge generation and low efficiency when low contaminant concentrations are present (Aziz *et al.*, 2008; Barakat, 2011).

Adsorption, on the other hand, has been widely used as a wastewater treatment alternative to most conventional methods. Adsorption is an effective, low-cost, simple and adaptable process that requires a low initial capital investment for the establishment of process units (Burakov *et al.*, 2018; Saleh *et al.*, 2016). The adsorbents used for the treatment of industrial wastewater are usually carbonaceous based materials such as activated carbon. Activated carbon has been the preferred adsorbent due to its high efficiency and versatile properties when used for industrial wastewater treatment applications (De Gisi *et al.*, 2016).

Activated carbon is a carbon-rich adsorbent with a highly porous structure and large effective surface area that promotes adsorption activities (Kong *et al.*, 2018). However, high production costs have limited the large-scale application of activated carbon for the removal of low concentrations of contaminants. Activated carbon is usually produced at high temperatures with expensive feedstock, such as coal and wood, and additional activation steps are required to activate the carbon once produced (Burakov *et al.*, 2018; Gratiuto *et al.*, 2008; Tan *et al.*, 2015). Therefore, to leverage the advantages of carbon-based adsorbents, alternative sources and

methods of production need to be found. One such method that has been focussed on in recent literature is the production of biochar for adsorbent applications (Tan *et al.*, 2015).

Biochar is a solid coal-like product, rich in carbon, that is produced from the thermal decomposition of biomass waste by employing either pyrolysis or hydrothermal liquefaction technologies (Gollakota *et al.*, 2018; Sohi, 2012). Pyrolysis and hydrothermal liquefaction are the two main thermochemical conversion processes commonly employed for the production of biochar, whereas hydrothermal liquefaction has become the preferred route amongst the two (Gollakota *et al.*, 2018).

Hydrothermal liquefaction (HTL) is a low-cost alternative to pyrolysis as the process requires low temperatures, low heating rates and no initial pre-treatment steps of the feedstock (Gollakota *et al.*, 2018; Liu *et al.*, 2013). Various studies have been performed to produce biochar from a variety of different waste materials such as pine waste, banana peels, sugarcane bagasse and papaya peels, and evaluated the adsorptive performance of the produced biochar in the presence of various pollutants (Abbaszadeh *et al.*, 2016; Amerkhanova *et al.*, 2017; Wong *et al.*, 2018; Zhou *et al.*, 2017). In most studies, the resulting bio-adsorbents performed better than commercial activated carbon (Tan *et al.*, 2015). This can be attributed to the favourable chemical nature of biochar that is rich in both oxygenated functional groups and mineral compounds that promote adsorption activities (Saleh *et al.*, 2016). However, limited literature is available on the usage of industrial waste products such as paper sludge as feedstock for the production of HTL biochar adsorbents for the removal of organic and inorganic pollutants such as phenol and calcium from an industrial wastewater stream.

Paper sludge is a waste product produced at a rate of between 300 and 350 million tons per year by the pulp and paper manufacturing industry on a global scale (Ioelovich, 2014). China, the United States, Western Europe and Japan have been found to produce approximately 12 million tons, eight million tons, six million tons and three million tons of paper sludge per year respectively, whereas South Africa produces roughly 0.50 million tons of paper sludge per year (Boshoff *et al.*, 2016; He *et al.*, 2009). Since large quantities of paper sludge are produced annually, the disposal thereof is a growing concern for paper mills all over the world.

Paper sludge is mainly landfilled at high disposal and land costs (Hojamberdiev *et al.*, 2008). According to Gurram *et al.* (2015), approximately 50% of the paper sludge currently produced is landfilled at significant disposal costs that are comparable with roughly 60% of the total operating costs required to operate the wastewater treatment plants of paper mills. This does not only result in economic changes but also environmental changes, as the leaching of groundwater resources are inevitable. Therefore, paper sludge should rather be used for bio-processes such as the

production of bio-adsorbents, as it will reduce the environmental impact of the pulp and paper industry and also prevent further contamination of groundwater resources.

Various studies have been performed in order to test the adsorptive performance of paper sludge-based biochar produced by pyrolysis for the removal of various organic and inorganic pollutants. Jaria *et al.* (2019) produced paper sludge-based biochar by pyrolysis and tested its adsorptive performance in the removal of various pharmaceuticals from both synthetic and real wastewater solutions. Hojamberdiev *et al.* (2008) also produced paper sludge-based biochar by pyrolysis but tested its adsorptive performance in the removal of phosphate and methylene blue from synthetic solutions. Méndez *et al.* (2009), on the other hand, tested the performance of paper sludge-based biochar in the removal of a common heavy metal such as copper from synthetic solutions.

To date, most of the studies that produced paper sludge-based biochar employed pyrolysis rather than hydrothermal liquefaction technologies. Also, the adsorptive performance of paper sludge-based biochar has not yet been tested for the removal of phenol and calcium from synthetic (single and binary) solutions, as well as in real industrial wastewater mediums. Therefore, in this study, the effectiveness of biochar, produced from paper sludge by hydrothermal liquefaction, was tested for the removal of phenol and calcium from both synthetic (single and binary) and real industrial wastewater environments.

1.2 Problem statement

South Africa is a water scarce country. The demand for freshwater grows on a continuous basis, putting a lot of pressure on existing freshwater resources. The discharge of contaminated industrial wastewater into nearby water resources further adds to the water scarcity already experienced in the country. The adsorbents currently used in industry, such as activated carbon, to treat contaminated industrial wastewater are expensive and require many expensive pre and post-treatment steps. Biochar as adsorbent is a low-cost alternative, but the performance of biochar produced from paper sludge by hydrothermal liquefaction for the removal of phenol and calcium has not yet been investigated.

1.3 Aim and objectives

The purpose of the study is to determine the effectiveness of paper sludge-based biochar as an adsorbent for the co-removal of phenol and calcium from an industrial paper mill's wastewater stream.

The main objectives of this study are:

- To understand the behaviour of the paper sludge-based biochar when subjected to synthetic phenol and calcium environments

- To understand how and why the affinity of the paper sludge-based biochar towards phenol changes in the presence of calcium
- To understand the performance of paper sludge-based biochar in a real industrial wastewater stream, compared to that of commercial activated carbon

1.4 Project scope

Paper sludge-based biochar will be produced at a temperature of 300°C through batch hydrothermal liquefaction of paper sludge collected from a local paper mill. The resulting biochar will be used as an adsorbent in different adsorption scenarios. The adsorption experiments will be performed at a constant temperature of $25^{\circ}\text{C} \pm 2^{\circ}\text{C}$, rotary speed of 150 rpm and solution pH of 8. The paper sludge-based biochar will be tested in single-component adsorption experiments with phenol (10 ppm - 150 ppm) and calcium (600 ppm - 1000 ppm), binary adsorption experiments with both phenol (10 ppm) and calcium (600 ppm), and lastly in the industrial wastewater collected from a local paper mill. The adsorbent dosage ($2 \text{ g.L}^{-1} - 12 \text{ g.L}^{-1}$) and the initial adsorbate concentration will be varied for both adsorbates. The experimental data will be analysed by isotherm and kinetic analysis. Activated carbon will be purchased and used for comparison purposes in the wastewater adsorption experiments.

In order to satisfy the aim and objectives of this project as stipulated in Section 1.3, this dissertation was divided into five chapters as follows:

- **Chapter 2 – Literature review:** discusses the impact and characteristics of the wastewater produced by the pulp and paper industry in detail. Conventional wastewater treatment methods are then briefly examined where focus is given to adsorption. The production of conventional activated carbon as adsorbent is explored where the attention is shifted to the production of activated carbon by low-cost materials. Thereafter, the potential of paper sludge as precursor for adsorbent production is reviewed followed by a brief discussion based on pyrolysis and hydrothermal liquefaction (HTL) where preference is given to HTL. The limitations of HTL produced paper sludge-based biochar are then considered, followed by a full theoretical review required for adsorption studies. Lastly, the chapter is ended with the concluding remarks.
- **Chapter 3 – Experimental design:** describes the materials and chemicals used for the biochar production and adsorption experiments. The biochar production method as well as the adsorption methodology followed is discussed in detail in this chapter. The characterisation methods used to characterise the paper sludge, biochar, activated carbon as well as the collected wastewater are also given. Lastly, the analytical methods used to quantify the phenol and calcium concentrations during the adsorption experiments are reported.

- **Chapter 4 – Results and discussion:** discusses the main results. Firstly, the biochar yield obtained by subjecting paper sludge to HTL conditions is given and briefly reviewed. Secondly, the characterisation results obtained for the paper sludge, paper sludge-based biochar and activated carbon are given and examined in detail. Thirdly, the results obtained by performing a complete adsorption study, including isotherm and kinetic analysis on the adsorption of phenol onto the produced biochar is given. Thereafter, the difficulties and possible explanations for the adsorption of calcium onto the produced biochar are discussed and evaluated. Lastly, the results of the binary adsorption studies for both the synthetic and real wastewater mediums are given. The performance of the biochar and the activated carbon are considered and compared to one another.
- **Chapter 5 – Conclusions and recommendations:** summarises the main conclusions for the project and makes recommendations for future investigations.

REFERENCES

- Abbaszadeh, S., Alwi, S.R.W., Webb, C., Ghasemi, N. & Muhamad, I.I. 2016. Treatment of lead-contaminated water using activated carbon adsorbent from locally available papaya peel biowaste. *Journal of Cleaner Production*, 118:210-222.
- Al-Malack, M.H. & Dauda, M. 2017. Competitive adsorption of cadmium and phenol on activated carbon produced from municipal sludge. *Journal of Environmental Chemical Engineering*, 5:2718-2729.
- Amat, A.M., Arques, A., Miranda, M.A. & López, F. 2005. Use of ozone and/or UV in the treatment of effluents from board paper industry. *Chemosphere*, 60:1111-1117.
- Amerkhanova, S., Shlyapov, R. & Uali, A. 2017. The active carbons modified by industrial wastes in process of sorption concentration of toxic organic compounds and heavy metals ions. *Colloids and Surfaces A*, 532:36-40.
- Aragaw, T.A. & Ayalew, A.A. 2019. Removal of water hardness using zeolite synthesized from ethiopian kaolin by hydrothermal method. *Water Practice and Technology*, 14(1):145-159.
- Ariffin, N., Abdullah, M.M.A.B., Mohd Arif Zainol, M.R.R., Murshed, M.F., Hariz-Zain, Faris, M.A. & Bayuaji, R. 2017. Review on adsorption of heavy metal in wastewater by using geopolymer. *MATEC Web of Conferences*, 97:1-8.
- Aziz, H.A., Adlan, M.N. & Ariffin, K.S. 2008. Heavy metals (Cd, Pb, Zn, Ni, Cu and Cr(III)) removal from water in Malaysia: Post treatment by high quality limestone. *Bioresource Technology*, 99:1578-1583.
- Barakat, M.A. 2011. New trends in removing heavy metals from industrial wastewater. *Arabian Journal of Chemistry*, 4:361-377.
- Boshoff, S., Gottumukkala, L.D., van Rensburg, E. & Görgens, J. 2016. Paper sludge (PS) to bioethanol: Evaluation of virgin and recycle mill sludge for low enzyme, high-solids fermentation. *Bioresource Technology*, 203:103-111.
- Burakov, A.E., Galunin, E. V., Burakova, I. V., Kucheroval, A.E., Agarwal, S., Tkachev, A.G. & Gupta, V.K. 2018. Adsorption of heavy metals on conventional and nanostructured materials for wastewater treatment purposes: A review. *Ecotoxicology and Environmental Safety*, 148:702-712.
- De Gisi, S., Lofrano, G., Grassi, M. & Notarnicola, M. 2016. Characteristics and adsorption

capacities of low-cost sorbents for wastewater treatment: A review. *Sustainable Materials and Technologies*, 9:10-40.

Gholizadeh, A., Kermani, M., Gholami, M. & Farzadkia, M. 2013. Kinetic and isotherm studies of adsorption and biosorption processes in the removal of phenolic compounds from aqueous solutions: Comparative study. *Journal of Environmental Health Science and Engineering*, 11(29):1-10.

Gollakota, A.R.K., Kishore, N. & Gu, S. 2018. A review on hydrothermal liquefaction of biomass. *Renewable and Sustainable Energy Reviews*, 81:1378-1392.

Gratuito, M.K.B., Panyathanmaporn, T., Chumnanklang, R.A., Sirinuntawittaya, N. & Dutta, A. 2008. Production of activated carbon from coconut shell: optimization using response surface methodology. *Bioresource Technology*, 99:4887-4895.

Gurram, R.N., Al-Shannag, M., Lecher, N.J., Duncan, S.M., Singasaas, E.L. & Alkasrawi, M. 2015. Bioconversion of paper mill sludge to bioethanol in the presence of accelerants or hydrogen peroxide pretreatment. *Bioresource Technology*, 192:529-539.

He, X., Wu, S., Fu, D. & Ni, J. 2009. Preparation of sodium carboxymethyl cellulose from paper sludge. *Journal of Chemical Technology and Biotechnology*, 84:427-434.

Hojamberdiev, M., Kameshima, Y., Nakajima, A., Okada, K. & Kadirova, Z. 2008. Preparation and sorption properties of materials from paper sludge. *Journal of Hazardous Materials*, 151:710-719.

Ioelovich, M. 2014. Waste paper as promising feedstock for production of biofuel. *Journal of Scientific Research and Reports*, 3(7):905-916.

Jaria, G., Calisto, V., Silva, C.P., Gil, M.V., Otero, M. & Esteves, V.I. 2019. Obtaining granular activated carbon from paper mill sludge – A challenge for application in the removal of pharmaceuticals from wastewater. *Science of the Total Environment*, 653:393-400.

Kong, J., Gu, R., Yuan, J., Liu, W., Wu, J. & Fei, Z. 2018. Adsorption behavior of Ni(II) onto activated carbons from hide waste and high-pressure steaming hide waste. *Ecotoxicology and Environmental Safety*, 156:294-300.

Liu, Z., Quek, A., Hoekman, S.K. & Balasubramanian, R. 2013. Production of solid biochar fuel from waste biomass by hydrothermal carbonization. *Fuel*, 103:943-949.

Méndez, A., Barriga, S., Fidalgo, J.M. & Gascó, G. 2009. Adsorbent materials from paper industry waste materials and their use in Cu(II) removal from water. *Journal of Hazardous*

Materials, 165:736-743.

Mubarik, S., Saeed, A., Mehmood, Z. & Iqbal, M. 2012. Phenol adsorption by charred sawdust of sheesham (Indian rosewood; *Dalbergia sissoo*) from single, binary and ternary contaminated solutions. *Journal of the Taiwan Institute of Chemical Engineers*, 43:926-933.

Rahman, M.M. & Kabir, K.B. 2010. Wastewater treatment options for paper mills using recycled paper/imported pulps as raw materials: Bangladesh perspective. *Chemical Engineering Research Bulletin*, 14:65-68.

Saleh, S., Kamarudin, K.B., Ghani, W.A.W.A.K. & Kheang, L.S. 2016. Removal of organic contaminant from aqueous solution using magnetic biochar. *Procedia Engineering*, 148:228-235.

Sohi, S.P. 2012. Carbon storage with benefits. *Science*, 338:1034-1036.

Tabassi, D., Harbi, S., Louati, I. & Hamrouni, B. 2017. Response surface methodology for optimization of phenol adsorption by activated carbon: Isotherm and kinetics study. *Indian Journal of Chemical Technology*, 24:239-255.

Tan, X., Liu, Y., Zeng, G., Wang, X., Hu, X., Gu, Y. & Yang, Z. 2015. Application of biochar for the removal of pollutants from aqueous solutions. *Chemosphere*, 125:70-85.

Vikrant, K., Kim, K., Ok, Y.S., Tsang, D.C.W., Tsang, Y.F., Giri, B.S. & Singh, R.S. 2018. Engineered/designer biochar for the removal of phosphate in water and wastewater. *Science of the Total Environment*, 616-617:1242-1260.

Wong, S., Ngadi, N., Inuwa, I.M. & Hassan, O. 2018. Recent advances in applications of activated carbon from biowaste for wastewater treatment: A short review. *Journal of Cleaner Production*, 175:361-375.

Zhou, N., Chen, H., Xi, J., Yao, D., Zhou, Z., Tian, Y. & Lu, X. 2017. Biochars with excellent Pb(II) adsorption property produced from fresh and dehydrated banana peels via hydrothermal carbonization. *Bioresource Technology*, 232:204-210.

CHAPTER 2 – LITERATURE REVIEW

In this chapter the importance of the treatment of industrial wastewater is discussed in depth. Sections 2.1 – 2.3 focus on the volumes, characteristics and composition of the wastewater produced by the pulp and paper industry. Section 2.4 highlights the impact that the wastewater produced by the pulp and paper industry has on both the environment and the economy. Sections 2.5 – 2.6 discuss the conventional methods employed for the treatment of industrial wastewater, where special attention is given to adsorption in Section 2.7. Section 2.8 focusses on commercial activated carbon as adsorbent, whereas Sections 2.9 – 2.13 focus on the production of alternative and cheaper adsorbents from biomass feedstock, such as paper sludge by hydrothermal liquefaction, the preferred processing method.

A detailed discussion based on the important factors to consider when employing the adsorption process, such as the processing conditions, isotherm and kinetic models and the possible mechanisms present during the adsorption process, is discussed in Sections 2.14 – 2.18. The limitations of binary adsorption studies are then also reviewed in Section 2.19. Lastly, concluding remarks are given in Section 2.20 which states the suitability of HTL paper sludge-based biochar as a possible adsorbent for the treatment of industrial wastewater produced by the pulp and paper industry.

2.1 Water usage in the pulp and paper industry

The pulp and paper industry utilises significant amounts of fresh water for the different stages of the paper manufacturing process. These stages include; wood debarking, pulp manufacturing, pulp bleaching, fibre recycling and paper manufacturing activities (Ashrafi *et al.*, 2015). Water in the pulp and paper industry is mainly used as suspension and transport fluid for fibres and fillers, solvent for chemical additive, and it serves as hydrogen bridging agent between the different fibres for product strength (Möbius, 2006).

According to Asghar *et al.* (2008), the pulp and paper industry has been ranked as the third largest consumer of freshwater resources globally, after the primary metals and chemical manufacturing industries. It has been found that paper mills typically use approximately 5 to 100 m³ of water per ton of paper produced and approximately 10 to 50 m³ of water per ton of paper produced for modern paper mills (Toczyłowska-Mamińska, 2017). The consumption of large amounts of fresh water therefore results in the generation of significant amounts of industrial wastewater. It has been found that pulp and paper mills generate between 1.5 to 60 m³ of wastewater per ton of paper produced, comparable with the starting amount of fresh water used per ton of paper produced (Asghar *et al.*, 2008). In South Africa, the consumption and production of industrial

wastewater by the pulp and paper industry is estimated at approximately 130 million m³ per annum and 60 m³ per ton of paper produced (Brink, 2017).

2.2 Characteristics of pulp and paper wastewater

The wastewater produced by the pulp and paper industry consists of a unique set of characteristics. The main characteristics include the chemical oxygen demand (COD), biological oxygen demand (BOD₅), BOD₅/COD ratio, total nitrogen content, total dissolved solids (TDS), total suspended solids (TSS) and pH of the wastewater produced (Ashrafi *et al.*, 2015). These characteristics depend on the processes employed, the raw materials used and to what extent used process water is being recycled (Kamali & Khodaparast, 2015; Raj *et al.*, 2007).

COD and BOD₅ concentrations are two of the most important parameters used to characterise the wastewater produced by paper mills. The COD concentration is an indication of the amount of chemicals present in the wastewater, where the BOD₅ concentration gives an indication of the microbial activity present in the wastewater produced. According to Kamali and Khodaparast (2015), the COD concentration of recycling paper mills are typically between 3380 and 4930 ppm, 1650 and 2565 ppm for the BOD₅ concentration, and the resulting BOD₅/COD ratio between 0.488 and 0.52.

BOD₅-to-COD ratio is commonly used in industry as an indication of the biodegradability of the wastewater produced. According to Al-Momani *et al.* (2002), wastewater with BOD₅/COD ratios in the range of 0.40 – 0.80 are considered readily biodegradable, whereas low BOD₅/COD ratios indicate that the high concentration of chemicals inhibit effective microbial activity. The biodegradability differs from one mill to another. For example, integrated pulp and paper mills produce wastewater that is not considered biodegradable, as the wastewater produced typically have a BOD₅/COD ratio of approximately 0.32 (Kamali & Khodaparast, 2015). Kraft and chlorine bleaching paper mills' wastewater is considered even less biodegradable, as a BOD₅/COD ratio of 0.237 is common for such mills (Raj *et al.*, 2007).

The pH of the industrial wastewater produced is another important parameter to take into account during the wastewater treatment and discharge activities. The different pulping processes produce wastewater with different pH values, depending on the type of process employed, Kraft or Soda, as different chemicals are used in each process (Mongkhonsiri *et al.*, 2018). Generally, the pH of the wastewater produced by the pulp and paper industry has been found to be in the alkaline range with pH values ranging between eight and nine (Raj *et al.*, 2007). The alkaline pH values can be attributed to the type of chemicals used in the production of paper-based products. Variations in the pH of the produced wastewater are however avoided as it influences the efficiency of the wastewater treatment steps employed to clean the received wastewater.

2.3 Composition of pulp and paper wastewater

Wastewater produced by the pulp and paper industry contains organic and inorganic pollutants. According to Amat *et al.* (2005), the degradation processes employed in the paper-making process have produced products like saccharides or carboxylic acids, and phenolic compounds are found in high concentrations in the wastewater produced by pulp and paper mills.

2.3.1 Organic pollutants

Phenol and phenol derivatives are volatile organics commonly found in the wastewater produced by the pulp and paper industry. According to Tuhkanen *et al.* (1997), the main contributors to the colour and COD of pulp and paper wastewater are phenol and its derivatives, originating from the degradation of lignin. Phenolic concentrations as high as 73 ppm have been reported for pulp and paper wastewater (Raj *et al.*, 2007). High phenolic concentrations are considered to be very dangerous even in low concentrations, due to their fatal impact on the environment and human life (Calace *et al.*, 2002). Human exposure to phenolic compounds can result in damage to the kidneys, blood, and respiratory and central nervous systems (Ali, 2014). Phenolic exposure is also fatal to the environment, as exposure has resulted in the death of aquatic organisms, inhibition of normal microbial activities and cancer in animals (Liu *et al.*, 2010a). Therefore, the maximum allowable limit of phenolic compounds present in wastewater is between 0.5 and 1 ppm (Polat *et al.*, 2006).

Considerable amounts of inorganic materials such as mineral compounds are also found in the wastewater produced by paper mills. According to Ichiura *et al.* (2011), the wastewater produced by the paper industry contains high calcium concentrations, since large quantities of calcium carbonate (CaCO_3) are used as filler during the papermaking process.

2.3.2 Inorganic pollutants

Alkali earth metals such as calcium (Ca) and magnesium (Mg) are divalent elements commonly found in industrial wastewater streams. Although these metals do not pose a direct threat to the health of living organisms, their presence is directly related to water hardness (Sepehr *et al.*, 2013). These divalent elements precipitate out of solutions, when heated, as calcium carbonate and magnesium hydroxide ($\text{Mg}(\text{OH})_2$), resulting in scale formation that clogs the water pipes used in the production processes (Kotzé *et al.*, 2014). The formation of these deposits adversely affect both the performance and lifetime of process equipment used in the manufacturing processes (Huuha *et al.*, 2010). Reduced capacity due to scale deposits on process equipment increases energy costs for production and separation, thus affecting plant productivity and profitability (Manahan, 2000).

The maximum allowable limit of water hardness constituents has not yet been defined, as it depends on the local environmental conditions. However, water can be classified as either soft or hard, depending on the concentration of calcium and its equivalent calcium carbonate present in the water. According to Kotzé *et al.* (2014), water is considered as hard water if the concentration of CaCO_3 exceeds 150 ppm, whereas concentrations above 300 ppm are considered as very hard water.

2.4 Impact of the pulp and paper industry

The pulp and paper industry has been ranked as the fourth largest industrial sector responsible for releasing Toxic Release Inventory chemicals (TRI) into water resources (Bajpai, 2015; Kamali & Khodaparast, 2015). The organic pollutants found in the wastewater produced by the pulp and paper industry results in mutagenic, carcinogenic, endocrinic and clastogenic consequences in living organisms, especially in aquatic ecosystems (Raj *et al.*, 2007). According to Pokhrel and Viraraghavan (2004), the discharge of pulp and paper wastewater has been found to result in the death of the zooplankton and fish present in discharging water bodies, as well as further influencing higher ecological food chains. Therefore, the industry has been urged to limit the amount of wastewater produced in order to comply with stricter environmental regulations and effluent limits.

The production of pulp and paper wastewater affects the efficiency and profitability of the production processes employed negatively. Since pulp and paper mills limit their fresh water consumption and wastewater production by recycling process water, accumulation of pollutants due to poorly treated process water can result in corrosion, bad odours and poor product characteristics (Asghar *et al.*, 2008). In addition, hefty penalties are issued by local authorities if the wastewater produced is above the acceptable effluent limits.

The impact of the produced wastewater is well-understood and acknowledged by the pulp and paper industry. Therefore, extensive research is being done and funded by the industry to find alternative solutions to the current wastewater treatment problems encountered.

Pulp and paper mills commonly employ conventional treatment methods to treat the wastewater produced in the process.

2.5 Conventional treatment methods

Conventional wastewater treatment plants used in industry employ primary and secondary treatment steps to purify the wastewater produced. However, conventional treatment facilities were designed to remove only simple organic matter and nutrients, and therefore the monitoring and removal of micropollutants is problematic (Goswami *et al.*, 2018). Also, the inhibitory and

toxic effects of pollutants found in industrial wastewater limits the performance of conventional biological/secondary treatment steps used in wastewater treatment plants (Soto *et al.*, 2011). Therefore, post-treatment methods such as physicochemical or alternative biological treatment techniques are required to remove residual micro-pollutants from traditionally treated wastewater streams. Various post-treatment methods have been developed to treat contaminated industrial wastewater.

2.6 Post-treatment methods

Industrial wastewater, with pollutant concentrations between 5 and 500 ppm, can be treated by physicochemical or biological methods, where physicochemical methods are the most common and the most effective methods used in industry (Beker *et al.*, 2010; Toczyłowska-Mamińska, 2017). The most common physicochemical methods include chemical precipitation, membrane filtration, chemical oxidation processes, ion exchange and adsorption (Gunatilake, 2015).

2.6.1 Chemical precipitation

The process of chemical precipitation is based on adjusting the solution pH through the addition of specific chemicals, which result in precipitation reactions of the pollutants (Carolín *et al.*, 2017). Chemicals that are most often used include lime (Ca(OH)_2), caustic soda (NaOH), soda ash (Na_2CO_3), sodium sulphide (Na_2S), sodium bicarbonate ($\text{Na(HCO}_3)_2$) and phosphate compounds (Chen *et al.*, 2018; Mohan *et al.*, 2014). The precipitated solids are then removed by physical means such as sedimentation and/or filtration (Chen *et al.*, 2018). The usage of chemical precipitation as a wastewater treatment method enables simple, adaptable and effective operation to remove micropollutants from the industrial wastewater produced (Barakat, 2011; Huuha *et al.*, 2010). However, chemical precipitation leads to the formation of large amounts of toxic chemical sludge that requires costly post-treatment and disposal steps in order to reduce contaminant concentrations below acceptable limits (Barakat, 2011; Mohan *et al.*, 2014). Chemical precipitation is also not recommended for industrial wastewater containing low concentrations of contaminants, due to the low efficiencies reported for its application (Carolín *et al.*, 2017). Membrane filtration, however, does not require the addition of chemicals to treat the contaminated industrial wastewater.

2.6.2 Membrane filtration

Membrane filtration is a pressure-driven wastewater treatment method that separates contaminants from a solution, based on its particle size, concentration, pH and the feed side pressure applied (Carolín *et al.*, 2017). Membrane filtration is a flexible process that requires simple operation, low energy input and smaller floor space to achieve high removal efficiencies

(Carolín *et al.*, 2017; Rosman *et al.*, 2018). However, membrane filtration is an expensive process that limits its large-scale implementation in industry (Ahmed & Ahmaruzzaman, 2016). High operating costs can be attributed to the cost associated with membrane materials and the occurrence of membrane fouling. Membrane fouling results in a declined flux, increased transmembrane pressure and biodegradation of the membrane materials (Barakat, 2011). However, an alternative solution to the occurrence of membrane fouling problems is the implementation of chemical oxidation processes.

2.6.3 Chemical oxidation processes

Chemically oxidation processes, especially advanced oxidation processes, have been extensively used for the treatment of contaminated industrial wastewater produced by the pulp and paper industry (Pokhrel & Viraraghavan, 2004). Chemical oxidation processes transform or mineralise hazardous pollutants through oxidation to their less harmful forms by the production of strong oxidants such as hydroxyl radicals (Rosman *et al.*, 2018). Advanced oxidation processes are nonselective with the ability to oxidise both the most complex and the simplest micropollutants at a high reaction rate to produce water, carbon dioxide and inorganic ions as end-products (Goswami *et al.*, 2018). However, the usage of advanced oxidation processes can lead to the production of harmful intermediates and additional treatment costs as the newly produced wastewater consists of an even higher degree of toxicity than the initial wastewater received, making it much harder to treat (Rosman *et al.*, 2018). In addition, oxidation of process equipment can occur that leads to corrosion and equipment failure (Carolín *et al.*, 2017). Therefore ion exchange is preferred above oxidation processes as it offers cost-effective solutions for wastewater treatment.

2.6.4 Ion exchange

The ion exchange process is based on the usage of a suitable ion exchanger to replace undesirable ions in a solution. The most commonly used ion exchangers are insoluble synthetic organic ion exchange resins (Gunatilake, 2015). During the process, absorption of anions or cations from an electrolyte solution onto active sites on the resin releases ions of an equivalent amount and charge back into the solution (Bochenek *et al.*, 2011; Gunatilake, 2015). The main advantage of employing ion exchange as post-treatment method is the associated cost. In comparison with the other wastewater treatment methods, ion exchange processes have the lowest capital and operating costs associated with its operation (Pintar *et al.*, 2001). However, ion exchange is an energy-intensive process where additional capital is required to regenerate saturated resins that may produce additional hazardous solutions in the process (Sepehr *et al.*, 2013). The capital saved during the operation of the process will then again be used for managing the hazardous solutions produced during the regeneration process of spent resins. Adsorption,

on the other hand, offers economical solutions for the regeneration of spent adsorbents through various desorption processes (Rathore *et al.*, 2016).

2.7 Adsorption

Adsorption is a well-known mass transfer process widely used to treat contaminated industrial wastewater containing organic and inorganic pollutants (Lin & Juang, 2009). The adsorption process entails the transfer of ions, the adsorbates, from the liquid phase to the surface of the solid phase, the adsorbent, where the adsorbates are then bounded to the surface of the adsorbent (Barakat, 2011). The adsorption of adsorbates takes place in three main steps, namely:

- External or film diffusion of the adsorbates from the bulk liquid across the boundary layer around the particles of the adsorbent;
- Intra-particle diffusion of the adsorbates from the outer surface of the adsorbent to and within the pores of the adsorbent. Adsorption on the outer surface of the adsorbent also occurs, but to a lesser extent compared to the internal surface adsorption;
- Adsorption of the adsorbates (chemical or physical) within the pores of the adsorbent (Singh *et al.*, 2012).

Adsorption on the surface or within the pores of an adsorbent take place depending on the type of attraction forces that exist between the adsorbate and the adsorbent. Adsorption, on the basis of attractive forces, takes place by either physical or chemical adsorption.

Physical adsorption is a reversible process where weak, non-specific intermolecular forces of attraction exist between adsorbates and adsorbents (Soto *et al.*, 2011). Physical adsorption is an exothermic process that produces relatively low enthalpy of adsorption values, lower than 25 kJ.mol^{-1} , and consists of low activation energies (Polat *et al.*, 2006). Physical adsorption can also result in the formation of a multilayer of adsorbates on the surface of the adsorbent (De Gisi *et al.*, 2016). Chemical adsorption, in contrast with physical adsorption, is an irreversible, highly specific process where strong covalent or ionic bonds of attraction are present, since chemical reactions take place (Burakov *et al.*, 2018). Chemical adsorption is also an exothermic process with high enthalpy of adsorption values, larger than 40 kJ.mol^{-1} (Polat *et al.*, 2006). Chemical adsorption can also result in the formation of a monolayer of adsorbates on the surface of the adsorbent (De Gisi *et al.*, 2016).

2.7.1 Adsorption capacity

The amount of adsorbate that can be adsorbed onto a specific adsorbent, independent of the type of adsorption taking place, is termed the adsorption capacity. The adsorption capacity at time t can be calculated by Equation (2-1) (adapted from Zhang *et al.*, 2015)

$$q_t = \frac{V_{sol}(C_i - C_t)}{m} \quad (2-1)$$

where q_t is the instantaneous adsorption capacity at time t (mg.g⁻¹), C_i is the initial adsorbate concentration (ppm), C_t is the instantaneous residual adsorbate concentration in the solution at time t (ppm), V_{sol} is the volume of the solution (L) and m is the mass of the adsorbent used (g).

The adsorption capacity can also be calculated, once equilibrium is reached, as given by Equation (2-2) (adapted from Zhang *et al.* (2015))

$$q_e = \frac{V_{sol}(C_i - C_e)}{m} \quad (2-2)$$

where q_e is the adsorption capacity at equilibrium (mg.g⁻¹) and C_e is the adsorbate concentration still left in the solution at equilibrium conditions (ppm). Once equilibrium is reached, the removal efficiency of the adsorption process can be calculated.

2.7.2 Removal efficiency

The removal efficiency can be calculated by Equation (2-3) (adapted from Rout *et al.* (2016))

$$Removal \% = \frac{C_i - C_e}{C_i} \quad (2-3)$$

From all the post-treatment methods commonly employed in industry, adsorption has been the preferred micropollutant treatment method used in most of the recent wastewater treatment literature published. From the removal of pharmaceuticals and heavy metals to the removal of volatile organics such as phenol and phenol derivatives from industrial wastewater produced by various industries (Mohammed *et al.*, 2018; Oliveira *et al.*, 2018; Sahu *et al.*, 2017; Villar da Gama *et al.*, 2018; Yoon *et al.*, 2017), the most commonly used adsorbent for adsorption applications is activated carbon.

2.8 Activated carbon

Activated carbon has many characteristics that make it ideal for use in adsorption purposes. These characteristics include having a large surface area, highly porous structure, high adsorption capacity and a fast adsorption rate (Hameed & Rahman, 2008; Liu *et al.*, 2010a). Characteristics such as surface area, pore size distribution, pore shape and surface chemistry are highly dependent on the type of feedstock, operating conditions and the type of activation method employed (Şentorun-Shalaby *et al.*, 2006).

Activated carbon is most commonly (and originally) produced from expensive feedstock such as coal and wood (Hameed & Rahman, 2008; Mohan *et al.*, 2014). The characteristics of typical activated carbon produced commercially are shown in Table 2-1.

Table 2-1: Commercial activated carbon characteristics

Characteristic name	Value	Reference
Surface area	400-2000 m ² .g ⁻¹	(Bhatnagar & Sillanpää, 2010; Mcdougall, 1991)
Pore diameters(d _p)		(Okolo <i>et al.</i> , 2014)
microporous	≤ 20 Å	
mesoporous	20 Å ≤ d _p ≤ 500 Å	
macroporous	≥ 500 Å	

Activated carbon is mostly microporous but can also contain mesopores, depending on the production method and application it is used for. Mesoporous and macroporous carbons are synthesised for the removal of relatively large molecules due to their large pore diameters that can accommodate larger molecules, as seen from Table 2-1 (De Gisi *et al.*, 2016). In contrast, microporous carbon is used for the removal of smaller molecules.

Different types of activated carbon can be produced with different sizes depending on the type of activation method selected. Activated carbon can be produced by physical or chemical activation.

2.8.1 Physical activation

Physical activation is a two-step process where the feedstock is firstly subjected to pyrolysis at high temperatures ranging between 400°C – 600°C, in an inert atmosphere (Abbaszadeh *et al.*, 2016; ElShafei *et al.*, 2017). The solid carbon/char produced is then activated by controlled gasification at temperatures between 800°C and 1100°C in the presence of steam or carbon dioxide as activating reagents (ElShafei *et al.*, 2017; Kilic *et al.*, 2011). The activated carbon produced by physical adsorption, however, consists of a limited porous structure, and therefore limited adsorptive characteristics due to the two-step process used. Also, physical activation is an energy-intensive process that leads to high energy costs associated with the high temperatures used in the pyrolysis and activation steps.

2.8.2 Chemical activation

Chemical activation produces activated carbon with a well-developed porous structure by performing the pyrolysis and activation step simultaneously (Abbaszadeh *et al.*, 2016). Chemical activation is based on the impregnation of the feedstock with dehydrating and oxidising agents,

and then subjecting the impregnated feedstock to pyrolysis at temperatures ranging between 400°C – 800°C in an inert atmosphere (ElShafei *et al.*, 2017; Yorgun & Yıldız, 2015). The most commonly used dehydrating and oxidising agents responsible for pore development are sulphuric acid, phosphoric acid, zinc chloride, potassium hydroxide and sodium hydroxide (Abbaszadeh *et al.*, 2016). After the chemical activation process has been completed, the last step of the preparation process entails washing the produced activated carbon with an acid or base, mixed with water, to remove the salts produced and the impregnating agents used (Yorgun & Yıldız, 2015).

Chemically activated carbon is the preferred activation method since the process requires lower operational and energy costs, and produces higher carbon yields and larger surface areas when compared to physically activated carbon (Kilic *et al.*, 2011). These characteristics make chemically activated carbon ideal for the adsorption process. However, chemical activation is still an expensive process due to the high cost of impregnating agents and large volumes of washing agents required to remove all the produced impurities. Also, the regeneration process of spent activated carbon is a costly process (Hossain *et al.*, 2014).

The costs associated with the production of activated carbon cannot justify its commercial production and industrial implementation for the treatment of industrial wastewater. Conventional feedstock like coal are too expensive and are considered non-renewable resources (Karakoyun *et al.*, 2011). Also, countries affected most by contaminated water sources do not have the financial support to purchase expensive adsorbents for wastewater treatment applications (Rathore *et al.*, 2016). Therefore, alternative feedstock for the production of activated carbon should be considered.

2.9 Low-cost activated carbon

Recent literature has been focussing on producing activated carbon from alternative feedstock sources such as biomass, a bio-renewable abundant natural resource which is not only inexpensive and environmentally friendly, but also offers waste management solutions (Abbaszadeh *et al.*, 2016; Amerkhanova *et al.*, 2017; Villar da Gama *et al.*, 2018; Zhou *et al.*, 2017a). The main sources of biomass can be classified as first, second, third and fourth generations, as shown in Table 2-2.

Table 2-2: Biomass generations (Yang *et al.*, 2015).

Generation	Description	Examples
First	Agricultural crops (edible)	Grains such as corn, sugarcane and wheat
Second	Non-food crops (non-edible organic waste products)	Corn cobs, wheat straw, barley straw, rice hulls and sugarcane bagasse
Third	Hydrophytes, microorganisms and engineered crops	Macroalgae, microalgae and bacteria
Fourth	Residues from the agricultural, municipal and industrial sectors	Swine waste, solid cattle manure, catering residues and paper-industry waste

Second- and fourth-generation biomass have been used as the main sources for the production of low-cost activated carbon. Second- and fourth-generation biomass are mainly waste products produced during agricultural, municipal and industrial activities. Therefore, low-cost activated carbon can be produced by avoiding the purchase of conventionally expensive feedstock. Shown in Table 2-3 are some of the second- and fourth-generation biomass feedstock successfully used for the production and implementation of low-cost activated carbon.

Table 2-3: Low-cost activated carbon adsorbents

Precursor	Adsorbate	BET surface area (m ² .g ⁻¹)	Adsorption capacity (mg.g ⁻¹)	Reference
Rice husk	Phenol	2138	201	(Fu <i>et al.</i> , 2019)
Tobacco residues	Phenol	1474 – 1634	17.83 – 45.49	(Kilic <i>et al.</i> , 2011)
Municipal sewage sludge	Cd (II)	319.50	9.72	(Al-Malack & Dauda, 2017)
Particleboard waste	Phenol	800 – 1300	500	(Girods <i>et al.</i> , 2009)
Sugarcane bagasse	Cd (II)	960	38.03	(Mohan & Singh, 2002)
	Zn (II)		31.11	
Soybean straw	Phenol	2271	278	(Miao <i>et al.</i> , 2013)
Wheat straw	Methylene blue	1258	165	(Xing <i>et al.</i> , 2019)
Corn straw		1102	166	
Sorghum straw		1061	164	
Coffee residue	Pb (II)	890	63	(Boudrahem <i>et al.</i> , 2009)
Cassava peels	Cu (II)	473	8.00	(De Gisi <i>et al.</i> , 2016)
	Pb (II)		5.80	

As seen from Table 2-3, the activated carbons produced from second- and fourth-generation biomass have surface areas in the range of 319.50 to 2271 m².g⁻¹ that is comparable with the

surface areas expected for commercial activated carbon, as seen from Table 2-1. The high surface areas of these low-cost activated carbons resulted in high adsorption capacities for common adsorbates such as phenol and divalent lead.

Although various second-generation sources have been utilised for the production of low-cost adsorbents, the usage of fourth-generation sources such as industrial waste products for the production of adsorbents are still limited, especially the usage of paper sludge.

2.10 Paper sludge as feedstock

Paper sludge is a fourth-generation biomass feedstock produced in large quantities by the pulp and paper industry. Paper sludge is a solid waste stream produced during the treatment of the process water used in the paper manufacturing process (Kizinievič *et al.*, 2018; Mäkelä *et al.*, 2018). According to Jaria *et al.* (2017), approximately between 40 and 50 kg of dry paper sludge is produced per ton of paper produced, where 70% accounts for primary sludge and the rest for biological sludge. There are two different types of paper sludge produced by wastewater treatment facilities, i.e. primary and secondary paper sludge (Faubert *et al.*, 2016). The different types of paper sludge produced during different parts of wastewater treatment operations are shown in Figure 2-1.

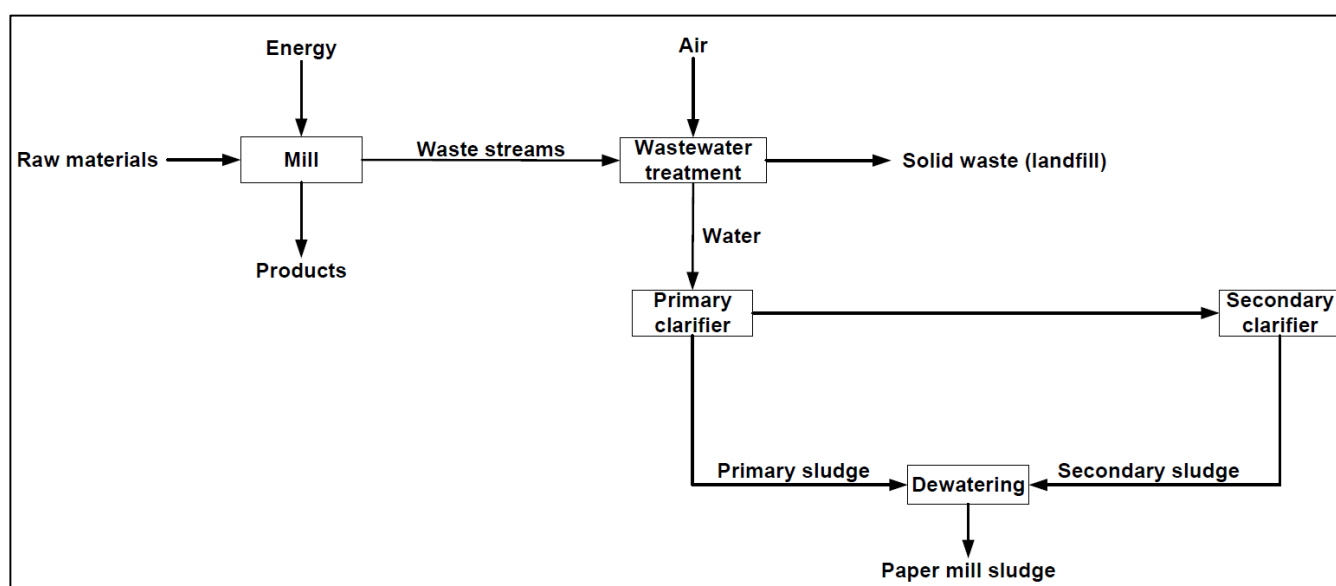


Figure 2-1: Paper sludge production process (adapted from Likon and Trebše, 2012)

Wastewater from the wastewater treatment plant firstly flows to the primary clarifier, as seen in Figure 2-1, where the solids are removed from the wastewater through sedimentation. According to Pokhrel and Viraraghavan (2004), sedimentation removes approximately 80% of suspended solids when employed by paper mills. Solids are removed from the bottom of the clarifier as a mixture of primary solids and water, referred to as the primary sludge. The overflow then flows to

the secondary clarifier, where microorganisms are used to convert the waste products to carbon dioxide and water, lowering the BOD and COD of the water (Faubert *et al.*, 2016). The remaining solids also known as secondary sludge, are also removed by clarification. The two sludge streams are then mixed and dewatered to produce paper sludge. The paper sludge dewatering is most commonly done by a belt press (Scott, 1995).

The composition of each paper mill's paper sludge is unique as its properties depend on the type of manufacturing processes employed at each mill. The manufacturing processes include how the pulp and paper is manufactured, whether recycled fibres (recycled paper) are used in the process, the type of wastewater treatment employed, and the type of wood preparation done (Jaria *et al.*, 2017). Paper sludge is generally composed of the following components:

- Organic fibres: cellulose, hemicellulose and lignin;
- Process wastewater;
- Coating material: limestone (CaCO_3), kaolinite ($\text{Al}_2\text{Si}_2\text{O}_5(\text{OH})_4$), and talcum ($\text{Mg}_3\text{Si}_4\text{O}_{10}(\text{OH})_2$); and
- Ash: magnesium (Mg), calcium (Ca), sodium (Na), aluminium (Al) and other metals such as iron (Fe) (Hojamberdiev *et al.*, 2008; Li *et al.*, 2018).

According to Yoon *et al.* (2017), paper sludge has been found to contain high concentrations of inorganic ash components such as calcium and iron, as similar chemicals are used in the paper production process. Paper sludge produced from recycled fibres contains high concentrations of ash components compared to using raw fibres, and a smaller fraction of organics ranging between 60% and 70% rather than between 80% and 90% (Calace *et al.*, 2002). De-inking paper sludge, on the other hand, has been found also to contain inorganic compounds that include ink constituents, de-inking chemicals, adhesive compounds and fillers such as kaolin, calcium carbonate and clay (Faubert *et al.*, 2016).

Since great quantities of paper sludge are produced and appropriate disposal of paper sludge is required because of strict environmental waste management regulations, the disposal of paper sludge is a growing global concern for the pulp and paper industry.

2.10.1 Conventional disposal methods

The most common methods used for paper sludge disposal are landfilling, energy recovery (incineration) and composting (Calisto *et al.*, 2014). However, due to stricter environmental legislation, alternative solutions for the minimisation of waste production are required, as traditional methods such as landfilling result in further environmental problems (Wajima, 2017). For example, landfilling has been found to result in the leaching of contaminants into groundwater resources as well as the production of greenhouse gasses (Jaria *et al.*, 2017). In addition, the

economic implications of landfilling make it financially unattractive, as disposal by landfilling is an expensive process due to the associated transportation and costs (Khalili *et al.*, 2000). Incineration and composting, on the other hand, are also costly processes as the paper sludge must firstly be dewatered to a specified moisture content before it can be used for incineration and composting purposes (Scott, 1995). Although methods such as incineration and composting are commonly employed by the pulp and paper industry, attention of the industry has been shifted to finding alternative disposal methods, as incineration and composting still have certain disadvantages associated with them.

2.10.2 Alternative disposal methods

Other methods for the disposal of paper sludge have been developed to utilise paper sludge in order to create new, value-added products. Incinerated paper sludge has been used as additive for the manufacturing of concrete (Wong *et al.*, 2015). Paper sludge has also been used in the production of cement bricks as substitute for natural additives which are commonly used (Kizinievič *et al.*, 2018). Other innovative applications for paper sludge include being used as heat insulation material, an additive for wood and paper, and also as an adsorbent for water remediation (Jaria *et al.*, 2017).

Calace *et al.* (2002) found that paper sludge showed a favourable adsorption capacity for common wastewater contaminants such as heavy metals, ionic surfactants and phenols from wastewater mediums. Battaglia *et al.* (2003) found that paper sludge mixed with soil can be used to remove cadmium and lead from a solution and the contaminants are contained in the paper sludge after the adsorption process. However, paper sludge can also be converted to carbon-based products to produce common adsorbents such as activated carbon. Paper sludge has been proposed to be a preferred precursor for activated carbon production, as it consists of a uniform chemical composition and a low concentration of contaminants (Khalili *et al.*, 2002).

However, the production of activated carbon still remains an expensive and time-consuming process due to the activation/modification steps required, although the costs associated with the precursor material can be reduced by the usage of waste products such as paper sludge. Biochar produced from paper sludge, on the other hand, can be used as an alternative to activated carbon, without the need for further activation steps.

2.11 Biochar production from paper sludge

Paper sludge-based biochar is a modification-free adsorbent that can be used for cost-effective and environmentally friendlier wastewater treatment solutions (Leng *et al.*, 2015; Liu *et al.*, 2011). According to Devi and Saroha (2015), the inherent chemical nature of paper sludge makes its corresponding biochar an attractive alternative to other adsorbents, due to its high mineral and

metal oxide content that promote adsorption activities. However, the physical nature and characteristics of the biochar produced depend strongly on the type of processing method selected for its production. The most common biochar processing method employed in literature is pyrolysis.

2.11.1 Pyrolysis

Pyrolysis is a process that converts dry biomass in the absence of oxygen under high operating temperatures such as 400 – 600°C, to produce gas, bio-oil and biochar at atmospheric pressures (Barreiro *et al.*, 2013). Pyrolysis is generally performed at low heating rates and long residence times (Amin, 2009). Although pyrolysis is commonly employed for the conversion of paper sludge to biochar, alternative options are being considered due to the disadvantages associated with the process, such as (Dimitriadis & Bezergianni, 2017):

- The feedstock must be dried before usage, which results in high energy cost (moisture content < 10 wt% (Mohan *et al.*, 2014);
- The feedstock must be grounded to particle sizes ≤ 1 mm (Mohammed *et al.*, 2018);
- Longer residence times such as 2 hours are required (Liu *et al.*, 2010b);
- High processing temperatures leads to corrosion of the equipment used;
- Biochar has the same characteristics as graphite since mostly all the oxygenated functional groups have been removed due to the high processing temperatures (Liu *et al.*, 2010b).

Therefore, attention is being given to alternative methods such as hydrothermal liquefaction to produce biochar adsorbents.

2.11.2 Hydrothermal liquefaction (HTL)

Hydrothermal liquefaction is based on the thermal conversion of wet biomass in the presence of hot pressurised water at subcritical conditions to produce bio-oil, an aqueous phase, biogas and biochar (Cao *et al.*, 2017; Kumar *et al.*, 2018). Hydrothermal liquefaction is carried out at temperatures ranging from 280°C to 370°C, system pressures ranging from 10 to 25 MPa and residence times ranging between 5 minutes and 60 minutes (De Caprariis *et al.*, 2017; Elliott *et al.*, 2015; Kumar *et al.*, 2018). The advantages of using hydrothermal liquefaction as biochar production method include (Cao *et al.*, 2017):

- No thermal drying of the wet biomass is required;
- The process is environmentally friendly since no other chemicals are required for the process. The water serves as the reaction medium and reactant in the process;

- Short residence times are used, limiting the need for long periods of energy usage (Liu & Zhang, 2009);
- The process is less prone to result in corrosion of the equipment used, compared to other alternatives such as pyrolysis;
- Biochar produced by hydrothermal liquefaction consists of a variety of oxygenated functional groups that promote adsorption activities (Jain *et al.*, 2016).

2.12 Paper sludge-based biochar

Although paper sludge-based biochar produced by hydrothermal liquefaction is a more attractive option as compared to pyrolysis biochar, limited literature is available on the usage of paper sludge-based biochar produced by hydrothermal liquefaction for adsorption applications, as seen in Table 2-4.

Table 2-4: Paper sludge-based biochar adsorbents' characteristics and performance

Biochar precursor	Conversion method	Temperature (°C)	BET surface area (m ² .g ⁻¹)	Pollutant removed	Adsorption capacity (mg.g ⁻¹)	Reference
De-inking paper sludge	Pyrolysis	650	88.40	Cu (II)	58.32	(Méndez <i>et al.</i> , 2009)
Effluent treatment paper sludge	Pyrolysis	270 – 720	13	As (II)	22.80	(Yoon <i>et al.</i> , 2017)
				Cd (II)	41.60	
Primary paper sludge	Pyrolysis	800	121	Fluoxetine	122.99	(Jaria <i>et al.</i> , 2015)
Primary paper sludge	Pyrolysis	800	209.12	Diclofenac	26.69	(Coimbra <i>et al.</i> , 2015)
				Salicylic acid	12.08	
				Ibuprofen	12.33	
Primary paper sludge	Pyrolysis	315 – 800	3.43 – 209.12	Citalopram	4.4 – 19.6	(Calisto <i>et al.</i> , 2014)
Biological paper sludge			0.77 – 2.36		2.2 – 4	
Primary paper sludge	Pyrolysis	800	414	Tricaine methanesulfonate	475	(Ferreira <i>et al.</i> , 2016)
				Benzocaine	299	
Biological paper sludge	Pyrolysis	800	258	Tricaine methanesulfonate	93	(Ferreira <i>et al.</i> , 2016)
				Benzocaine	51.40	

As seen in Table 2-4, paper sludge-based biochar can be used for the removal of both organic and inorganic pollutants such as heavy metals and pharmaceuticals. However, the surface area of the biochar produced by pyrolysis is lower ($< 400 \text{ m}^2.\text{g}^{-1}$) than the surface area of the low-cost activated carbons also produced by pyrolysis, as shown in Table 2-3. The lower surface area of the biochar can be attributed to the absence of additional activation steps, as in the case of activated carbon, that would have resulted in the formation of additional pores. A lower surface area will also result in lower adsorption capacities, as the smaller number of active sites available will limit the adsorptive capabilities of the biochar for various adsorbates.

As seen in Table 2-4, biological paper sludge-based biochar had the lowest surface area, and therefore a very low adsorption capacity of below $4 \text{ mg}.\text{g}^{-1}$. This can be attributed to the blockage of the pores by the impurities produced in the process and also by not subjecting the biochar to further activation steps. Although the surface area of biochar can be increased by washing the biochar with strong HCl solutions to remove impurities such as ash, the surface area of activated paper sludge-based biochar of $671 \text{ m}^2.\text{g}^{-1}$ remains much higher than that of the unmodified biochar produced in literature (Jaria *et al.*, 2019).

Surface area is, however, not the only determining factor in adsorption processes. Wong *et al.* (2018) and Méndez *et al.* (2009) found that adsorbents with a high concentration of surface oxygenated functional groups have higher adsorption capacities compared to adsorbents with larger surface areas. Therefore, focus should be given to the production of adsorbents with more oxygenated functional groups, such as HTL produced adsorbents, than adsorbents produced at high pyrolysis processing temperatures resulting in the decomposition of nearly all the oxygenated functional groups during the process (Liu *et al.*, 2010b).

2.13 HTL produced biochar

HTL-produced adsorbents are receiving increasing interest since the resulting biochar is rich in oxygenated functional groups due to the low processing temperatures used (Tan *et al.*, 2015). Liu *et al.* (2010b) compared the adsorptive performance of HTL biochar (300°C) with that of pyrolysis biochar (700°C) and found that the HTL biochar contained more oxygenated functional groups that promoted adsorption than the pyrolysis char. The authors concluded that although the pyrolysis char had a larger surface area, the adsorption only took place due to physical adsorption. In contrast, adsorption took place on the HTL biochar by ion-exchange mechanisms due to the nature of the biochar's surface. However, only a limited number of studies have been performed on the production of paper sludge-based biochar produced through HTL. Zhang *et al.* (2011) produced biochar from secondary paper sludge and newspaper waste through HTL. However, the focus of the study was to produce bio-oil rather than using the biochar for adsorption purposes. Therefore, since the implementation of paper sludge-based biochar produced through

HTL is limited, the usage of paper sludge-based biochar should be investigated in order to determine its adsorptive performance, optimum adsorptive conditions, isotherm and kinetic responses, as well as the mechanisms responsible for the adsorption taking place.

2.14 Adsorption processing conditions

The adsorption capacity of any adsorbate onto an adsorbent is highly dependent on the process conditions of the adsorption process. The conditions determine the type of adsorption taking place, the main mechanisms present, the adsorption capacity and charge of the adsorbent, and the ionic state of the adsorbate. It is therefore important to optimise the different adsorption parameters such as the solution pH, adsorbent dosage and the adsorbate concentration to achieve the best possible adsorption result.

2.14.1 Solution pH

Solution pH plays a critical role in the adsorption of organic and inorganic pollutants, as it influences the surface charge of the adsorbent and the extent of ionisation of the adsorbate (Wang *et al.*, 2017). In order to optimise the adsorption performance for a given system, it is necessary to determine the optimum solution pH that will produce the best adsorption performance. Studies on the solution pH of adsorption are commonly adjusted to different starting values by the addition of either 0.1 M HCl or 0.1 M NaOH (Reguyala *et al.*, 2017). Therefore, the pH of the solution will determine the concentration of hydrogen ions (H^+) and hydroxide ions (OH^-) in the solution.

Solutions containing a high concentration of hydrogen ions result in a more acidic solution. According to Abbaszadeh *et al.* (2016), lower pH values result in lower cation removal efficiencies, as the cationic adsorbate competes with the hydrogen ions in the solution for available active sites on the surface of the adsorbent. However, as the pH of the solution increases, the competition between the two ions weakens, resulting in an increase in the cation adsorption performance as the cationic adsorbate then replaces the hydrogen ions attached to the active sites. Therefore, the adsorption of cationic species is favourable at pH values close to the neutral pH, as there is a limitation on the amount and adsorption of hydrogen ions. However, more alkaline conditions might result in a decrease in the removal efficiencies as high pH values could promote precipitation reactions forming metal salts (Aman *et al.*, 2008).

This behaviour of adsorbate species is not limited to cationic species, as anionic species may also adsorb at low pH values, depending on the surface charge of the adsorbent. Dursun *et al.* (2005) found that the best phenol adsorption on beet-pulp activated carbon was achieved at a solution pH of 6, whereas the adsorption of phenol decreased as the pH of the solution was increased.

Alkaline solutions contain high concentrations of hydroxide ions as the pH of the solution is increased above a pH of 7. An increase in hydroxide ions in the solution results in competition between the hydroxide ions and anionic species for active sites (Abdelwahab & Amin, 2013). The adsorption of the hydroxide ions is therefore favoured as the pH increases, resulting in a negatively charged adsorbent surface that repulses anionic adsorbates (Rengaraj *et al.*, 2002). Consequently, the adsorption of anionic species is favourable at pH values close to the neutral pH, as there is a limitation on the amount and adsorption of hydroxide ions. Kilic *et al.* (2011) found that phenol adsorption was favourable at pH values from 7 – 8 for tobacco residue activated carbons. Singh and Balomajumber (2016) also found that the best pH for maximum phenol removal with coconut shell activated carbon was at a pH of 8. However, the optimal solution pH of any adsorption system is still a function of the surface charge of the adsorbent, which changes with the pH of the solution.

2.14.1.1 Point of zero charge of adsorbent

In order to determine the surface charge of adsorbents at specific pH values, it is necessary to determine the point of zero charge, pH_{PZC} , for the adsorbent. The point of zero charge is an indication of the pH value where the net surface charge of the adsorbent is zero (Beker *et al.*, 2010). The charge of the adsorbent will change as the pH of the solution changes below or beyond the pH_{PZC} . According to Liu *et al.* (2010a) an adsorbent will be positively charged if the solution $pH < pH_{PZC}$ and negatively charged if the solution $pH > pH_{PZC}$. Depending on the type of adsorbate used, common electrostatic repulsive or attractive forces will exist between the surface of the adsorbent and the adsorbate. According to Leng *et al.* (2015), the adsorption of cations will be favoured if the solution $pH > pH_{PZC}$, whereas the adsorption of anions will be favoured if the solution $pH < pH_{PZC}$. The adsorption of cations and anions at solution pH values other than those recommended by Leng *et al.* (2015) will possibly result in electrostatic repulsive forces. However, electrostatic forces are not the only mechanisms responsible or present during an adsorption process. Therefore, adsorption can still take place where the adsorbate and the adsorbent have the same charge due to the presence of other mechanisms as stated in Section 2.17.

2.14.1.2 pKa value of adsorbate

The nature of some adsorbates, such as phenol and phenol derivatives, are also dependant on the pH of the solution as it determines the degree of dissociation of the adsorbates. The degree of dissociation of an adsorbate can be explained by its unique dissociation constant, pK_a (Calace *et al.*, 2002). The adsorbate will be protonated if the solution $pH < pK_a$ and deprotonated if the solution $pH > pK_a$ (Liu *et al.*, 2010a). According to Beker *et al.* (2010), phenol will be negatively charged at pH values higher than 9 due to the formation of phenoxide ions, since the pK_a value of phenol is 9.89.

2.14.2 Adsorbent dosage

The adsorbent dosage is an important parameter that affects the economic feasibility of an adsorption process. The main goal of determining the optimum adsorbent dosage is to find the minimum dosage for the maximum adsorption. If the minimum amount of adsorbent can remove the desired amount of adsorbate, then there is no need to use more adsorbent than necessary.

Low and high adsorbent dosages have different effects on the adsorption capacity and the removal efficiency. High adsorbent dosages result in an increase in the removal efficiency. The removal efficiency will increase as the solution concentration of the adsorbate decreases. According to El-Naas *et al.* (2010), the adsorbate concentration will decrease when more adsorbent is added to the solution, since more active sites are available for adsorption, resulting in an enhanced removal efficiency. However, an increase in the mass of adsorbent will result in a decrease in the adsorption capacity, as seen from Equation (2-1). The adsorption capacity will decrease as there will be more active sites available than initially required to adsorb the amount of adsorbate particles present in the solution. This will lead to more active sites on the surface of the adsorbent left unoccupied during the adsorption process (Abbaszadeh *et al.*, 2016).

The influence of a low adsorbent dosage will have the opposite effect on the removal efficiency compared to high dosages. Low adsorbent dosages result in a limited number of active sites available for adsorption and thus a low removal efficiency is achieved. However, since the adsorbent only has a limited number of active sites available, the chances of unoccupied sites are rare. The adsorbent will therefore use all its active sites which result in a higher adsorption capacity for the adsorbent.

The adsorbent dosage, high or low, can only be optimised with regards to the initial adsorbate concentration. The adsorbent concentration can be adjusted in order to remove the required concentration of the adsorbate.

2.14.3 Initial adsorbate concentration

Higher adsorbate concentrations will require a higher adsorbent dosage and more time to remove the desired concentration of the adsorbate. Low and high initial adsorbate concentrations have different effects on the adsorption capacity and the removal efficiency. High initial adsorbate concentrations will increase the adsorption capacity of the adsorbent. According to Kumar and Jena (2016) an increase in the initial concentration of methylene blue from 100 ppm to 500 ppm supplied the system with an enhanced driving force to overcome mass transfer limitations. However, the higher initial concentration required more time (60 minutes) compared to the lower concentration (20 minutes) to reach equilibrium. But, a higher concentration of adsorbates in the solution will cause the adsorption process to proceed much faster (initially), compared to lower

adsorbate concentrations, due to the high concentration gradient in the solution, enhancing mass transfer (Mahdi *et al.*, 2018). The removal efficiency will, however, decrease as the process proceeds until the adsorbate concentration has reached equilibrium and no further change in the concentration of the solution is observed. Once all the active sites are occupied, adsorption and desorption of ions from and to the active sites take place at the same rate, resulting in a constant removal efficiency at equilibrium. In contrast, low initial concentrations will result in a decrease in the adsorption capacity since mass transfer limitations are applicable due to the limited number of adsorbates.

2.15 Operating conditions: single-component systems

Various single-component adsorption studies have been performed for both activated carbon and biochar adsorbents at different operating conditions, as shown in Table 2-5.

As seen from Table 2-5, most of the adsorption studies performed varied the initial solution pH from 1 to 11 in order to find the best initial solution pH for phenol adsorption. However, the solution pH that resulted in the highest and best phenol adsorption ranged from 5 to 8, as indicated in Table 2-5. This can be attributed to the surface charge of the adsorbent used and the ionic state of the phenol at pH values approaching more alkaline conditions. Since phenol is mostly positively charged at pH values below 9.89, as discussed in Section 2.14.1.2, a pH of 5 to 8 will result in attractive forces between phenol and the surface of the adsorbent. According to Beker *et al.* (2010), phenol was adsorbed better at a solution pH of 6.5, since the activated carbon was negatively charged, with a point of zero charge between a pH of 1 – 3. At solution pH values lower than the point of zero charge or higher than the pK_a value of phenol, the competition of hydrogen and hydroxide ions are too significant for phenol adsorption to take place. Therefore the adsorption of phenol is preferred at solution pH values close to a neutral pH.

The adsorption of various heavy metal species is mostly performed at pH values below a neutral pH, since heavy metal species are pH limited due to the possibility of precipitation reactions occurring at pH values close to 7. Divalent ions such as calcium and magnesium, on the other hand, are not pH limited as compared to heavy metals, as they can exist as ions at alkaline conditions depending on the operating temperature employed. Since calcium is mostly removed by other wastewater treatment methods like ion exchange, literature available on the removal of calcium by adsorption is limited. One such study was conducted by Sepehr *et al.* (2013), who found that the best calcium adsorption on natural and unmodified pumice stones took place at a pH of 6, close to the point of zero charge of the two adsorbents of 6.3 and 6.5, where electrostatic interactions did not influence the adsorption process.

Most adsorption studies are preferably performed at pH values close to the point of zero charge or at the point of zero charge in order to ensure that the state of the adsorbent and the adsorbate does not play a role. By performing the adsorption studies at the point of zero charge of the adsorbent, a better understanding can be developed of the actual interaction between the surface of the adsorbent and the adsorbate. A better understanding of the actual adsorption process taking place will enable the optimisation of the process to produce better adsorption capacities.

When considering the economic factors associated with the adsorption process, it is important to find the minimum dosage to remove the maximum required concentration of adsorbate. As seen in Table 2-5, the adsorbent dosages typically used for the phenol and calcium adsorption experiments varied from 0.5 g.L⁻¹ to 10 g.L⁻¹. Although increasing the adsorbent dosage will typically remove more of the adsorbate due to the availability of more active sites, increasing the adsorbent dosage will not always result in an increased removal efficiency. According to Mohammed *et al.* (2018), increasing the adsorbent dosage higher than 8 g.L⁻¹ had no effect on the adsorption of phenol. As in the case with most of the other studies, adsorbent dosages close to 10 g.L⁻¹ were most frequently used to remove the required amount of adsorbate, as shown in Table 2-5. However, also shown in Table 2-5 is some of the adsorption studies which were successfully performed with lower adsorbent dosages, and therefore low and high adsorption dosages should be considered when performing adsorption studies.

The initial adsorbate concentration selected for the adsorption experiments performed for phenol is typically between 0.5 ppm and 800 ppm and for calcium between 25 ppm and 150 ppm. However, the initial adsorbate concentration is dependent on the objective of each study. As most adsorption studies are based on treating contaminated water sources containing the adsorbate in question, the initial adsorbate concentration is selected based on the typical concentration of adsorbate found in real contaminated water sources.

Furthermore, a rotary speed of approximately 150 rpm is most commonly selected for various adsorption studies, independent of the type of adsorbate used. Also, most adsorption studies are performed at or close to room temperature (25°C).

Table 2-5: Adsorption parameter ranges for the batch adsorption of organic and inorganic pollutants

Adsorbent	Adsorbate	pH	Rotary speed (rpm)	Adsorbent dosage (g.L ⁻¹)	Initial concentration (ppm)	Reference
Pine fruit shells biochar	Phenol	2, 6.5, 10 (6.5)	250	1 – 10	20 – 100	(Mohammed <i>et al.</i> , 2018)
Cherry stone activated carbon	Phenol	6.5 – 9.0 (6.5)	120	0.10 – 1.0	25	(Beker <i>et al.</i> , 2010)
Tobacco residue activated carbon	Phenol	8	-	0.50 – 8.0	1 – 12	(Kilic <i>et al.</i> , 2011)
Beet pulp activated carbon	Phenol	2 – 12 (6)	150	0.50	25 – 500	(Dursun <i>et al.</i> , 2005)
Paper mill activated carbon	Phenol	-	-	1.0	100 – 500	(Khalili <i>et al.</i> , 2000)
Eggshell activated carbon	Phenol	5.7	150	10	45 – 800	(Giraldo & Moreno-piraján, 2014)
Effluent treatment paper sludge biochar	As (II)	6.2	200	1.0	20.90 – 189.50	(Yoon <i>et al.</i> , 2017)
	Cd (II)				21.0 – 218.70	
Papaya peels activated carbon	Pb (II)	3 – 7 (5)	150	0.10 – 2.0	10 – 200	(Abbaszadeh <i>et al.</i> , 2016)
De-inking paper sludge biochar	Cu (II)	5	300	2.50	50	(Méndez <i>et al.</i> , 2009)
Activated carbon fibres	Phenol	1 – 11 (7)	150	1.0	141.17	(Liu <i>et al.</i> , 2010a)
Pumice stones activated carbon	Ca ²⁺ , Mg ²⁺	2 – 10 (6)	200	2.0 – 10	25 – 150	(Sepehr <i>et al.</i> , 2013)

Optimising the operating conditions of an adsorption process requires equilibrium studies. Equilibrium studies are used to determine the maximum adsorption capacity of an adsorbent for a specific adsorbate and the interaction between the adsorbent and the adsorbate (Abbaszadeh *et al.*, 2016). Equilibrium data can be interpreted by the usage of appropriate adsorption isotherm models.

2.16 Adsorption isotherms

Adsorption isotherms are mathematical models based on equilibrium data used to determine the mechanism of adsorption. Isotherm models are based on assumptions related to:

- The homogeneity or heterogeneity of the type of adsorbent used;
- The type of surface coverage (monolayer or multilayer);
- If there is interaction between the adsorbed species (Abdelkreem, 2013).

There are various isotherm models available in literature to describe the equilibrium data of a given system, i.e. Langmuir, Freundlich, Redlich-Peterson, Temkin, Dubinin-Radushkevich and Toth models (Giraldo & Moreno-piraján, 2014; Kilic *et al.*, 2011; Lin & Juang, 2009). However, the Langmuir and Freundlich isotherm models are the most widely used for wastewater treatment applications (El-Naas *et al.*, 2010; Escrig & Morell, 1998; Son *et al.*, 2018).

2.16.1 Langmuir isotherm

The Langmuir isotherm model is based on the following assumptions:

- The adsorbent's surface is homogenous (Kong *et al.*, 2018);
- Monolayer adsorption takes place on the surface of the adsorbent (Hameed & Rahman, 2008);
- The adsorbent's surface consists of a finite number of identical and equivalent adsorption sites (Abbaszadeh *et al.*, 2016; Hameed *et al.*, 2008);
- The affinity of all the active sites are the same and without preference (Kong *et al.*, 2018);
- There is no interaction or steric hindrances between adjacent adsorbed molecules (Inyang *et al.*, 2016).

The Langmuir isotherm model for a single-component system is therefore given by Equation (2-4) (adapted from Liu *et al.*, 2010a)

$$q_e = \frac{q_{max} K_L C_e}{1 + K_L C_e} \quad (2-4)$$

where q_{max} is the maximum adsorption capacity and K_L is the Langmuir constant related to the free energy of adsorption (L.mg⁻¹).

After algebraic manipulation and rearrangement, the Langmuir isotherm model can be rewritten as a straight line equation as shown by Equation (2-5)

$$\frac{1}{q_e} = \frac{1}{K_L q_{max} C_e} + \frac{1}{q_{max}} \quad (2-5)$$

where the slope is given by $\frac{1}{K_L q_{max}}$ and the intercept is given by $\frac{1}{q_{max}}$. The Langmuir constants can be calculated from the slope and intercepted by the plotting $\frac{1}{q_e}$ versus $\frac{1}{C_e}$ (Abdelkreem, 2013).

Furthermore, the feasibility of the Langmuir isotherm to describe a set of experimental data points can be determined by its characteristic separation factor. The separation factor, R_L , is a dimensionless factor that can be calculated by Equation (2-6) (adapted from Liu *et al.*, 2010a)

$$R_L = \frac{1}{1 + K_L C_i} \quad (2-6)$$

where the adsorption described by the Langmuir isotherm can be considered as:

- Irreversible if $R_L = 0$
- Favourable if $0 < R_L < 1$
- Linear if $R_L = 1$
- Unfavourable if $R_L > 1$

However, most adsorbents do not have homogeneous surfaces with identical active sites. Therefore, the Freundlich isotherm is more frequently employed to fit experimental adsorption data.

2.16.2 Freundlich isotherm

The Freundlich isotherm model can be used to describe non-ideal adsorption systems based on the following assumptions (Inyang *et al.*, 2016):

- The adsorbent's surface is heterogeneous;

- Multilayer adsorption takes place on the surface of the adsorbent;
- The adsorbent's surface consists of a finite number of identical and equivalent adsorption sites;
- Stronger active sites on the adsorbent surface will receive preference above another.

The Freundlich isotherm model for a single-component system is therefore given by Equation (2-7) (adapted from Abbaszadeh *et al.* (2016) and Hameed *et al.* (2008)),

$$q_e = K_F C_e^{\frac{1}{n}} \quad (2-7)$$

where K_F is an indicator of the adsorption capacity ($mg^{(1-\frac{1}{n})} \cdot L^{(n)} \cdot g^{-1}$) and $(\frac{1}{n})$ is the adsorption intensity or the favourability of the adsorption process.

After algebraic manipulation and rearrangement, the Freundlich isotherm model can be rewritten as a straight line equation as shown in Equation (2-8),

$$\ln(q_e) = \ln(K_F) + \left(\frac{1}{n}\right) \ln(C_e) \quad (2-8)$$

where the slope is given by $(\frac{1}{n})$ and the intercept is given by $\ln(K_F)$. The Freundlich parameters can be calculated from the slope and intercepted by the plotting of $\ln(q_e)$ versus $\ln(C_e)$. However, at very low adsorbate concentrations, the Freundlich isotherm model has been found to reduce to Henry's law as the parameter n , and will have a value of one.

2.16.3 Henry's law

Henry's law is the simplest isotherm model available in literature as it consists of only one parameter. Henry's law for single-component systems are given by Equation (2-9) (adapted from Tran *et al.* (2017)),

$$q_e = K_H C_e \quad (2-9)$$

where K_H is known as the Henry constant or distribution coefficient ($L \cdot mg^{-1}$). The applicability of Henry's law to describe equilibrium data indicates that the adsorption capacity is proportional to the residual adsorbate concentration in the liquid phase at equilibrium conditions. Therefore, higher adsorption capacities can be obtained by increasing the adsorbate concentration in the solution.

Adsorption isotherms can be used to determine how the adsorption of an adsorbate took place on the surface of the adsorbent as time progressed. As each adsorbent is unique, the

adsorption of an adsorbate can be different depending on the type of mechanism that takes place at the surface of the adsorbent.

2.17 Adsorption mechanisms

Different mechanisms have been proposed to describe the adsorption of different adsorbates onto the surface of biochar adsorbents. Adsorption mechanisms are important as they offer explanations on how the adsorption at the surface of the adsorbent took place. A better understanding of the adsorption mechanisms present during an adsorption process will allow researchers to optimise the adsorption conditions in order to enhance the working of the main mechanisms present. Different mechanisms are present during the adsorption of organic and inorganic pollutants onto biochar adsorbents.

2.17.1 Organic adsorption mechanisms

The main mechanisms present during the adsorption of organic adsorbates onto biochar adsorbents are: electrostatic forces, hydrogen bonding, π - π and hydrophobic interactions, as well as pore-filling mechanisms.

2.17.1.1 Electrostatic forces

Electrostatic forces have been found to be the dominant mechanism present during organic and inorganic pollutant adsorption onto biochar (Tan *et al.*, 2015). Electrostatic forces exist between two objects due to the difference in electrical charges emitted by each object. The electrical charges between the two objects can have the same charges (repulsive forces) or opposite charges that lead to attractive forces existing between the two. In the case of adsorption, electrostatic interactions will exist between the adsorbate and the surface of the adsorbent, depending on the solution pH and the pH_{PZC} of the biochar, as stated in Section 2.14.1.1 (Al-Malack & Dauda, 2017).

Biochar, especially unmodified biochar, has been found to consist of a negatively charged surface, as it is concentrated with oxygenated functional groups such as carboxylic, hydroxyl and phenolic groups on its surface (Li *et al.*, 2017). According to Ahmad *et al.* (2014), cations will easily adsorb onto the surface of biochar due to its typically negatively charged surface. Anionic species, on the other hand, will adsorb to the mineral-rich sites on the biochar surface that are positively charged. The biochar's surface, rich with oxygenated functional groups, can also result in the formation of hydrogen bonds between the adsorbate and the adsorbent.

2.17.1.2 Hydrogen bonding

Hydrogen bonding is present during the adsorption of organic pollutants such as phenol and phenol derivatives. Hydrogen bonding takes place between the positively charged hydrogen atom of the phenolic hydroxyl group and the electron negative oxygen atom of the oxygenated surface functional groups of the biochar (Polat *et al.*, 2006). According to Ahmad *et al.* (2014), electrostatic repulsion forces between anionic organic species and biochar have been found to result in the formation of hydrogen bonds and therefore promotes adsorption.

However, the hydroxyl group of these phenolic compounds is not the only group that results in interactions with the surface of the adsorbent.

2.17.1.3 π - π interaction

The aromatic nature of organic compounds recreates a platform for the presence of π - π interactions with the surface of the biochar (Purnomo *et al.*, 2012). The occurrence of π - π interactions exist due to the interaction between the π -orbital electrons of the aromatic molecules with the π -orbital electrons of the aromatic groups on the biochar's surface (Wu *et al.*, 2011). According to Liu *et al.* (2010a) phenol molecules are prone to form π - π stacking interactions with an adsorbent's surface that results in the formation of a multi-layer adsorption system.

However, the occurrence of π interactions is not limited to organic compounds as cation- π interactions between the positively charged inorganic ions and the π -orbital electrons of the biochar's surface groups can also occur (Li *et al.*, 2017; Wang *et al.*, 2018). Furthermore, the aromatic nature and the electrical charges of organic molecules are not the only factors contributing to the adsorption performance of aromatic compounds.

2.17.1.4 Hydrophobic interactions

Hydrophobic interactions also have an influence on the adsorption of organic molecules. The hydrophobic nature of organic molecules is related to the solubility of these compounds (Rosales *et al.*, 2017). Organic molecules with more non-polar functional groups are more likely to adsorb onto the hydrophobic regions of the biochar, whereas organic molecules with more polar functional groups will easily adsorb to the hydrophilic regions since biochar has a heterogeneous surface (Ahmad *et al.*, 2014). The characteristic heterogeneous surface of biochar also contributes to the surface available for adsorption to take place effectively.

2.17.1.5 Pore-filling

The filling of pores by adsorbates are directly affected by the surface characteristics of the biochar. According to Inyang and Dickenson (2015), the adsorption of organic ions by pore-filling is a function of the total micropore and mesopore volumes of the biochar. High pore volumes will increase the possibility of adsorption as more pores of the right sizes will be available and accessible by adsorbate species. The pore size also determines the type of adsorbates that can adsorb onto the surface of the biochar. As the size of a phenol molecule has been found to be 0.62 nm and biochar has been found to consist of a well-developed pore network with both micropores and mesopores within its surface, phenol adsorption by biochar is possible (Mukherjee *et al.*, 2011; Terzyk, 2003).

Compared to the performance of biochar with organic molecules, the adsorption of inorganic molecules onto the surface of biochar takes place by the occurrence of two different types of mechanisms.

2.17.2 Inorganic adsorption mechanisms

The main mechanism present during the adsorption of inorganic adsorbates are ion exchange as well as surface complexation and precipitation mechanisms.

2.17.2.1 Ion exchange

Ion exchange is one of the most common mechanisms present during the adsorption of inorganic species and is highly dependent on the chemical nature of the biochar. Ion exchange takes place when ionisable protons or cations from the surface of the biochar are exchanged with inorganic ions (Inyang *et al.*, 2016). According to Goldschmidt's classification, elements in groups 1 to 3 on the periodic table such as Na, K, Ca, Li, Mg, Be and Sc are common cations to exchange with inorganic ions such as heavy metals, due to their comparable electrical charges and sizes (Hollabaugh, 2007). Inorganic ions can also react with functional groups on the surface of the biochar to form surface complexes.

2.17.2.2 Surface complexation and precipitation

Surface complexation occurs when inorganic ions bind with surface functional groups to form complex precipitates on the surface of the biochar (Inyang *et al.*, 2016). However, the solution pH has a large influence on the behaviour of surface functional groups. According to Li *et al.* (2017), ionisation of carboxyl groups occurs at pH values between 3 and 4, where an increase in the solution pH results in the deprotonation of the carboxyl groups. The deprotonated carboxyl groups are then free to form complexes with the positively charged inorganic ions,

which results in the formation of precipitates on the biochar's surface. Also, an increase in the solution pH will result in an increased hydroxyl ion concentration that produces insoluble complexes with the inorganic cations in the solution (Al-Malack & Dauda, 2017).

Adsorption isotherms and the corresponding mechanisms offer a better understanding on how adsorption processes take place. However, the time required for the adsorption process to reach equilibrium is essential when the financial implications, and therefore the industrial implementation of adsorption processes, are being considered.

2.18 Adsorption kinetics

The evaluation of adsorption kinetics is an important aspect to consider in understanding the dynamic behaviour of any adsorption process. Adsorption increases as the contact time is increased until the surface of the adsorbent is saturated and equilibrium conditions are reached (Abbaszadeh *et al.*, 2016).

Kinetic parameters can be used to predict the rate of adsorption, and thus the contact time required for the process to be completed can be determined. Knowledge of the contact time can then be used to assist with the modelling and designing of an adsorption process (Ali *et al.*, 2018; Mohammed *et al.*, 2018; Rout *et al.*, 2016). Various kinetic models are available for the determination of the adsorption kinetics for both organic and inorganic adsorbates. The two kinetic models most commonly used are the pseudo-first and pseudo-second-order rate models (Abdelkreem, 2013; Dursun *et al.*, 2005; El-Naas *et al.*, 2010; Kong *et al.*, 2018; Mahdi *et al.*, 2018; Yang *et al.*, 2014; Zhang *et al.*, 2015).

2.18.1 Pseudo-first-order model

The pseudo-first-order rate equation of Lagergren (1898) is given by Equation (2-10) (adapted from El-Naas *et al.* (2010)),

$$\frac{dq_t}{dt} = k_1(q_e - q_t) \quad (2-10)$$

where k_1 is the pseudo first-order rate constant (min^{-1}). The pseudo-first-order rate equation can also be written in its linearized form as given by Equation (2-11),

$$\ln(q_e - q_t) = \ln(q_e) - k_1 t \quad (2-11)$$

where the slope, $-k_1$ and the intercept, $\ln(q_e)$ can be calculated by plotting $\ln(q_e - q_t)$ versus t . It has been reported by Hameed *et al.* (2008) that the pseudo-first-order rate equation

cannot describe the dynamic behaviour of an adsorption process for the entire contact period. Therefore, the pseudo-first-order rate equation can only be used to describe the initial stages of an adsorption process.

2.18.2 Pseudo-second-order model

The pseudo-second-order rate equation can predict the behaviour of an adsorption process for the entire contact period of the process (Kilic *et al.*, 2011). The pseudo-second-order rate equation is given by Equation (2-12) (adapted from Dursun *et al.*, 2005),

$$\frac{dq_t}{dt} = k_2(q_e - q_t)^2 \quad (2-12)$$

where k_2 is the pseudo-second-order rate constant ($\text{g.mg}^{-1} \text{ min}^{-1}$). The pseudo-second-order rate equation can also be written in its linearized form, as given by Equation (2-13),

$$\frac{t}{q_t} = \frac{1}{k_2 q_e^2} + \frac{t}{q_e} \quad (2-13)$$

where the slope, $\frac{1}{q_e}$ can be used to calculate q_e and the intercept, $\frac{1}{k_2 q_e^2}$ to calculate k_2 by plotting $\frac{t}{q_t}$ versus t . Furthermore, the calculated parameters can then be used to determine the initial rate of adsorption, h_o , as shown in Equation (2-14)

$$h_o = k_2 q_e^2 \quad (2-14)$$

However, adsorption kinetic models such as the pseudo-first and second-order-rate expressions cannot be used to predict the rate-limiting step(s), as these models are based on chemical reaction kinetics without considering the actual diffusion steps present during an adsorption process (Bonilla-Petriciolet *et al.*, 2017). Therefore, diffusional models such as the intra-particle diffusion model was also considered.

2.18.3 Intra-particle diffusion

The intra-particle diffusion model has been extensively used to determine the main diffusion mechanisms and to provide a better understanding of the rate-limiting steps (Bhatnagar & Sillanpää, 2010). Intra-particle diffusion is affected by the following factors (El-Naas *et al.*, 2010):

- Physical properties of the adsorbent (pore size, pore size distribution);
- Initial adsorbate concentration in the solution;

- Temperature at which the experiments are performed;
- The rotary speed used in batch adsorption to ensure effective mixing.

Furthermore, the intra-particle diffusion model was formulated by taking the following assumptions into account (Kong *et al.*, 2018):

- External resistance at the start of the process will only affect the process for a short time;
- Diffusion takes place in a radical direction;
- The pore diffusivity remains constant.

Based on the above assumptions, the intra-particle diffusion model is given by Equation (2-15) (adapted from Singh *et al.*, 2012),

$$q_t = k_{id} t^{0.5} + C \quad (2-15)$$

where the slope, k_{id} is the intra-particle diffusion rate constant ($\text{mg.g}^{-1}.\text{time}^{0.5}$) and the intercept, C is a constant that is proportional to the thickness of the external boundary layer, calculated by the plotting of q_t versus $t^{0.5}$. From the plot, different conclusions regarding the diffusion mechanism and rate-limiting steps can be made. These conclusions are as follows (Kilic *et al.*, 2011; Ooi *et al.*, 2019):

- If the plot is linear, then intra-particle diffusion is applicable;
- If the plot also passes through the origin, then intra-particle diffusion is the rate-limiting step;
- If the straight-line plot does not pass through the origin, then intra-particle diffusion is not the only rate-limiting step present, and therefore film diffusion may be applicable.

It should also be noted that some adsorption processes result in the plotting of multiple straight lines, indicating that different diffusion mechanisms influenced the adsorption rate at some stage of the process (El-Naas *et al.*, 2010; Ooi *et al.*, 2019). The use of applicable diffusion models is limited as most studies do not include its evaluation in their adsorption kinetics. As adsorbents are mostly porous in nature, diffusional effects of adsorbates throughout the adsorption process should be included in the evaluation of the adsorption kinetics (Tsibranska & Hristova, 2011).

As mentioned, different diffusional steps like film and intra-particle diffusion can influence the overall rate of adsorption. Therefore, the overall diffusion coefficient must be calculated in order to establish which mass transfer step played the dominant role during the adsorption process.

2.18.4 Overall diffusion coefficient

The overall diffusion coefficient, $D_{overall}$, can be determined by firstly calculating the film diffusion coefficient, D_{film} and the intra-particle diffusion coefficient, D_{intra} ($\text{cm}^2.\text{s}^{-1}$) as given in Equation (2-16) and Equation (2-17) (adapted from Girish and Murty (2016)),

$$F = 6 \left(\frac{D_{film}}{\pi r_p^2} \right)^{0.5} t^{0.5} \quad (2-16)$$

$$\ln \left(\frac{1}{1 - F(t)^2} \right) = \left(\frac{\pi D_{intra}}{r_p^2} \right) t \quad (2-17)$$

where r_p is the average particle size of the adsorbent (cm) and the fractional attainment F can be calculated by Equation (2-18) (adapted from Itodo *et al.*, 2010).

$$F = \frac{q_t}{q_e} \quad (2-18)$$

Since film and intra-particle diffusion proceeds after one another in series, the overall diffusion coefficient can be calculated by Equation (2-19),

$$D_{overall} = D_{film} + D_{intra} \quad (2-19)$$

where the contribution (%) of the film and intra-particle diffusion can be determined. By determining which diffusional step had the largest influence on the overall rate of adsorption, a better understanding of the rate-limiting step can be obtained. This will enable the possible improvement of future adsorption studies to be performed with the adsorbent and/or the adsorbate in question.

Adsorption studies are most commonly performed on single-component systems. However, real industrial wastewater effluents do not contain only a single organic or inorganic contaminant, but rather a combination of organic and inorganic contaminants (Sellaoui *et al.*, 2017; Singh & Balomajumder, 2016; Villar da Gama *et al.*, 2018; Zhou *et al.*, 2017b). Therefore, to understand the behaviour of real-life industrial effluent adsorption processes, it is essential to evaluate the binary adsorption performance of an adsorbent in the presence of both an organic and inorganic contaminant.

2.19 Binary adsorption systems

Limited literature is available on the binary adsorption of contaminants since the main focus of adsorption experiments has been the adsorption of individual contaminants (Rout *et al.*, 2016). The performance of various adsorbents in the presence of binary adsorbates are therefore not fully understood, especially different combinations of either organic or inorganic contaminants or both.

Binary adsorption systems are much more complex than single-component systems, as the presence of one contaminant can influence the adsorption of another. According to Villar da Gama *et al.* (2018), the presence of more than one component will affect the selectivity and adsorption capacity of an adsorbent for a target pollutant. The possibility of competition and interaction between two pollutants for the same active sites may also arise, which affect the adsorption of a specific pollutant (Padilla-Ortega *et al.*, 2013; Rout *et al.*, 2016).

Shown in Table 2-6 is a summary of some of the binary adsorption studies performed for organic-organic, inorganic-inorganic and organic-inorganic contaminants, where a variety of activated carbon and biochar adsorbents were used.

As seen in Table 2-6, most of the binary adsorption studies are also performed at pH values close to 7, as in the case with single-component systems. The adsorbent dosages selected for most of the studies lie between 0.40 g.L^{-1} and 10 g.L^{-1} , indicating that binary adsorption systems also require moderate adsorbent dosages. However, the adsorbent dosage used for the binary experiments of two adsorbates is often determined by performing single adsorption experiments for each of the two adsorbates. The adsorbent dosage that produced the best adsorptive performance for both of the adsorbates is then selected as the dosage used for the binary adsorption experiments of the two adsorbates to follow. Furthermore, a rotary speed of 150 rpm and a temperature of 25°C are also preferred for most of the binary studies, as in the case of single-component systems.

Table 2-6: Binary batch adsorption studies performed in literature

Adsorbent	Adsorbent dosage (g.L ⁻¹)	pH	Rotary speed (rpm)	Adsorbate(s)	Concentration (ppm)	Reference
Coconut shell activated carbon	5.0 – 60	4 – 12	120	Phenol CN ⁻	100 – 1000 10 – 100	(Singh & Balomajumder, 2016)
Peanut shell activated carbon	2 – 40	6.2	300	Phenol Cd ²⁺	0 – 100	(Villar da Gama <i>et al.</i> , 2018)
Modified chitin	10	6	150	Co ²⁺	0 – 450	(Sellaoui <i>et al.</i> , 2017)
Fe/Zn doped biochar	1.0	6	150	Methylene blue p-nitrophenol Pb ²⁺	10 – 300 35 – 73	(Wang <i>et al.</i> , 2017)
Raw pumice stones	6.0	6	200	Ca ²⁺ Mg ²⁺	100	(Sepehr <i>et al.</i> , 2013)
Pumice stones activated carbon	6.0	6	200	Ca ²⁺ Mg ²⁺	100	(Sepehr <i>et al.</i> , 2013)
Dolochar	5.0	7	150	(PO ₄) ⁻³ (NO ₃) ⁻	16 65	(Rout <i>et al.</i> , 2016)
Fox nutshell activated carbon	0.4 – 5.0	7 – 11	150	Phenol Methylene blue	100 – 500	(Kumar & Jena, 2016)
Bagasse fly ash	10	6	150	Cd ²⁺ – Ni ²⁺	10 – 100	(Srivastava <i>et al.</i> , 2006)

2.20 Concluding remarks

Adsorption is the preferred wastewater treatment method due to its low operation and maintenance costs, low energy requirements, lower production of toxic sludge in the process, simple design and operation, as well as the economic regeneration of spent adsorbents. Adsorption, compared to other conventional wastewater treatment methods, also offers waste management solutions when waste products such as paper sludge can be used for the production of value-added products rather than being landfilled at additional disposal costs. Also, by utilising paper sludge for bio-purposes, the environmental footprint of a large industry such as the pulp and paper industry will be reduced on a large scale, as their waste can now be used to clean the wastewater produced during the paper manufacturing process. Proper treatment of the wastewater that is produced will reduce the amount of fresh water required for production processes, lifting the pressure on freshwater resources, thus resulting in drastically reduced volumes of wastewater being discharged to downstream receiving/discharging bodies. Also, by employing production processes such as HTL for biochar adsorbent production, economic solutions are developed not only to reduce paper sludge volumes, but also to produce an end-product with economic and commercial usage at a fraction of the energy and treatment costs as required by pyrolysis.

Since paper sludge-based biochar has been proven to have the potential to remove not only organic but also various inorganic pollutants, the usage of paper sludge-based biochar has the potential to replace current adsorbents used in tertiary treatment facilities.

To the best of the author's knowledge, limited studies are available on:

- The use of HTL produced paper sludge-based biochar as adsorbent;
- The use of paper sludge-based biochar as adsorbent for the removal of phenol from a synthetic solution;
- The use of paper sludge-based biochar as adsorbent for the removal of calcium from a synthetic solution;
- The use of paper sludge-based biochar as adsorbent for the binary adsorption of phenol and calcium from a synthetic wastewater solution;
- The use of paper sludge-based biochar as adsorbent for the binary adsorption of phenol and calcium from a real industrial wastewater stream produced by a South African paper mill.

REFERENCES

- Abbaszadeh, S., Alwi, S.R.W., Webb, C., Ghasemi, N. & Muhamad, I.I. 2016. Treatment of lead-contaminated water using activated carbon adsorbent from locally available papaya peel biowaste. *Journal of Cleaner Production*, 118:210-222.
- Abdelkreem, M. 2013. Adsorption of phenol from industrial wastewater using olive mill waste. *APCBEE Procedia*, 5:349-357.
- Abdelwahab, O. & Amin, N.K. 2013. Adsorption of phenol from aqueous solutions by *Luffa cylindrica* fibers: Kinetics, isotherm and thermodynamic studies. *Egyptian Journal of Aquatic Research*, 39:215-223.
- Ahmad, R., Upamali, A., Lim, J.E., Zhang, M., Bolan, N., Mohan, D., Vithanage, M., Lee, S.S. & Ok, Y.S. 2014. Biochar as a sorbent for contaminant management in soil and water: A review. *Chemosphere*, 99:19-33.
- Ahmed, J.K. & Ahmaruzzaman, M. 2016. A review on potential usage of industrial waste materials for binding heavy metal ions from aqueous solutions. *Journal of Water Process Engineering*, 10:39-47.
- Al-Malack, M.H. & Dauda, M. 2017. Competitive adsorption of cadmium and phenol on activated carbon produced from municipal sludge. *Journal of Environmental Chemical Engineering*, 5:2718-2729.
- Al-Momani, F., Touraud, E., Degorce-dumas, J.R., Roussy, J. & Thomas, O. 2002. Biodegradability enhancement of textile dyes and textile wastewater by VUV photolysis. *Journal of Photochemistry and Photobiology A: Chemistry*, 153:191-197.
- Ali, M. 2014. Removal of phenol from water different types of carbon – A comparative analysis. *APCBEE Procedia*, 10:136-141.
- Ali, M.E.M., Abd El-Aty, A.M., Badawy, M.I. & Ali, R.K. 2018. Removal of pharmaceutical pollutants from synthetic wastewater using chemically modified biomass of green alga *Scenedesmus obliquus*. *Ecotoxicology and Environmental Safety*, 151:144-152.
- Aman, T., Kazi, A.A., Sabri, M.U., Bano, Q., Ahmad, A., Usman, M. & Bano, Q. 2008. Potato peels as solid waste for the removal of heavy metal copper(II) from waste water/industrial effluent. *Colloids and Surfaces B: Biointerfaces*, 63:116-121.

Amat, A.M., Arques, A., Miranda, M.A. & López, F. 2005. Use of ozone and/or UV in the treatment of effluents from board paper industry. *Chemosphere*, 60:1111-1117.

Amerkhanova, S., Shlyapov, R. & Uali, A. 2017. The active carbons modified by industrial wastes in process of sorption concentration of toxic organic compounds and heavy metals ions. *Colloids and Surfaces A*, 532:36-40.

Amin, S. 2009. Review on biofuel oil and gas production processes from microalgae. *Energy Conversion and Management*, 50:1834-1840.

Asghar, M.N., Khan, S. & Mushtaq, S. 2008. Management of treated pulp and paper mill effluent to achieve zero discharge. *Journal of Environmental Management*, 88:1285-1299.

Ashrafi, O., Yerushalmi, L. & Haghighat, F. 2015. Wastewater treatment in the pulp-and-paper industry: A review of treatment processes and the associated greenhouse gas emission. *Journal of environmental management*, 158:146-157.

Bajpai, P. 2015. Environmental consequences of pulp and paper manufacture. (*In Green Chemistry and Sustainability in Pulp and Paper Industry*. Switzerland: Springer International Publishing. p. 41).

Barakat, M.A. 2011. New trends in removing heavy metals from industrial wastewater. *Arabian Journal of Chemistry*, 4:361-377.

Barreiro, D.L., Prins, W., Ronsse, F., Brilman, W., López Barreiro, D., Prins, W., Ronsse, F. & Brilman, W. 2013. Hydrothermal liquefaction (HTL) of microalgae for biofuel production: State of the art review and future prospects. *Biomass and Bioenergy*, 53:113-127.

Battaglia, A., Calace, N., Nardi, E., Petronio, B.M. & Pietroletti, M. 2003. Paper mill sludge-soil mixture: Kinetic and thermodynamic tests of cadmium and lead sorption capability. *Microchemical Journal*, 75(2):97-102.

Beker, U., Ganbold, B., Dertli, H., Gülbayir, D.D. & Duranog, D. 2010. Adsorption of phenol by activated carbon: Influence of activation methods and solution pH. *Energy Conversion and Management*, 51:235-240.

Bhatnagar, A. & Sillanpää, M. 2010. Utilization of agro-industrial and municipal waste materials as potential adsorbents for water treatment-A review. *Chemical Engineering Journal*, 157:277-296.

Bochenek, R., Sitarz, R. & Antos, D. 2011. Design of continuous ion exchange process for the wastewater treatment. *Chemical Engineering Science*, 66:6209-6219.

Bonilla-Petriciolet, A., Mendoza-Castillo, D.I. & Reynel-Ávila, H.E. 2017. Adsorption processes for water treatment and purification. Switzerland: Springer International Publishing.

Boudrahem, F., Aissani-Benissad, F. & Aït-Amar, H. 2009. Batch sorption dynamics and equilibrium for the removal of lead ions from aqueous phase using activated carbon developed from coffee residue activated with zinc chloride. *Journal of Environmental Management*, 90:3031-3039.

Brink, A. 2017. Combined biological and advance oxidation processes for paper and pulp effluent treatment. Johannesburg: University of the Witwatersrand. (Dissertation: MSc).

Burakov, A.E., Galunin, E.V., Burakova, I.V., Kucheroval, A.E., Agarwal, S., Tkachev, A.G. & Gupta, V.K. 2018. Adsorption of heavy metals on conventional and nanostructured materials for wastewater treatment purposes: A review. *Ecotoxicology and Environmental Safety*, 148:702-712.

Calace, N., Nardi, E., Petronio, B.M. & Pietroletti, M. 2002. Adsorption of phenols by papermill sludges. *Environmental Pollution*, 118(3):315-319.

Calisto, V., Ferreira, C.I.A., Santos, S.M., Gil, M.V., Otero, M. & Esteves, V.I. 2014. Production of adsorbents by pyrolysis of paper mill sludge and application on the removal of citalopram from water. *Bioresource Technology*, 166:335-344.

Cao, L., Zhang, C., Chen, H., Tsang, D.C.W., Luo, G., Zhang, S. & Chen, J. 2017. Hydrothermal liquefaction of agricultural and forestry wastes: state-of-the-art review and future prospects. *Bioresource Technology*, 245:1184-1193.

Carolin, C.F., Kumar, P.S., Saravanan, A., Joshiba, G.J. & Naushad, M. 2017. Efficient techniques for the removal of toxic heavy metals from aquatic environment: A review. *Journal of Environmental Chemical Engineering*, 5:2782-2799.

Chen, Q., Yao, Y., Li, X., Lu, J., Zhou, J. & Huang, Z. 2018. Comparison of heavy metal removals from aqueous solutions by chemical precipitation and characteristics of precipitates. *Journal of Water Process Engineering*, 26:289-300.

Coimbra, R.N., Calisto, V., Ferreira, C.I.A., Esteves, V.I. & Otero, M. 2015. Removal of pharmaceuticals from municipal wastewater by adsorption onto pyrolyzed pulp mill sludge. *Arabian Journal of Chemistry*, 12(8):3611-3620.

- De Caprariis, B., De Filippis, P., Petruccio, A. & Scarsella, M. 2017. Hydrothermal liquefaction of biomass: Influence of temperature and biomass composition on the bio-oil production. *Fuel*, 208:618-625.
- De Gisi, S., Lofrano, G., Grassi, M. & Notarnicola, M. 2016. Characteristics and adsorption capacities of low-cost sorbents for wastewater treatment: A review. *Sustainable Materials and Technologies*, 9:10-40.
- Devi, P. & Saroha, A.K. 2015. Simultaneous adsorption and dechlorination of pentachlorophenol from effluent by Ni-ZVI magnetic biochar composites synthesized from paper mill sludge. *Chemical Engineering Journal*, 271:195-203.
- Dimitriadis, A. & Bezergianni, S. 2017. Hydrothermal liquefaction of various biomass and waste feedstocks for biocrude production: A state of the art review. *Renewable and Sustainable Energy Reviews*, 68:113-125. Elsevier.
- Dursun, G., Çiçek, H., Dursun, A.Y. & Handan, C. 2005. Adsorption of phenol from aqueous solution by using carbonised beet pulp. *Journal of Hazardous Materials*, B125:175-182.
- El-Naas, M.H., Al-Zuhair, S. & Alhaija, M.A. 2010. Removal of phenol from petroleum refinery wastewater through adsorption on date-pit activated carbon. *Chemical Engineering Journal*, 162:997-1005.
- Elliott, D.C., Biller, P., Ross, A.B., Schmidt, A.J. & Jones, S.B. 2015. Hydrothermal liquefaction of biomass: Developments from batch to continuous process. *Bioresource Technology*, 178:147-156.
- ElShafei, G.M.S., ElSherbiny, I.M.A., Darwish, A.S. & Philip, C.A. 2017. Artichoke as a non-conventional precursor for activated carbon: Role of the activation process. *Journal of Taibah University for Science*, 11:677-688.
- Escrig, I. & Morell, I. 1998. Effect of calcium on the soil adsorption of cadmium and zinc in some Spanish sandy soils. *Water, Air, and Soil Pollution*, 105:507-520.
- Faubert, P., Barnabé, S., Bouchard, S., Côté, R. & Villeneuve, C. 2016. Pulp and paper mill sludge management practices: What are the challenges to assess the impacts on greenhouse gas emissions? *Resources, Conservation and Recycling*, 108:107-133.
- Ferreira, C.I.A., Calisto, V., Otero, M., Nadais, H. & Esteves, V.I. 2016. Comparative adsorption evaluation of biochars from paper mill sludge with commercial activated carbon for the removal

of fish anaesthetics from water in Recirculating Aquaculture Systems. *Aquacultural Engineering*, 74:76-83.

Fu, Y., Shen, Y., Zhang, Z., Ge, X. & Chen, M. 2019. Activated bio-chars derived from rice husk via one- and two-step KOH-catalyzed pyrolysis for phenol adsorption. *Science of the Total Environment*, 646:1567-1577.

Giraldo, L. & Moreno-piraján, J.C. 2014. Study of adsorption of phenol on activated carbons obtained from eggshells. *Journal of Analytical and Applied Pyrolysis*, 106:41-47.

Girish, C.R. & Murty, V.R. 2016. Mass transfer studies on adsorption of phenol from wastewater using Lantana camara, forest waste. *International Journal of Chemical Engineering*. 2016.

Girods, P., Dufour, A., Fierro, V., Rogaume, Y., Rogaume, C., Zoulalian, A. & Celzard, A. 2009. Activated carbons prepared from wood particleboard wastes: Characterisation and phenol adsorption capacities. *Journal of Hazardous Materials*, 166:491-501.

Goswami, L., Kumar, R.V., Narayan, S. & Manikandan, N.A. 2018. Membrane bioreactor and integrated membrane bioreactor systems for micropollutant removal from wastewater: A review. *Journal of Water Process Engineering*, 26:314-328.

Gunatilake, S.K. 2015. Methods of removing heavy metals from industrial wastewater. *Journal of Multidisciplinary Engineering Science Studies (JMESS)*, 1(1):12-18.

Hameed, B.H. & Rahman, A.A. 2008. Removal of phenol from aqueous solutions by adsorption onto activated carbon prepared from biomass material. *Journal of Hazardous Materials*, 160:576-581.

Hameed, B.H., Tan, I.A.W. & Ahmad, A.L. 2008. Adsorption isotherm, kinetic modelling and mechanism of 2,4,6-trichlorophenol on coconut husk-based activated carbon. *Chemical Engineering Journal*, 144:235-244.

Hojamberdiev, M., Kameshima, Y., Nakajima, A., Okada, K. & Kadirova, Z. 2008. Preparation and sorption properties of materials from paper sludge. *Journal of Hazardous Materials*, 151:710-719.

Hollabaugh, C.L. 2007. Modification of Goldschmidt's geochemical classification of the elements to include arsenic, mercury, and lead as biophile elements. (In Sarkar, D., Datta, R. & Hannigan, R. eds. Concepts and applications in environmental geochemistry. Amsterdam: Elsevier Ltd.).

- Hossain, M.A., Ngo, H.H., Guo, W.S., Nghiem, L.D., Hai, F.I., Vigneswaran, S. & Nguyen, T. V. 2014. Competitive adsorption of metals on cabbage waste from multi-metal solutions. *Bioresource Technology*, 160:79-88.
- Huuha, T.S., Kurniawan, T.A. & Sillanpää, M.E.T. 2010. Removal of silicon from pulping whitewater using integrated treatment of chemical precipitation and evaporation. *Chemical Engineering Journal*, 158:584-592.
- Ichiura, H., Nakatani, T., & Ohtani, Y. 2011. Separation of pulp and inorganic materials from paper sludge using ionic liquid and centrifugation. *Chemical Engineering Journal*, 173:129-134.
- Itodo, A., Abdulrahman, F., Hassan, L., Maigandi, S.A. & Itodo, H. 2010. Intraparticle diffusion and intraparticulate diffusivities of herbicide on derived activated carbon. *Researcher*, 2(2):74-86.
- Inyang, M. & Dickenson, E. 2015. The potential role of biochar in the removal of organic and microbial contaminants from potable and reuse water: A review. *Chemosphere*, 134:232-240.
- Inyang, M.I., Gao, B., Yao, Y., Xue, Y., Zimmerman, A., Mosa, A., Pullammanappallil, P., Ok, Y.S. & Cao, X. 2016. A review of biochar as a low-cost adsorbent for aqueous heavy metal removal. *Critical Reviews in Environmental Science and Technology*, 46(4):406-433.
- Jain, A., Balasubramanian, R. & Srinivasan, M.P. 2016. Hydrothermal conversion of biomass waste to activated carbon with high porosity: A review. *Chemical Engineering Journal*, 283:789-805.
- Jaria, G., Calisto, V., Gil, M.V., Otero, M. & Esteves, V.I. 2015. Removal of fluoxetine from water by adsorbent materials produced from paper mill sludge. *Journal of Colloid and Interface Science*, 448:32-40.
- Jaria, G., Calisto, V., Silva, C.P., Gil, M.V., Otero, M. & Esteves, V.I. 2019. Obtaining granular activated carbon from paper mill sludge – A challenge for application in the removal of pharmaceuticals from wastewater. *Science of the Total Environment*, 653:393-400.
- Jaria, G., Silva, C.P., Ferreira, C.I.A., Otero, M. & Calisto, V. 2017. Sludge from paper mill effluent treatment as raw material to produce carbon adsorbents: An alternative waste management strategy. *Journal of Environmental Management*, 188:203-211.
- Kamali, M. & Khodaparast, Z. 2015. Review on recent developments on pulp and paper mill wastewater treatment. *Ecotoxicology and Environmental Safety*, 114:326-342.

- Karakoyun, N., Kubilay, S., Aktas, N., Turhan, O., Kasimoglu, M., Yilmaz, S. & Sahiner, N. 2011. Hydrogel-Biochar composites for effective organic contaminant removal from aqueous media. *Desalination*, 280:319-325.
- Khalili, N.R., Campbell, M., Sandi, G. & Golaś, J. 2000. Production of micro- and mesoporous activated carbon from paper mill sludge. *Carbon*, 38:1905-1915.
- Khalili, N.R., Vyas, J.D., Weangkaew, W., Westfall, S.J., Parulekar, S.J. & Sherwood, R. 2002. Synthesis and characterization of activated carbon and bioactive adsorbent produced from paper mill sludge. *Separation and Purification Technology*, 26:295-304.
- Kilic, M., Apaydin-varol, E. & Pütün, E. 2011. Adsorptive removal of phenol from aqueous solutions on activated carbon prepared from tobacco residues: equilibrium, kinetics and thermodynamics. *Journal of Hazardous Materials*, 189:397-403.
- Kizinievič, O., Kizinievič, V. & Malaiškienė, J. 2018. Analysis of the effect of paper sludge on the properties, microstructure and frost resistance of clay bricks. *Construction and Building Materials*, 169:689-696.
- Kong, J., Gu, R., Yuan, J., Liu, W., Wu, J., & Fei, Z. 2018. Adsorption behavior of Ni(II) onto activated carbons from hide waste and high-pressure steaming hide waste. *Ecotoxicology and Environmental Safety*, 156:294-300.
- Kotzé, N., Johnston, S., Harper, C.L., Masters, G.M. & Maier, P. 2014. The impact of engineering on society. 2nd ed. Harlow: Pearson.
- Kumar, A. & Jena, H.M. 2016. Removal of methylene blue and phenol onto prepared activated carbon from Fox nutshell by chemical activation in batch and fixed-bed column. *Journal of Cleaner Production*, 137:1246-1259.
- Kumar, M., Olajire Oyedun, A. & Kumar, A. 2018. A review on the current status of various hydrothermal technologies on biomass feedstock. *Renewable and Sustainable Energy Reviews*, 81:1742-1770.
- Leng, L.J., Yuan, X.Z., Huang, H.J., Wang, H., Wu, Z. Bin, Fu, L.H., Peng, X., Chen, X.H. & Zeng, G.M. 2015. Characterization and application of bio-chars from liquefaction of microalgae, lignocellulosic biomass and sewage sludge. *Fuel Processing Technology*, 129:8-14.
- Li, H., Dong, X., Evandro, B., De Oliveira, L.M., Chen, Y., Ma, L.Q., Silva, E., Chen, Y. & Ma, L.Q. 2017. Mechanisms of metal sorption by biochars: biochar characteristics and modifications. *Chemosphere*, 178:466-478.

- Li, T., Guo, F., Li, X., Liu, Y., Peng, K., Jiang, X. & Guo, C. 2018. Characterization of herb residue and high ash-containing paper sludge blends from fixed bed pyrolysis. *Waste Management*, 76:544-554.
- Likon, M., Trebše, P. 2012. Recent advances in paper mill sludge management. (*In* Industrial Waste. Slovenia: Intechopen. p. 73-74). <https://www.intechopen.com/books/industrial-waste/papermill-sludge-as-valuable-raw-material> Date of access: 24 Jan. 2019.
- Lin, S.H. & Juang, R.S. 2009. Adsorption of phenol and its derivatives from water using synthetic resins and low-cost natural adsorbents: A review. *Journal of Environmental Management*, 90:1336-1349.
- Liu, Q., Zheng, T., Wang, P., Jiang, J. & Li, N. 2010a. Adsorption isotherm, kinetic and mechanism studies of some substituted phenols on activated carbon fibers. *Chemical Engineering Journal*, 157:348-356.
- Liu, W.J., Zeng, F.X., Jiang, H. & Zhang, X.S. 2011. Preparation of high adsorption capacity biochars from waste biomass. *Bioresource Technology*, 102:8247-8252.
- Liu, Z. & Zhang, F.S. 2009. Removal of lead from water using biochars prepared from hydrothermal liquefaction of biomass. *Journal of Hazardous Materials*, 167:933-939.
- Liu, Z., Zhang, F.S. & Wu, J. 2010b. Characterization and application of chars produced from pinewood pyrolysis and hydrothermal treatment. *Fuel*, 89:510-514.
- Mahdi, Z., Yu, Q.J. & El Hanandeh, A. 2018. Investigation of the kinetics and mechanisms of nickel and copper ions adsorption from aqueous solutions by date seed derived biochar. *Journal of Environmental Chemical Engineering*, 6(1):1171-1181.
- Mäkelä, M., Forsberg, J., Söderberg, C., Larsson, S.H. & Dahl, O. 2018. Process water properties from hydrothermal carbonization of chemical sludge from a pulp and board mill. *Bioresource Technology*, 263:654-659.
- Manahan, S.E. 2000. Water treatment. 7th ed. Environmental chemistry. Lewis publishers: New York. New York: Lewis publishers.
- Mcdougall, G. 1991. The physical nature and manufacture of activated carbon. *Journal of the South African institute of mining and metallurgy*, 91(4):109-120.
- Méndez, A., Barriga, S., Fidalgo, J.M. & Gascó, G. 2009. Adsorbent materials from paper industry waste materials and their use in Cu(II) removal from water. *Journal of Hazardous Materials*, 165:736-743.

- Miao, Q., Tang, Y., Xu, J., Liu, X., Xiao, L. & Chen, Q. 2013. Activated carbon prepared from soybean straw for phenol adsorption. *Journal of the Taiwan Institute of Chemical Engineers*, 44:458-465.
- Möbius, C.H. 2006. Water use and wastewater treatment in papermills. Norderstedt: Books on Demand GmbH.
- Mohammed, N.A.S., Abu-zurayk, R.A., Hamadneh, I. & Al-Dujaili, A.H. 2018. Phenol adsorption on biochar prepared from the pine fruit shells: equilibrium, kinetic and thermodynamics studies. *Journal of Environmental Management*, 226:377-385.
- Mohan, D., Sarswat, A., Ok, Y.S. & Pittman, C.U. 2014. Organic and inorganic contaminants removal from water with biochar, a renewable, low cost and sustainable adsorbent – A critical review. *Bioresource technology*, 160:191-202.
- Mohan, D. & Singh, K.P. 2002. Single- and multi-component adsorption of cadmium and zinc using activated carbon derived from bagasse – an agricultural waste. *Water Research*, 36:2304-2318.
- Mongkhonsiri, G., Gani, R., Malakul, P. & Assabumrungrat, A. 2018. Integration of the biorefinery concept for the development of sustainable processes for pulp and paper industry. *Computers and Chemical Engineering*, 119:70-84.
- Mukherjee, A., Zimmerman, A.R. & Harris, W. 2011. Surface chemistry variations among a series of laboratory-produced biochars. *Geoderma*, 163:247-255.
- Okolo, G.N., Everson, R.C., Neomagus, H.W.J.P.J.P., Roberts, M.J., Sakurovs, R. & Okolo, G.N. 2014. Comparing the porosity and surface areas of coal as measured by gas adsorption, mercury intrusion and SAXS techniques. *Fuel*, 141:293-304.
- Oliveira, G., Calisto, V., Santos, S.M., Otero, M., & Esteves, V.I. 2018. Paper pulp-based adsorbents for the removal of pharmaceuticals from wastewater: A novel approach towards diversification. *Science of the Total Environment*, 631-632:1018-1028.
- Ooi, C.H., Ling, Y.P., Pung, S.Y. & Yeoh, F.Y. 2019. Mesoporous hydroxyapatite derived from surfactant-templating system for p-Cresol adsorption: Physicochemical properties, formation process and adsorption performance. *Powder Technology*, 342:725-734.
- Padilla-Ortega, E., Leyva-Ramos, R. & Flores-Cano, J.V. 2013. Binary adsorption of heavy metals from aqueous solution onto natural clays. *Chemical Engineering Journal*, 225:536-546.

- Pintar, A., Batista, J. & Levec, J. 2001. Integrated ion exchange/catalytic process for efficient removal of nitrates from drinking water. *Chemical Engineering Science*, 56:1551-1559.
- Pokhrel, D. & Viraraghavan, T. 2004. Treatment of pulp and paper mill wastewater – A review. *Science of the Total Environment*, 333(1–3):37-58.
- Polat, H., Molva, M. & Polat, M. 2006. Capacity and mechanism of phenol adsorption on lignite. *International Journal of Mineral Processing*, 79:264-273.
- Purnomo, C.W., Salim, C. & Hinode, H. 2012. Effect of the activation method on the properties and adsorption behavior of bagasse fly ash-based activated carbon. *Fuel Processing Technology*, 102:132-139.
- Raj, A., Reddy, M.K. & Chandra, R. 2007. Decolourisation and treatment of pulp and paper mill effluent by lignin-degrading *Bacillus* sp. *Journal of Chemical Technology and Biotechnology*, 82:399-406.
- Rathore, V.K., Dohare, D.K. & Mondal, P. 2016. Competitive adsorption between arsenic and fluoride from binary mixture on chemically treated laterite. *Journal of Environmental Chemical Engineering*, 4:2417-2430.
- Reguyala, F., Sarmaha, A.K. & Gao, W. 2017. Synthesis of magnetic biochar from pine sawdust via oxidative hydrolysis of FeCl_2 for the removal sulfamethoxazole from aqueous solution. *Journal of Hazardous Materials*, 321:868-878.
- Rengaraj, S., Moon, S.H., Sivabalan, R., Arabindoo, B. & Murugesan, V. 2002. Agricultural solid waste for the removal of organics: Adsorption of phenol from water and wastewater by palm seed coat activated carbon. *Waste Management*, 22:543-548.
- Rosales, E., Meijide, J., Pazos, M. & Sanromán, M.A. 2017. Challenges and recent advances in biochar as low-cost biosorbent: From batch essays to continuous-flow systems. *Bioresource Technology*, 246:176-192.
- Rosman, N., Salleh, W.N.W., Azuwa, M., Jaafar, J., Ismail, A.F. & Harun, Z. 2018. Hybrid membrane filtration-advanced oxidation processes for removal of pharmaceutical residue. *Journal of Colloid and Interface Science*, 532:236-260.
- Rout, P.R., Dash, R.R. & Bhunia, P. 2016. Nutrient removal from binary aqueous phase by dolochar: Highlighting optimization, single and binary adsorption isotherms and nutrient release. *Process Safety and Environmental Protection*, 100:91-107.

- Sahu, O., Rao, D.G., Gabbiye, N., Engidayehu, A. & Teshale, F. 2017. Sorption of phenol from synthetic aqueous solution by activated saw dust: Optimizing parameters with response surface methodology. *Biochemistry and Biophysics Reports*, 12:46-53.
- Scott, G.M. 1995. Sludge characteristics and disposal alternatives for the pulp and paper industry. International Environmental Conference. TAPPI Press: Atlanta. TAPPI Press: Atlanta, pp. 269-279.
- Sellaoui, L., Franco, D.S.P., Dotto, G.L., Lima, É.C. & Lamine, A. Ben. 2017. Single and binary adsorption of cobalt and methylene blue on modified chitin: Application of the Hill and exclusive extended Hill models. *Journal of Molecular Liquids*, 233:543-550.
- Şentorun-Shalaby, Ç., Uçak-Astarlioğlu, M.G., Artok, L. & Sarici, Ç. 2006. Preparation and characterization of activated carbons by one-step steam pyrolysis/activation from apricot stones. *Microporous and Mesoporous Materials*, 88:126-134.
- Sepehr, M., Mansur, Z., Hossein, K., Abdeltif, A., Kamiar, Y., Hamid, R.G., Sepehr, M., Mansur, Z., Hossein, K., Abdeltif, A., Kamiar, Y. & Hamid, R.G. 2013. Removal of hardness agents, calcium and magnesium, by natural and alkaline modified pumice stones in single and binary systems. *Applied surface science*, 274:295-305.
- Singh, N. & Balomajumder, C. 2016. Simultaneous removal of phenol and cyanide from aqueous solution by adsorption onto surface modified activated carbon prepared from coconut shell. *Journal of Water Process Engineering*, 9:233-245.
- Singh, S.K., Townsend, T.G., Mazyck, D. & Boyer, T.H. 2012. Equilibrium and intra-particle diffusion of stabilized landfill leachate onto micro- and meso-porous activated carbon. *Water Research*, 46:491-499.
- Son, E.B., Poo, K.M., Chang, J.S. & Chae, K.J. 2018. Heavy metal removal from aqueous solutions using engineered magnetic biochars derived from waste marine macro-algal biomass. *Science of the Total Environment*, 615:161-168.
- Soto, M.L., Moure, A., Domínguez, H. & Parajó, J.C. 2011. Recovery, concentration and purification of phenolic compounds by adsorption: A review. *Journal of Food Engineering*, 105:1-27.
- Srivastava, V.C., Mall, I.D. & Mishra, I.M. 2006. Equilibrium modelling of single and binary adsorption of cadmium and nickel onto bagasse fly ash. *Chemical Engineering Journal*, 117:79-91.

- Tan, X., Liu, Y., Zeng, G., Wang, X., Hu, X., Gu, Y. & Yang, Z. 2015. Application of biochar for the removal of pollutants from aqueous solutions. *Chemosphere*, 125:70-85.
- Terzyk, A.P. 2003. Further insights into the role of carbon surface functionalities in the mechanism of phenol adsorption. *Journal of Colloid and Interface Science*, 268:301-329.
- Toczyłowska-Mamińska, R. 2017. Limits and perspectives of pulp and paper industry wastewater treatment – A review. *Renewable and Sustainable Energy Reviews*, 78:764-772.
- Tran, H.N., You, S.J., Hosseini-Bandegharai, A. & Chao, H.P. 2017. Mistakes and inconsistencies regarding adsorption of contaminants from aqueous solutions: A critical review. *Water Research*, 120:88-116.
- Tsibranska, I. & Hristova, E. 2011. Comparison of different kinetic models for adsorption of heavy metals onto activated carbon from apricot stones. *Bulgarian Chemical Communications*, 43(3):370-377.
- Tuhkanen, T., Naukkarinen, M., Blackburn, S. & Tanskanen, H. 1997. Ozonation of pulp mill effluent prior to activated sludge treatment. *Environmental Technology*, 18:1045-1051.
- Villar da Gama, B.M., Elisandra do Nascimento, G., Silva Sales, D.C., Rodríguez-Díaz, J.M., Bezerra de Menezes Barbosa, C.M. & Menezes Bezerra Duarte, M.M. 2018. Mono and binary component adsorption of phenol and cadmium using adsorbent derived from peanut shells. *Journal of Cleaner Production*, 201:219-228.
- Wajima, T. 2017. A new carbonaceous adsorbent for heavy metal removal from aqueous solution prepared from paper sludge by sulfur-impregnation and pyrolysis. *Process Safety and Environmental Protection*, 112:342-352.
- Wang, P., Tang, L., Wei, X., Zeng, G., Zhou, Y., Deng, Y., Wang, J., Xie, Z. & Fang, W. 2017. Synthesis and application of iron and zinc doped biochar for removal of p-nitrophenol in wastewater and assessment of the influence of co-existed Pb(II). *Applied Surface Science*, 392:391-401.
- Wang, Q., Wang, B., Lee, X., Lehmann, J. & Gao, B. 2018. Sorption and desorption of Pb(II) to biochar as affected by oxidation and pH. *Science of The Total Environment*, 634:188-194.
- Wong, H.S., Barakat, R., Alhilali, A., Saleh, M. & Cheeseman, C.R. 2015. Hydrophobic concrete using waste paper sludge ash. *Cement and Concrete Research*, 70:9-20.

- Wong, S., Ngadi, N., Inuwa, I.M. & Hassan, O. 2018. Recent advances in applications of activated carbon from biowaste for wastewater treatment: A short review. *Journal of Cleaner Production*, 175:361-375.
- Wu, T., Cai, X., Tan, S., Li, H., Liu, J. & Yang, W. 2011. Adsorption characteristics of acrylonitrile, p-toluenesulfonic acid, 1-naphthalenesulfonic acid and methyl blue on graphene in aqueous solutions. *Chemical Engineering Journal*, 173:144-149.
- Xing, X., Jiang, W., Li, S., Zhang, X. & Wang, W. 2019. Preparation and analysis of straw activated carbon synergetic catalyzed by $\text{ZnCl}_2\text{-H}_3\text{PO}_4$ through hydrothermal carbonization combined with ultrasonic assisted immersion pyrolysis. *Waste Management*, 89:64-72.
- Yang, X., Choi, H.S., Park, C. & Kim, S.W. 2015. Current states and prospects of organic waste utilization for biorefineries. *Renewable and Sustainable Energy Reviews*, 49:335-349.
- Yang, Y., Wei, Z., Zhang, X., Chen, X., Yue, D., Yin, Q., Xiao, L. & Yang, L. 2014. Biochar from *Alternanthera philoxeroides* could remove Pb(II) efficiently. *Bioresource Technology*, 171:227-232.
- Yoon, K., Cho, D.W., Tsang, D.C.W.W., Bolan, N., Rinklebe, J. & Song, H. 2017. Fabrication of engineered biochar from paper mill sludge and its application into removal of arsenic and cadmium in acidic water. *Bioresource Technology*, 246:69-75.
- Yorgun, S. & Yıldız, D. 2015. Preparation and characterization of activated carbons from Paulownia wood by chemical activation with H_3PO_4 . *Journal of the Taiwan Institute of Chemical Engineers*, 53:122-131.
- Zhang, D., Huo, P. & Liu, W. 2015. Behavior of phenol adsorption on thermal modified activated carbon. *Chinese Journal of Chemical Engineering*, 24:446-452.
- Zhang, L., Champagne, P. & Xu, C.C. 2011. Bio-crude production from secondary pulp/paper-mill sludge and waste newspaper via co-liquefaction in hot-compressed water. *Energy*, 36(4):2142-2150.
- Zhou, N., Chen, H., Xi, J., Yao, D., Zhou, Z., Tian, Y. & Lu, X. 2017a. Biochars with excellent Pb(II) adsorption property produced from fresh and dehydrated banana peels via hydrothermal carbonization. *Bioresource Technology*, 232:204-210.
- Zhou, Y., Liu, X., Xiang, Y., Wang, P., Zhang, J., Zhang, F., Wei, J., Luo, L., Lei, M. & Tang, L. 2017b. Modification of biochar derived from sawdust and its application in removal of tetracycline

and copper from aqueous solution: adsorption mechanism and modelling. *Bioresource Technology*, 245:266-273.

CHAPTER 3 – RESEARCH METHODOLOGY

The purpose of this chapter is to explain the materials and experimental pathways selected for the HTL and adsorption experiments in order to achieve the set objectives. The chapter also reports on all the analyses done on the industrial wastewater, paper sludge, biochar and activated carbon samples, as well as the analytical methods used in order to determine the phenol and calcium concentrations after the adsorption experiments.

3.1 Materials

3.1.1 Paper mill materials

Paper sludge, as shown in Figure 3-1, was collected from Mpact's Springs mill situated in South Africa. The mill mainly utilises re-pulped, recycled fibres as feedstock. The collected paper sludge corresponds to the primary sludge produced after the primary treatment and dewatering activities.



Figure 3-1: The paper sludge as collected on-site

Industrial wastewater was also collected from the paper mill in order to evaluate the performance of the biochar compared with that of activated carbon (powered) in a real industrial wastewater medium. The activated carbon was purchased from Associated Chemical Enterprises (ACE), South Africa. The wastewater collected from the mill corresponds to the effluent after primary treatment steps were employed. The mill recirculates approximately 78% of the treated

wastewater, whereas the rest is discharged into municipality resources. Both the paper sludge and industrial wastewater were stored in a refrigerator at 4°C after collection.

3.1.2 Chemicals

The chemicals required for the biochar production and batch adsorption experiments are summarised in Table 3-1.

Table 3-1: Chemicals required for biochar production and adsorption experiments

Chemical name	Purity (%)	Supplier	Purpose
Acetone ($(\text{CH}_3)_2\text{CO}$)	99.50	Rochelle Chemicals	Cleaning of all the equipment used
Deionised, ultra-pure water (conductivity of $0.055 \mu\text{S}\cdot\text{cm}^{-1}$)	-	SG – Labostar ultra-pure water and reverse osmosis system	Cleaning of all the equipment used and preparation of all solutions
Nitrogen gas	UHP	Afrox	Inert gas used for the HTL experiments
Dichloromethane (DCM) (CH_2Cl_2)	99	ACE	Extractive solvent used to remove the bio-oil and aqueous phase from the biochar
Potassium bromide (KBr)	≥ 99	Sigma-Aldrich	Used as blank sample for FTIR analysis
Calcium nitrate tetrahydrate ($\text{Ca}(\text{NO}_3)_2 \cdot 4\text{H}_2\text{O}$)	98	ACE	Preparation of synthetic calcium stock solution
Phenol crystals ($\text{C}_6\text{H}_5\text{OH}$)	99.90	ACE	Preparation of synthetic phenol stock solution
Nitric acid (HNO_3)	70	ACE	Used for the ICP-OES mobile phase and inorganic adsorption sample preparation
Formic acid (CH_2O_2)	99.90	ACE	Used for the HPLC mobile phase and organic adsorption sample preparation
Acetonitrile (CH_3CN)	99.90	E-Lab Direct Limited	Used for the HPLC mobile phase
pH buffer solutions (pH 4 and pH 7)	-	ACE	Calibration of the pH meter
Sodium hydroxide (NaOH)	98.00	ACE	Used for pH modification of the adsorption solutions (alkaline)
Hydrochloric acid (0.1 M HCl)	-	ACE	Used for pH modification of the adsorption solutions (acidic)

3.2 Biochar preparation from paper sludge

The biochar used in this study was produced in different batches to ensure that enough biochar was available as required for the adsorption studies to follow.

3.2.1 Experimental setup

Batch hydrothermal liquefaction experiments were performed in an SS316 autoclave with a working volume of 945 ml, equipped with heating mantels, as shown in Figure 3-2.

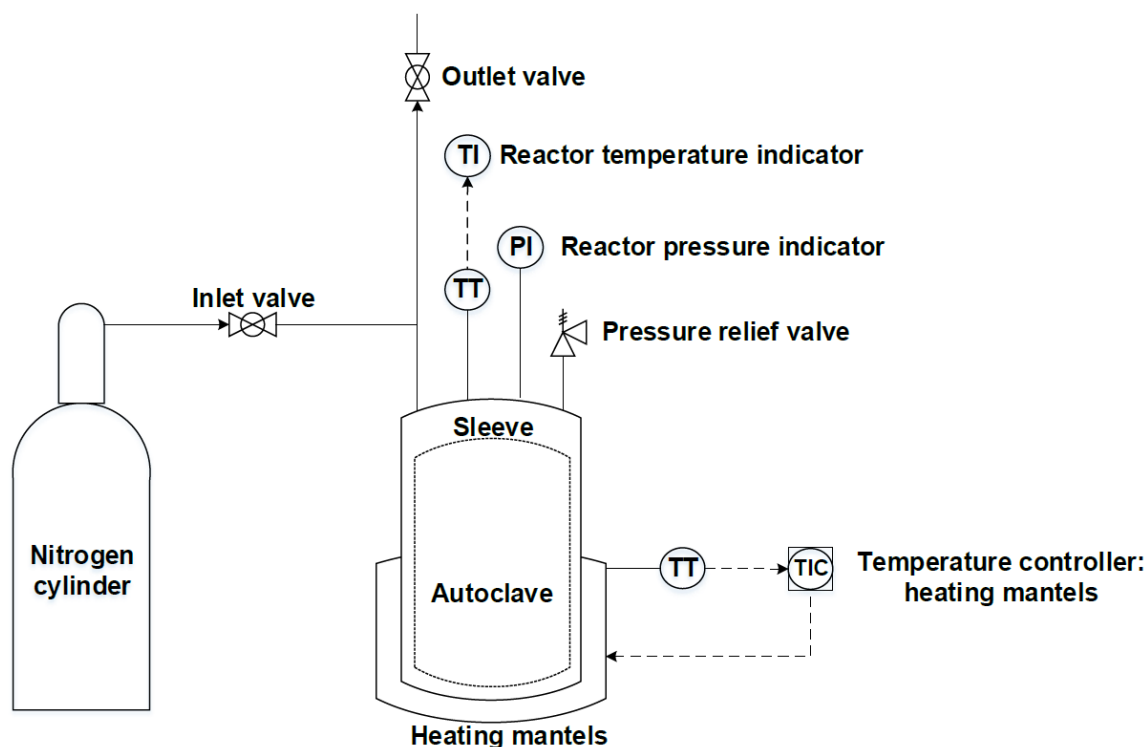


Figure 3-2: Schematic representation of the batch HTL reactor experimental setup

The autoclave was filled with approximately 200 g of paper sludge by filling the removable stainless steel reactor sleeve. No additional water was added to the reactor, as the paper sludge already contained sufficient water for the HTL reactions to proceed. The autoclave was pressurised to an initial pressure of 0.50 MPa at room temperature. The reaction was carried out at a temperature of 300°C with a residence time of 15 minutes. The average heating rate for the experiments were 3.42°C.min⁻¹. The heating rate could not be controlled.

3.2.2 Experimental procedure

Various steps were required for the start-up, operation and shutdown of the autoclave. The HTL process was performed according to the standard operating procedure for the specific autoclave used, as given in Appendix A.

3.2.2.1 Autoclave start-up

Before the start of each experimental run, the autoclave and corresponding equipment (steel feedstock cups, copper seal, etc.) were thoroughly cleaned with acetone and, where applicable,

left to dry in an oven at 60°C to ensure that all the acetone has evaporated. The required glassware was firstly washed with soap and water, rinsed with acetone and lastly rinsed three times with deionised water and left to dry in a Series 2000 Scientific oven at 60°C.

A clean steel cup was removed from the oven and left to cool for a few minutes. The cooled empty reactor sleeve was weighed, the mass was recorded and the scale was zeroed. The paper sludge container was then removed from the fridge and approximately 200 g of paper sludge was added to the steel reactor sleeve. The mass was once again recorded. The filled reactor sleeve was then inserted into the bottom half of the autoclave, as shown in Figure 3-3. Once secured, the top half (fitted with a copper seal) was carefully fitted onto the bottom half, ensuring that the holes of the top and bottom half align.



Figure 3-3: Paper sludge loaded into the autoclave

Once aligned, one bolt at a time was lubricated with copper slip, inserted in a criss-cross pattern into the flange of the autoclave, and lightly tightened by hand. Once all twelve M10 Allen cap bolts have been inserted, the bolts were then torqued 40 N.m, 60 N.m and finally 70 N.m with an appropriate torque wrench. A random point check was done after the torqueing has been completed for safety purposes.

After the point check, the inlet gas supply tube was attached to the corresponding reactor inlet and the fixture was tightened. The inlet valve of the gas supply was closed as well as the outlet valve fitted onto the reactor. The fume hood was switched on. The regulator fitted onto the nitrogen cylinder was closed before the cylinder was opened. Once closed, the nitrogen cylinder was opened. The regulator was opened to 5 MPa.

Once the nitrogen gas supply was available, the inlet valve to the reactor was opened. The reactor was pressurised to 5 MPa and the inlet valve was once again closed. A leak check was then performed by applying soap water to all the fittings of the reactor as well as around the flange, where the copper seal was fitted. If no bubbles were produced and there was no pressure loss inside the reactor, the leak check was considered successful. The outlet valve was then opened and the reactor was depressurised. The reactor was pressurised three times thereafter to remove any residual oxygen from the reactor. After the third time, the reactor was finally pressurised to the starting pressure of the experiment. The nitrogen cylinder was then closed and the gas supply line was purged.

3.2.2.2 Autoclave operation

Once the reactor has been pressurised to the desired starting pressure, the two heating mantels were fitted into position, located around the autoclave body. Three K-type thermocouples in total were used throughout the process. The first thermocouple, measuring the temperature inside the reactor, was plugged into its corresponding temperature indicator equipment. The other two thermocouples, measuring the temperature of each of the heating mantels, were plugged into their corresponding temperature controller.

The temperature of the heating mantels was firstly set to 100°C and once the temperature was reached, the setpoint temperature of each heating mantle was then increased in 50°C – 100°C intervals until the maximum allowable temperature of 550°C was reached. The temperature and pressure were recorded every five minutes until the desired temperature inside the reactor was reached. Once a temperature of 300°C was reached inside the reactor, the timer was started and the temperature and pressure were recorded until the reaction was completed. The reaction was allowed to continue for the specified residence time. The heating mantels was switched off to stop the reactor temperature of overshooting. Further heating of the reactor was due to the residual heat still available.

Once the reaction has been completed, the heating mantels were immediately removed from the reactor and placed away from the reactor to ensure effective cooling of the reactor could take place. Various electric fans were placed around the reactor and left until the reactor cooled down to a temperature of approximately 40°C.

3.2.2.3 Autoclave shutdown

Once the reactor had cooled down, the outlet valve was opened very slowly in order to depressurise the reactor to atmospheric pressure. Once the reactor had been depressurised, the bolts were loosened in a criss-cross manner. The fitting of the inlet gas supply was also loosened. All the sensors were unplugged, and the top half of the reactor was removed and placed aside.

The reactor sleeve with the product mixture was then carefully removed from the reactor and immediately weighed and the mass recorded. The product mixture was a combination of biochar, bio-oil and an aqueous phase, as shown in Figure 3-4.



Figure 3-4: Reactor product mixture after cool down

3.2.2.4 Bio-oil and aqueous phase removal

The contents of the reactor sleeve were emptied onto the filter paper of a Buchner funnel, as shown in Figure 3-5, attached to a conical flask and corresponding B&W vacuum pump.



Figure 3-5: Reactor product mixture before filtration

The reactor product mixture was washed several times with DCM in order to remove the bio-oil and aqueous phases trapped between the biochar particles.

3.2.2.5 Biochar drying

The Buchner funnel with washed biochar was then placed into a Series 2000 Scientific oven and allowed to dry for 2 – 3 hours at 60°C in order to evaporate any residual DCM. Once the biochar had dried, the Buchner funnel with the dried biochar was weighed again, and the mass was recorded. The difference between the empty Buchner funnel with filter paper and the Buchner funnel-biochar combination was the mass of biochar produced for the run. The yield of the biochar produced could then be calculated. The final biochar produced is shown in Figure 3-6.



Figure 3-6: Biochar after drying

3.2.3 Washing of the biochar

To ensure that the all loose ash components (metal oxides) had been removed from the biochar, the biochar was thoroughly washed with deionised water. The total mass of biochar was divided between four flasks, each containing a magnetic stirrer, placed onto separate magnetic stirrer plates. The flasks were filled with deionised water until the magnetic stirrer could effectively stir the biochar-water mixture. The flasks were then covered with parafilm to ensure that no foreign matter could contaminate the biochar-water mixtures. The biochar-water mixtures were left to mix for 24 hours consecutively to ensure for effective ash removal. After 24 hours, the biochar-water mixtures were subjected to vacuum filtration with deionised water in order to remove the concentrated ash water from the biochar. The newly washed biochar was once again dried for 24 hours to ensure that all the water used in the washing process has been evaporated.

3.2.4 Homogeneous sample preparation

The biochar used for the adsorption experiments were produced on different days in different batches. Therefore, it is possible that the biochar from each batch may differ from one to another. Homogenous sample preparation was therefore employed to ensure that the biochar, used for

the adsorption experiments, would not deviate from one experiment to another. All the dried biochar was added to the hopper of an SMC rotary sample splitter, as shown in Figure 3-7.

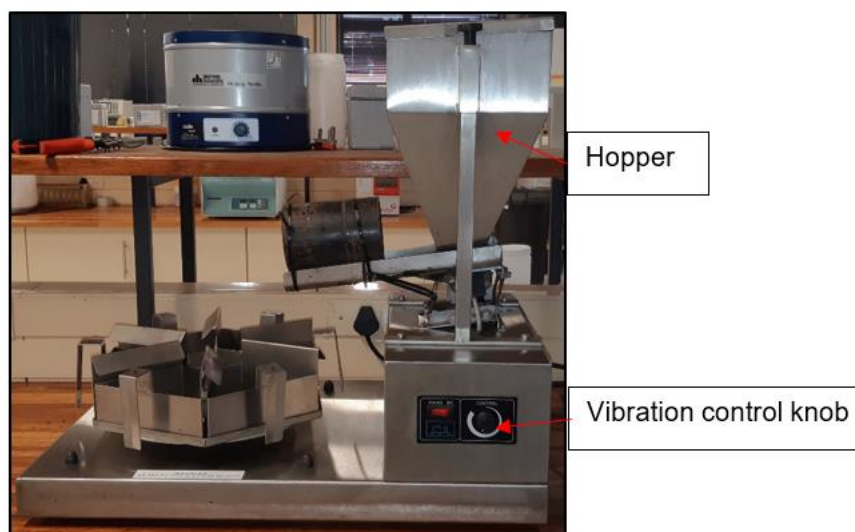


Figure 3-7: Sample splitter

The splitter was switched on and the vibration control knob was turned to a moderate setting. The biochar splitting process continued for approximately two hours, in order to split the combined mass of biochar produced. The homogenous biochar samples were then thrown into different plastic containers and crushed with a mortar and pestle until a fine powder was produced. The powdery biochar was then dried in an oven for 2 – 3 hours at 105°C. The dried biochar was stored in a desiccator before, during and after the adsorption experiments. The biochar was further denoted as paper sludge-based biochar.

3.3 Physicochemical characterisation of paper sludge, paper sludge-based biochar and activated carbon

Physicochemical analyses were performed on the paper sludge, biochar (paper sludge-based) and activated carbon samples. Chemical characterisation was done using elemental analysis, Fourier-transform infrared spectroscopy (FTIR) analysis, proximate analysis, X-ray powder diffraction (XRD) analysis and X-ray fluorescence (XRF) analysis. The point of zero charge for each adsorbent was also determined. Fibre analysis was only performed on the paper sludge. Physical characterisation was done by performing Brunauer-Emmett-Teller (BET) and scanning electron microscope (SEM) analysis. Also, the average particle size of the biochar was determined for the diffusion studies to follow.

3.3.1 Elemental analysis

The elemental composition of each sample was determined based on the ISO 12902 – CHN instrumental method. The oxygen content was calculated by difference. Sample preparation was done according to ISO 13909-4: 2001.

3.3.2 Proximate analysis

Proximate analysis was performed according to SANS 17246:2011 in conjunction with SANS 589 and SANS 50 in order to determine the moisture content and volatile matter. The ash content was determined by placing the crucible into a Lenton muffle furnace at 900°C and only removing the samples after 18 hours or when constant mass was achieved.

3.3.3 Brunauer-Emmett-Teller (BET) analysis

The surface area and porosity properties of the biochar and activated carbon were determined by physical adsorption of carbon dioxide at 0°C and nitrogen at -196°C with a Micromeritics ASAP 2020 surface area and porosity analyser. Approximately 0.50 g of each sample was firstly dried at 105°C for three hours to ensure that the moisture could not influence the analysis. The samples were removed from the oven after three hours and a carefully weighed mass of each sample was transferred to a ball glass tube. Then the sample tube was closed with a plug. All the samples were degassed for at least twelve hours before BET analysis. The resulting adsorption data produced was automatically processed by the ASAP 2020 v4.0 software. Furthermore, the microporous surface area was calculated by the Dubinin-Raduchkevich equation, the mesoporous surface area was calculated by the Brunauer-Emmett-Teller equation, whereas the average micropore diameter was calculated by the Horvath-Kawazoe equation and the mesopore diameter by the Barrett-Joyner-Halenda (BJH) method, as suggested by Okolo *et al.* (2015).

3.3.4 Fibre analysis

In addition, fibre analysis was also performed on the paper sludge in order to determine its hemicellulose, cellulose and lignin content. The fibre analysis was done according to the Van Soest method (Van Soest, 1963). The protein content was determined according to ASM 078 and the fat content according to ASM 044.

3.3.5 Scanning electron microscope (SEM) analysis

The surface morphology of the paper sludge was studied by a Phenom Prox benchtop scanning electron microscope equipped with an energy dispersive X-ray (EDX) detector. The surface morphology of the activated carbon and biochar samples were analysed by a Quanta FEG 250

Fei Scanning Electron Microscope. The samples prepared for both SEM analysers were placed on a carbon background to ensure that the sample would not get charged too much. The samples used for the Quanta FEG 250 Fei SEM were however plated with a platinum gold layer to further reduce the effect of the surface getting too charged. In addition, EDX analysis was also done on the samples with the Phenom Prox benchtop SEM.

3.3.6 X-ray powder diffraction (XRD)

The crystallinity of the biochar was analysed with an X'Pert Pro XRD with a Co tube. The phases were identified using X'Pert HighScore Plus software, PAN ICSD and an ICDD database. Sample preparation entailed sieving enough sample through a stainless steel 75 μm sieve and weighing off approximately 5 g required for the XRD analysis.

3.3.7 X-ray fluorescence (XRF)

The major elemental composition of the biochar, XRF, was determined using WROXI standards and an Axios Max. Sample preparation entailed sieving enough sample through a stainless steel 75 μm sieve and weighing-off approximately 20 g – 30 g required for the XRF analysis.

3.3.8 Fourier-transform infrared spectroscopy (FTIR)

The functional groups present in each sample were determined by using an IRAffinity 1 Fourier transform infrared spectrophotometer supplied by Shimadzu. The FTIR spectrums were determined at wavelengths in the range of 400 cm^{-1} to 4000 cm^{-1} with a resolution of 4 cm^{-1} and 45 scans per sample. The samples were prepared by mixing 1% sample with 99% potassium bromide (KBr) and then crushing the mixture to a fine powder by using a pestle and mortar.

3.3.9 Point of zero charge

The point of zero charge for each adsorbent was determined by preparing eight solutions of deionised water with initial pH values ranging from 3 to 9. The pH of each solution was adjusted with either a 0.1 M HCl or 0.1 M NaOH solution. Approximately 1.2 g of each adsorbent was added to each solution and shaken constantly at 150 rpm in a Labcon platform incubator shaker at $25^\circ\text{C} \pm 2^\circ\text{C}$. The final pH of each solution was measured after 24 hours. The point of zero charge was determined by plotting the $\text{pH}_f - \text{pH}_i$ versus pH_i and obtaining the value where the curve crossed the x-axis.

3.3.10 Particle size diameter

The average biochar particle size was determined by a Hydro 2000 MU Malvern Mastersizer.

3.4 Wastewater characterisation

The collected wastewater was characterised by measuring the pH, conductivity and COD, BOD₅, TDS, TSS, total calcium and total phenolic content of the wastewater. The COD concentration was determined by using a Macherey-Nagel 100 – 1500 ppm COD test kit (code: 985029). The total phenol concentration was determined by using a Merck 0.002 – 5 ppm phenol test kit (code: 100856). A Macherey-Nagel PF-12 photometer was used to determine the final concentrations. BOD₅ analysis was outsourced and performed according to the W044-43-W reference method. The TSS and TDS concentrations were determined according to SANS 6049:2010 and SANS 5213:2013. The pH of the wastewater was measured by a Metrohm 692 pH/ion meter, whereas the conductivity of the wastewater was measured by an EDT instrument FE 280 conductivity meter. The metal (calcium) concentration in the wastewater was determined by inductively coupled plasma optical emission spectrometry (ICP-OES), discussed in Section 3.7.1.

3.5 Adsorption experiments

The adsorptive performance of the biochar and activated carbon was characterised by performing various adsorption experiments.

3.5.1 Experimental setup

Batch adsorption experiments were performed in a temperature-controlled Labcon platform incubator shaker as shown in Figure 3-8. Initially, single-component adsorption experiments were performed with phenol and calcium individually in order to determine the optimum adsorbent dosage at a maximum initial concentration of 150 ppm for phenol and 1000 ppm for calcium. Once the optimum biochar dosage of 12 g.L⁻¹ was determined, kinetic experiments were performed at various initial adsorbate concentrations (10 ppm – 150 ppm for phenol and 600 ppm – 1000 ppm for calcium) to determine the kinetic constants and adsorption isotherm parameters for each adsorbate.



Figure 3-8: Actual batch adsorption experimental setup

Binary adsorption experiments with phenol and calcium were then performed at initial concentrations of 10 ppm phenol and 600 ppm calcium, corresponding to that found in the collected wastewater. The binary adsorption experiments were also performed at the optimum adsorbent dosage of 12 g.L^{-1} . Lastly, the wastewater adsorption experiments with real industrial wastewater were performed with 1.2 g of each different adsorbent.

Control experiments were performed with 1.2 g of biochar in deionised water in order to determine what components will be added to the adsorption medium during adsorption experiments by the biochar. In addition, preliminary experiments showed that no adsorption of the two adsorbates took place onto the wall of the sample bottles used in the adsorption experiments, as no change in the concentration was observed. All the experiments were conducted at a temperature of $25^{\circ}\text{C} \pm 2^{\circ}\text{C}$ and a rotary speed of 150 rpm. A solution pH of 8 was used for all the experiments as it corresponds to the pH of the industrial wastewater collected.

3.5.2 Experimental planning

The adsorbent dosage and initial adsorbate concentration were selected as the manipulated variables in order to achieve the set of objectives for the project. The reasoning behind each is shown in Table 3-2.

Table 3-2: Reasoning behind manipulated variables

Manipulated variable	Component	Range	Reason for ranges
Adsorbent dosage	Phenol, calcium	2 g.L ⁻¹ – 12 g.L ⁻¹	The most commonly used adsorbent dosages in literature for phenol and calcium adsorption experiments were between 2 g.L ⁻¹ – 12 g.L ⁻¹ .
Initial adsorbate concentration	Phenol	10 ppm – 150 ppm	Selected based on the maximum phenolic concentration in the industrial wastewater and the maximum phenol concentration removed by the biochar, as shown by the preliminary results in Appendix B.
	Calcium	600 ppm – 1000 ppm	Selected based on the maximum calcium concentration in the industrial wastewater as well as taking possible fluctuations in the calcium concentration into account.

3.5.3 Experimental procedure

The biochar and activated carbon adsorbents were used for the adsorption experiments. The adsorption experiments were conducted according to standard adsorption operating procedures as found in literature.

3.5.3.1 Preparation of glassware

Before the start of each experiment, all the glassware was washed with soap and water, rinsed three times with regular tap water, rinsed once with acetone, and lastly rinsed three times with deionised water. The glassware was dried in a Series 2000 Scientific oven at 105°C. All the glassware was removed from the oven and left to cool down to room temperature. Once the glassware was cooled, a one 1 L Duran bottle was used to prepare the required stock solution (phenol or calcium) in.

3.5.3.2 Preparation of adsorption medium

The phenol and calcium 1000 ppm stock solutions were prepared beforehand and stored in a refrigerator at 4°C. The phenol solution was prepared by dissolving 1 g of pure phenol crystals in 1 L deionised water. The calcium solution was prepared by dissolving 5.90 g of calcium nitrate tetrahydrate in 1 L deionised water. The solutions were mixed until all the solid particles were dissolved. The different phenol (10 ppm – 150 ppm) and calcium (600 ppm – 1000 ppm) concentrations were obtained by diluting the stock solutions of each adsorbate with deionised

water to make a 1 L solution of each. The calculated volume of each stock solution was firstly added to a 1 L volumetric flask. Deionised water was then added up to the 1 L mark. The mixture was thoroughly mixed and kept at $25^{\circ}\text{C} \pm 2^{\circ}\text{C}$ for 24 hours before usage.

3.5.3.3 Weighing of the adsorbent

The required mass (0.20 g – 1.20 g) of adsorbent was measured by using a weighing boat on an analytical scale and added to each 250 ml Duran sample bottle. The actual mass was recorded for each sample bottle. The sample bottle was closed with its corresponding cap until the adsorption medium was finally introduced.

3.5.3.4 Preparation of the adsorbate solution

The adsorbate solution used for each experiment was adjusted to an initial pH of 8 before the start of each experiment (single-component and synthetic binary experiments). Firstly, a Metrohm 692 pH/Ion meter was calibrated beforehand with pH 4 and pH 7 buffer solutions. Depending on the initial concentration and type of adsorbate solution, an appropriate amount of 0.1 M HCl or 0.1 M NaOH was added to the stock solution, dropwise, by a 5 ml syringe, to reach its desired initial pH of 8. Once the desired pH was reached, the adsorption experiment could be started.

3.5.3.5 The adsorption process

The stock solution (100 ml) with the specified initial concentration and pH was added to each sample bottle with different adsorbent masses, two minutes apart from one another. Once the stock solution had been added to a sample bottle, the bottle was then closed and shaken before placing it on an incubator shaker and closing the door. The same procedure was followed for the rest of the sample bottles. The temperature of the incubator shaker was fixed at $25^{\circ}\text{C} \pm 2^{\circ}\text{C}$ with a rotary speed of 150 rpm.

3.5.3.6 Sampling

Sampling was done with a plastic 5 ml syringe at various time intervals, in order to continuously track the progress of the adsorption experiment. Approximately 2.60 ml of sample was taken at 30, 60, 90, 120, 180, 240, 360 and after 1440 minutes or 24 hours from each sample bottle. The samples taken during each sampling period was immediately filtered with either 0.22 μm Gf/tech syringe filters for the pure-water experiments or with 0.45 μm Pall GHP membrane syringe filter for the wastewater experiments (due to the wastewater's high dissolved solids content). Each sample was filtered into its corresponding sample vial or tube. The phenol samples were only filtered into 2 ml glass HPLC vials and closed with its corresponding screw cap with a

fitted septum before HPLC analysis was done. The calcium samples were filtered and diluted 10 times with ICP mobile phase in 50 ml centrifuge tubes before ICP analysis was done.

3.6 Data analysis

The experimental data obtained from the single adsorption experiments were used to fit the pseudo first and pseudo-second-order kinetic models. The experimental data was also analysed by adsorption diffusional models, such as the intra-particle diffusion model, to determine the rate-limiting step(s) of the adsorption system. Adsorption isotherm models were also used to determine the equilibrium behaviour of the system. The Langmuir and Freundlich isotherm models, as well as Henry's law, were fitted to the equilibrium data. In general, the linearised forms of each model were fitted to the experimental data where the corresponding constants and regression coefficients for each model were determined. Microsoft Excel's add-on, the data analysis tool, was used for the calculation of the constants and corresponding regression coefficients.

3.7 Analytical methods: adsorption

The calcium and phenol concentrations were quantified by using ICP-OES and HPLC analysis, as shown in Section 3.7.1 and Section 3.7.2.

3.7.1 Inductively coupled plasma optical emission spectrometry (ICP-OES)

The residual concentration of inorganic components, such as the calcium and other trace elements, were quantified by an Agilent Technologies 725-ES ICP-OES with a radical torch, as shown in Figure 3-9. The argon flow to the plasma was 15 L.min⁻¹ with auxiliary and nebuliser flow rates of 1.50 L.min⁻¹ and 0.75 L.min⁻¹, and a viewing height of 12 mm. The ICP-OES used a 1% nitric acid solution as mobile phase for analysis.

The sample preparation entailed diluting each sample 10 times with mobile phase in a centrifuge tube that was then mixed thoroughly before each analysis. The instrument was calibrated each time by one blank sample (deionised water) and three calibration samples. All samples were analysed three times, 15 s per replicate, where an average value was then calculated. The instrument has a stabilisation delay of 15 s.



Figure 3-9: ICP-OES

3.7.2 High-performance liquid chromatography (HPLC)

The residual concentration of the organic components, such as phenol and various phenol derivatives, were quantified by an Agilent Technologies 1260 Infinity II HPLC, as shown in Figure 3-10. The HPLC was fitted with an InfinityLab Poroshell 120 EC-C18 4.6 x 100 mm column. The HPLC had two mobile phases namely: A – 1% Formic acid in water and 1% formic acid in acetonitrile, mixed initially: 92% A, 8% B, and at 10 minutes: 70% A, 30% B. The column temperature was set as 40°C. An injection volume of 10 μ L was used with a Diode Array Detector with a wavelength of 275 nm and bandwidth of 4 nm.

The sample preparation entailed pipetting 1 ml of each sample into a glass sample tube. No dilution was required as the phenol concentrations used in the adsorption experiments were well below the limit of the phenol calibration curve. The calibration curve for phenol is given in Appendix A.



Figure 3-10: Phenolic HPLC

REFERENCES

Okolo, G.N., Everson, R.C., Neomagus, H.W.J.P., Roberts, M.J. & Sakurovs, R. 2015. Comparing the porosity and surface areas of coal as measured by gas adsorption, mercury intrusion and SAXS techniques. *Fuel*, 141:293-304.

Van Soest, P.J. 1963. Use of detergents in the analysis of fibrous feeds. II. A rapid method for the determination of fiber and lignin. *The Journal of AOAC International*, 46(5):829-835.

CHAPTER 4 – RESULTS AND DISCUSSION

This chapter discusses and interprets the main results. Yields obtained for the production of paper sludge-based biochar through hydrothermal liquefaction (HTL) are reported in Section 4.1. Section 4.2 focusses on the characterisation of the paper sludge as well as the adsorbents used in this study, i.e. biochar and activated carbon. The results of the single-component adsorption of phenol onto biochar are discussed in Section 4.3. The derivation of adsorption isotherms and adsorption kinetics are discussed in Section 4.4 and Section 4.5. Section 4.6 focusses on single-component studies of calcium adsorption onto biochar and Section 4.7 reports on the adsorptive performance of biochar in the presence of both phenol and calcium in a synthetic wastewater environment. Lastly, the performance of biochar as an adsorbent for phenol and calcium using industrial wastewater is compared to that of commercial activated carbon in Section 4.8, and the concluding remarks are given in Section 4.9. Additional data on the material discussed in this chapter can be found in Appendix B.

4.1 Yield of paper sludge-based biochar

The collected paper sludge consisted of a high moisture content of $54.79 \text{ wt.\%} \pm 1.60 \text{ wt.\%}$. The high moisture content of the paper sludge was beneficial for HTL processing since sufficient water was present to ensure that the HTL reactions could proceed. A biochar yield of $722.09 \text{ g.kg}^{-1} \pm 83.51 \text{ g.kg}^{-1}$ (dry basis) was obtained at a reaction temperature of 300°C , which was comparable to the biochar from paper sludge yield of 640 g.kg^{-1} reported by Jaria *et al.* (2015) at 800°C under pyrolysis conditions. Devi and Saroha (2015) also produced biochar from paper sludge under pyrolysis conditions and obtained a yield of 707.90 g.kg^{-1} at a much lower reaction temperature of 300°C . The HTL results obtained in this study thus show that HTL can be used to obtain biochar yields similar to that obtained by pyrolysis without the need for energy-intensive pre-treatment steps such as thermal drying and mechanical grinding.

4.2 Characterisation of paper sludge, biochar and activated carbon

4.2.1 Proximate and elemental analysis

Proximate and elemental analyses were performed on the paper sludge as well as the two adsorbents used in this study and the results are shown in Table 4-1.

Table 4-1: Proximate and elemental analysis of paper sludge, biochar and activated carbon (g.g⁻¹, dry basis)

	Paper sludge	Biochar	Activated carbon
Elemental analysis			
Carbon (C)	0.35	0.39	0.83
Hydrogen (H)	0.047	0.035	0.020
Nitrogen (N)	0.0037	0.0044	0.0030
Oxygen (O)	0.60	0.58	0.15
Proximate analysis*			
Volatile matter	0.70 ± 0.007	0.42 ± 0.01	0.067 ± 0.007
Ash content	0.22 ± 0.007	0.41 ± 0.04	0.023 ± 0.007
Fixed carbon	0.079 ± 0.005	0.16 ± 0.02	0.91 ± 0.005

*moisture contents calculated as 0.55 g.g⁻¹ ± 0.02 g.g⁻¹, 0.02 g.g⁻¹ ± 0.005 g.g⁻¹ and 0.064 g.g⁻¹ ± 0.02 g.g⁻¹ for the paper sludge, biochar and activated carbon respectively

As seen in Table 4-1, the elemental composition of the biochar was very similar to that of the paper sludge as seen by the CHNO content of each. The similar carbon contents of the biochar and paper sludge suggest that the carbon had undergone little to no conversion to gaseous products or depolymerisation reactions to the aqueous phase, indicating that most of the carbon was concentrated in the biochar phase. However, the biochar showed a lower volatile matter content as compared to the paper sludge and can be attributed to the occurrence of dehydration reactions during the HTL process, as the paper sludge consisted of a relatively high moisture content (Lin *et al.*, 2015).

Furthermore, the paper sludge was found to be rich in inorganic ash species, as seen in Table 4-1. The large inorganic fraction of the paper sludge can be attributed to the chemicals used in the paper manufacturing process. According to Mäkelä *et al.* (2016), the high ash content in paper sludge is due to the high calcium concentrations originating from the paper coating materials, such as calcium carbonate, used during the paper manufacturing process. Since Mpact's Springs mill utilises calcium-based coating materials for the production of coated board, high calcium concentrations are expected in the resulting paper sludge produced during the wastewater treatment activities. Therefore, the biochar was found to have consisted of a high ash content, as calcium carbonate exhibits a low solubility in water and would then be found mainly in the biochar phase, and to a lesser extent in the aqueous phase.

A large ash content and a low carbon content is commonly found in literature for paper sludge. Ash contents of 0.20 g.g⁻¹ to 0.36 g.g⁻¹ on a dry basis have been reported for paper sludge with a carbon content of approximately 0.34 g.g⁻¹ (Areeprasert *et al.*, 2015; Khalili *et al.*, 2002; Mu'azu *et al.*, 2017). The biochar obtained from the paper sludge can generally be classified as a Class two biochar due to having a carbon content between 0.30 g.g⁻¹ and 0.60 g.g⁻¹ (Mohan *et al.*, 2014). Furthermore, the high oxygen and low nitrogen content observed in the biochar produced in this study is an indication of the presence of oxygenated functional groups on the surface of the biochar (Al-Malack & Dauda, 2017), which has been found to promote adsorption activities (Wong *et al.*, 2018). The results of the proximate and elemental obtained in this study were comparable with those found in literature (Devi & Saroha, 2015; Oliveira *et al.*, 2018).

4.2.2 Surface area and porosity

Surface area analysis was done on the biochar and activated carbon and the results are shown in Table 4-2.

Table 4-2: Surface area and porosity of the biochar and activated carbon

	Microporous surface area (m ² .g ⁻¹)	Mesoporous surface area (m ² .g ⁻¹)	d _{p,micro} (Å)	d _{p,meso} (Å)
Biochar	24.78	1.54	3.84	431.39
Activated carbon	550.45	277.72	3.72	53.64

As seen from the different surface areas given in Table 4-2, approximately 94% of the surface area of the biochar and 66% of the surface area of the activated carbon is due to micropores, despite the diameters of the micropores in the two adsorbents being similar. The mesopores in the biochar were much larger than that of the mesopores in the activated carbon, which is probably the reason for the much lower mesoporous surface area in the biochar (Zhang *et al.*, 2019). The latter can be attributed to the different production processes employed for the two adsorbents.

Activated carbon is usually produced at very high temperatures (650 – 800°C) and the biochar was produced at a much lower temperature (300°C). Higher temperatures enhance the formation of pores through the evolution of volatiles, but a high ash content could result in the blockage of mesopores by mineral aggregates (Yoon *et al.*, 2017). Given the high ash content of the biochar, it can be deduced that the low mesoporous surface area is most likely the result of pore blockage through mineral matter present in the biochar. The large mesoporous diameter, d_{p,meso} is, however, large enough for a phenol molecule (approximately 6.2 Å) to fit into while the micropores are smaller than the size of one phenol molecule. It is therefore expected that phenol adsorption

will proceed through the mesoporous structure rather than the microporous structure of the biochar.

Calisto *et al.* (2014) produced biochar from paper sludge at a temperature of 315°C and calculated the mesoporous surface area as 3.43 m².g⁻¹, comparable with the mesoporous surface area of the biochar produced in this study. In contrast, the mesoporous surface areas obtained for biochar from paper sludge produced at higher temperatures (650°C) was found to be in the range of 38.38 m².g⁻¹ and 42.51 m².g⁻¹ (Méndez *et al.*, 2009).

4.2.3 Organic composition of the paper sludge

The paper sludge was composed out of cellulose, hemicellulose and lignin as seen from Table 4-3. Cellulose is mainly present in the form of cellulosic fibres of different lengths due to the different processes employed during the paper manufacturing process (Kuokkanen *et al.*, 2008).

Table 4-3: Composition of the paper sludge (dry basis)

Fibre analysis	(wt.%)
Neutral Detergent Fibre (NDF)	85.49
Acid Detergent Fibre (ADF)	73.46
Acid Detergent Lignin (ADL)	38.59
Hemicellulose	12.03
Cellulose	34.88
Lignin	24.54
Cutin	14.05
Protein	2.25
Fat (ether extraction)	1.01

However, the paper sludge used in this study contained a larger fraction of lignin (24.54 wt.%) as compared to other paper sludge showing lignin contents of 5.18 wt.% (Veluchamy & Kalamdhad, 2017). The presence of a larger lignin fraction can be attributed to the main type of raw material used by the paper mill in question. Mpact's Springs mill uses mostly recycled fibre as feedstock. The recycled fibre consists of corrugated boxes amongst other materials such as newspapers, magazines and office paper. Some processes (not all) that produce corrugated boxes do so through a pulping process that can result in larger quantities of residual lignin remaining in the pulp for increased product stiffness (Antonides, 2000). Corrugated material in South Africa has a good recycling rate and thus the material produced from one pulping process can be the recycled

fibre fed into another process. Thus, the paper sludge produced in the process still contains a considerable amount of lignin.

4.2.4 Surface morphology

The surface morphology of the paper sludge, biochar and activated carbon was studied using scanning electron microscopy (SEM) and the micrographs are shown in Figure 4-1, 4-2 and 4-3, respectively. The surface of the paper sludge (Figure 4-1) is an agglomerate mixture of short, broken down organic fibres and a large fraction of fine white, spherical-like particles between fibres. Energy dispersive X-ray (EDX) analysis done on the small white particles mixed in-between the organic fibres revealed that the particles were mineral-based and composed mainly out of calcium, silicon and aluminium. Méndez *et al.* (2009) also found that the small mineral particles were ash constituents composed out of calcium, silicon and aluminium. Kizinievič *et al.* (2018) reported that the fine white particles in-between the cellulosic fibres were lime-based particles.



Figure 4-1: SEM micrograph of the dried paper sludge

The irregular distribution and texture of the organic fibres are characteristic of the pulping process. According to Hojamberdiev *et al.* (2008), paper sludge is usually produced from residual organic/cellulosic fibres that have been recycled various times during the paper manufacturing process. Therefore, the number of cellulosic fibres in the paper sludge will decrease depending on the number of times the fibres have been recycled. The paper sludge used in this study was mostly produced from recycled fibres that are in agreement with the low cellulose content, as shown in Table 4-3. Although the fibres found in the paper sludge are mainly recycled and broken-down, some of the pit fields of the original fibres can still be seen in Figure 4-1. Pit fields are

essential components found in the wall of plant cells required to ensure the transport of water in complex plant species (Choat *et al.*, 2008).

No visible pore structure can be seen in Figure 4-1. However, a large pore structure can be seen in the produced biochar and no short cellulosic fibres are observed, confirming that structural changes to the paper sludge took place during HTL. According to Devi and Saroha (2015), the disappearance of the cellulosic fibres can be attributed to the carbonisation of cellulose that resulted in rough and uneven surfaces in the resulting biochar. Furthermore, as can be seen from Figure 4-2(a), the biochar surface structure also shows a high degree of melting and fusion of the paper sludge constituents, which is typical of HTL-based biochar.

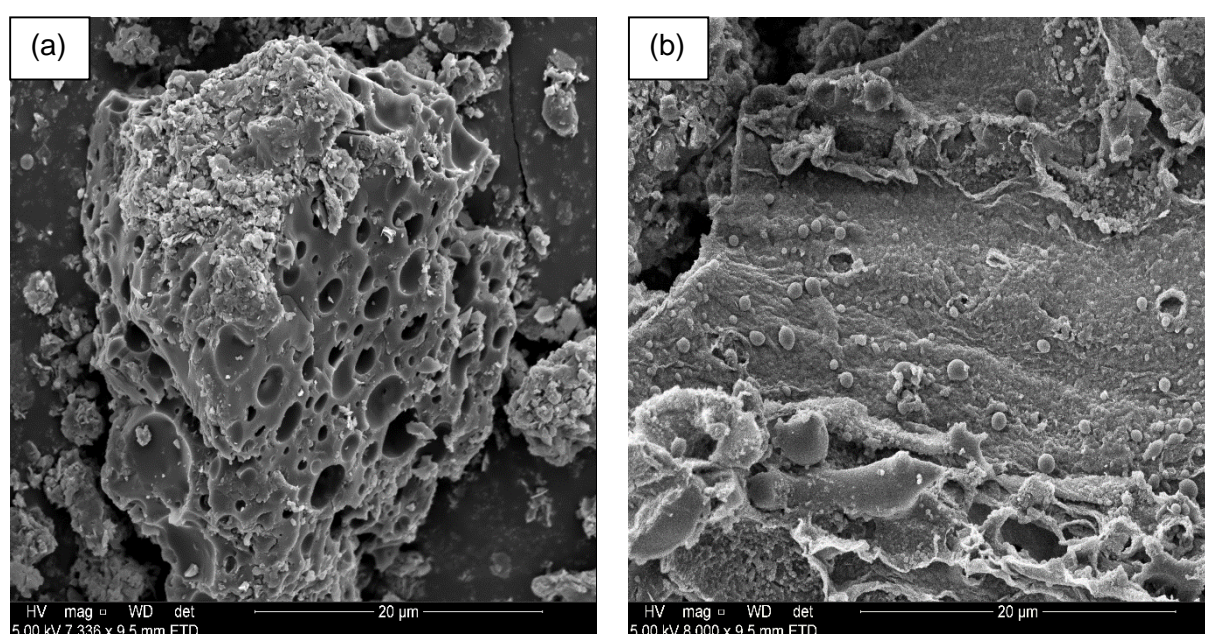


Figure 4-2: SEM micrographs of the produced biochar, showing the presence of irregularly sized pores (a) and volatiles (b) on the surface of the biochar

The overall morphology of the biochar was found to be coarse and irregular, consisting of pores of different shapes and sizes, as shown in Figure 4-2. The latter is in agreement with the low surface areas calculated from BET analysis and reported in Table 4-2. The larger pores can be attributed to the loss of volatiles from the biomass matrix that caused the surface to become brittle and collapse as the reaction proceeded (Liu *et al.*, 2010). The relatively high volatile matter content in the biochar reported in Table 4-1 shows that not all the volatiles were released during the HTL process, and this can be seen in Figure 4-2(b) where volatiles are still trapped in the biochar matrix, as seen by the bubbles near the surface of the biochar. EDX analysis revealed that the main constituents of the biochar were carbon and mineral elements such as calcium, aluminium and silicon.

The overall morphology of the activated carbon showed many smooth external surfaces, with small coarse particles of all sizes found on its surface as seen from Figure 4-3(a). The inside surface structure of the activated carbon was very porous with small pores that result in a sponge-like morphology, as shown in Figure 4-3(b). The latter is typical for activated carbon activated at high temperatures (approximately 900°C) (Kilic *et al.*, 2011) and are in agreement with the small pore diameters and large surface areas calculated from BET analysis of activated carbon and reported in Table 4-2.

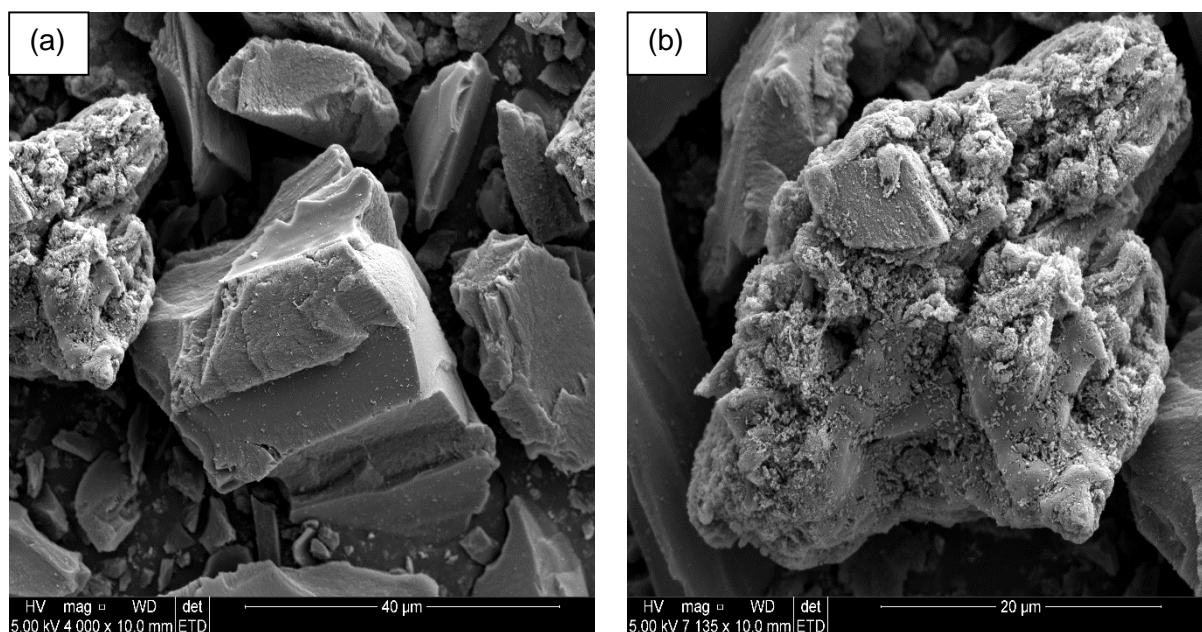


Figure 4-3: SEM micrographs of the commercial activated carbon, showing its external (a) and internal (b) surfaces

4.2.5 Crystalline constituents and major mineral composition of biochar

X-ray power diffraction (XRD) analysis was performed in order to study the mineralogy of the biochar since the proximate and surface morphology analysis showed a relatively high ash content. From the XRD spectra in Figure 4-4, it can be seen that the main mineral constituent of the biochar was calcite (CaO), as shown by the sharp narrow peaks at $2\theta = 27^\circ, 34.2^\circ, 42^\circ, 46.1^\circ, 50.6^\circ, 55.2^\circ, 55.9^\circ, 57^\circ, 67.9^\circ$ and 76.8° . Yoon *et al.* (2017) also reported sharp and narrow peaks at $2\theta = 29.4^\circ, 36.2^\circ, 39.4^\circ, 43.3^\circ, 47.4^\circ, 48.5^\circ$ and 57.4° , which were assigned to the presence of calcite. As calcite is used as filler during the paper manufacturing process, large concentrations of calcite were present in the paper sludge. Furthermore, calcite is also formed during the HTL process as main product, when calcium carbonate is heated and precipitate out of the solution. The observed calcite and kaolinite peaks were found to be very sharp and narrow, indicating that these compounds were part of the biochar's crystalline structure (Zhang *et al.*, 2012). The biochar

also contained kaolinite ($\text{Al}_2\text{Si}_2\text{O}_5(\text{OH})_4$), but to a smaller extent as shown by the smaller narrow peaks produced at $2\theta = 14.2^\circ$ and 28.9° .

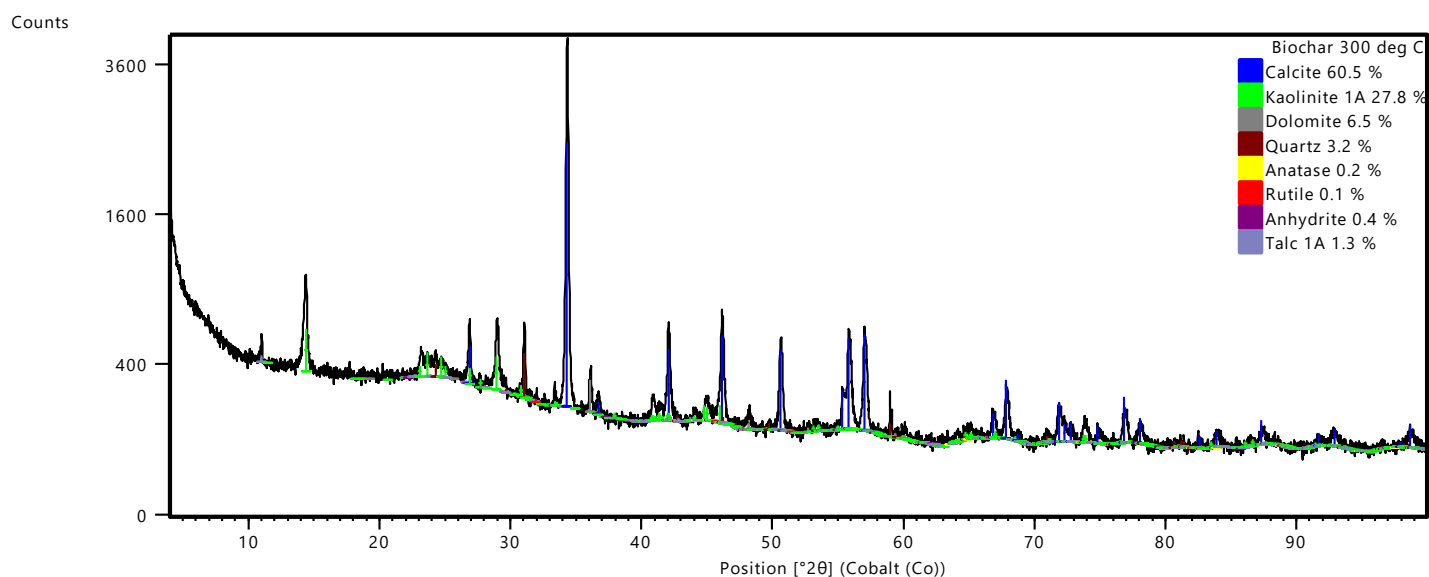


Figure 4-4: XRD spectra of the biochar produced

X-ray fluorescence (XRF) analysis showed that the biochar was rich in mineral constituents as tabulated in Table 4-4. According to the XRF analysis, the biochar contained mostly calcite, quartz and aluminium oxide, validating the results from the EDX analysis. These compounds are constituents of some of the main filler materials such as calcium carbonate, kaolinite and talc used during the paper manufacturing process (Okada *et al.*, 2003). According to Bajpai (2015), the main mineral matter found in paper sludge are calcium oxides, silicon and aluminium oxides, originating from the calcium carbonate and kaolin used in recycled fibre manufacturing. A large mineral matter content is thus expected to be present in the biochar produced from paper sludge.

Hojamberdiev *et al.* (2008) found that biochar produced from paper sludge at 700°C was mainly composed of quartz (31.1%), alumina (27.2%) and calcite (14.2%) with only 5.5% of carbon present in the samples. However, the biochar produced by Hojamberdiev *et al.* (2008) contained more quartz than calcite as compared to the biochar produced in this study. The difference can be attributed to the composition of the paper sludge used, as each paper mill produces paper sludge with a unique composition depending on the chemical used as well as manufacturing processes employed.

Table 4-4: XRF analysis of the biochar produced

	CaO	SiO ₂ (Quartz)	Al ₂ O ₃ (alumina)	MgO	Fe ₂ O ₃	SO ₃	TiO ₂	K ₂ O	P ₂ O ₅	BaO
Composition (wt.%)	47.68	27.23	18.50	2.52	1.85	0,94	0,70	0,42	0,37	0,19

4.2.6 Functional group analysis

XRD and XRF analysis showed that the biochar was not only rich in mineral matter but also in oxygenated groups, and therefore FTIR analysis was used to determine the surface functional groups of the biochar. The FTIR spectra for the paper sludge, biochar and activated carbon are shown in Figure 4-5 and the peak allocation is given in Table 4-5.

Table 4-5: FTIR classification of bond vibrations in compounds

Wavelength (cm ⁻¹)	Bond allocation	Functional group/compounds
875, 1426	CO ₃	Calcium carbonate in the calcite phase (Ichiura <i>et al.</i> , 2011; Méndez <i>et al.</i> , 2009)
950 – 1350, 1624, 3500 – 4000	O – H C – O	Hydroxyl containing groups such as alcohols, phenolics and carboxylic acids (Abdel-Ghani <i>et al.</i> , 2015; Liu <i>et al.</i> , 2013; Yao <i>et al.</i> , 2017)
3300, 3385	O – H	Cellulose (Zhuang <i>et al.</i> , 2019)
1420 – 1737	C = C	Lignin (Lupoi <i>et al.</i> , 2015; Yao <i>et al.</i> , 2017)
1600 – 1850	C – O	Carbonyl compounds such as carboxylic acids, ketones, aldehydes and esters (Davis <i>et al.</i> , 1999; Méndez <i>et al.</i> , 2009; Yao <i>et al.</i> , 2017)
2450 – 2600	C = O	
2400 – 2700	O – H	
2800 – 3000	C – H	Aliphatic groups such as hydrocarbons (Gascó <i>et al.</i> , 2018)
432, 470, 520, 1030, 3619, 3694	Si – O – Si	Kaolinite or quartz (Al-Malack & Dauda, 2017; Méndez <i>et al.</i> , 2009; Ouallal <i>et al.</i> , 2019)

The calcium carbonate observed in the XRD/XRF analysis was also seen in the spectra of the paper sludge as a sharp peak at a wavelength of 876 cm⁻¹ and a broad peak at a wavelength of 1437 cm⁻¹. Kaolinite is represented by the sharp peaks at wavelengths of 1032 cm⁻¹, 3619 cm⁻¹ and 3694 cm⁻¹. The biochar showed similar mineral-based peaks that were intensified as the release of volatile species concentrated ash compounds during the HTL process.

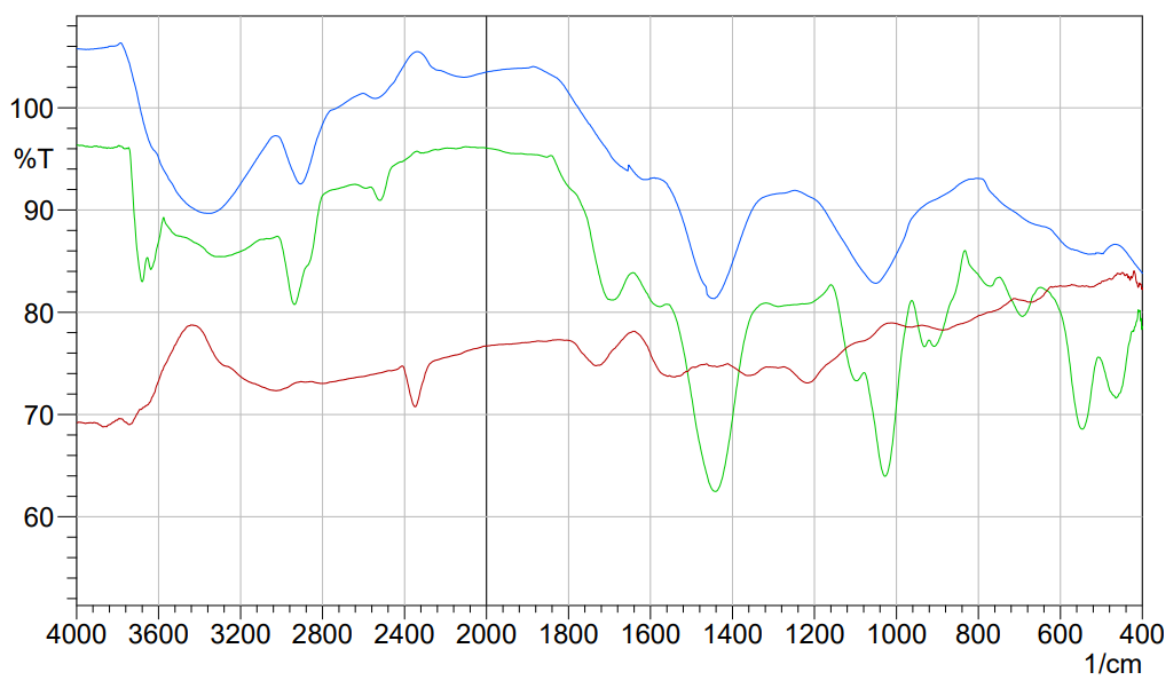


Figure 4-5: FTIR spectra of paper sludge (—), biochar (—) and activated carbon (—)

The presence of cellulose, as seen in the SEM micrograph of the paper sludge, was also observed in the FTIR spectra of the paper sludge as a broad peak at a wavelength of 3400 cm^{-1} . The intensity of the cellulosic peak, however, decreased in the biochar produced, due to the decomposition of cellulose to form monomeric and oligomeric sugars which contain hydroxyl groups, as shown by an increase in the hydroxyl-containing groups at different wavelengths in the spectra.

The FTIR spectra of the paper sludge also confirmed the presence of lignin, as seen from the fibre analysis, by various peaks at wavelengths of 1420 cm^{-1} to 1737 cm^{-1} . The biochar produced contained similar but more pronounced peaks in the same wavelength range, due to the formation of monophenolic hydroxyl groups during the HTL process. The decomposition of lignin also resulted in the formation of nonphenolic oxygenated hydrocarbons, such as carbonyl and alcohol compounds in the biochar, as seen by the pronounced peaks observed at wavelengths of 1700 cm^{-1} to 1850 cm^{-1} and 950 cm^{-1} to 1350 cm^{-1} . According to Kang *et al.* (2013), hydrolysis and breakage of ether and C-C bonds will result in the formation of hydroxylated benzene compounds as well as oxygenated hydrocarbons such as carbonyl and hydroxyl compounds when lignin is subjected to HTL conditions. The presence of various oxygenated functional groups as seen by the FTIR spectra, is in agreement with the high oxygen content calculated for the biochar, as shown by the elemental analysis reported in Table 4-1. The presence of oxygenated functional groups such as carbonyl and hydroxyl are beneficial for phenol adsorption, and therefore adsorption of phenol onto the biochar produced is expected (Mu'azu *et al.*, 2017).

The FTIR spectrum for the activated carbon showed a limited amount of surface functional groups, especially oxygenated functional groups present on its surface. This can be attributed to the high processing temperatures used to produce activated carbon which resulted in the decomposition of most oxygenated surface functional groups (Al-Malack & Dauda, 2017; Liu *et al.*, 2010). These results are also in agreement with the low oxygen content calculated for the activated carbon, as shown by the results of the elemental analysis reported in Table 4-1.

4.2.7 Point of zero charge

The point of zero charge of the biochar (8.1) and activated carbon (6.8) were almost similar as seen from the results shown in Figure 4-6. Therefore, the surface charge of both adsorbents were the comparable during the adsorption studies.

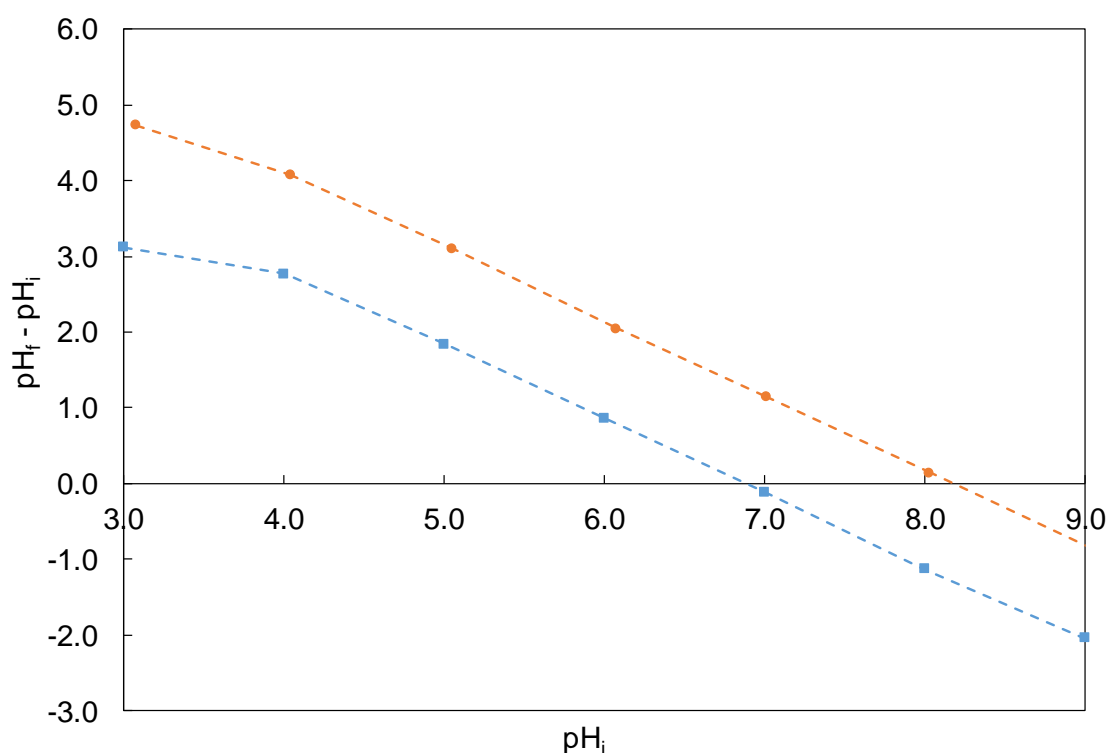


Figure 4-6: Determination of point of zero charge for the biochar (●) and activated carbon (■) samples

A high point of zero charge was expected for the biochar because of its high mineral content. Oliveira *et al.* (2018) found that adsorbents with more basic than acidic functional groups, such as carbonyl groups, will have a higher point of zero charge. The biochar produced in this study contained many surface functional groups but had a lower point of zero charge than adsorbents produced through pyrolysis (Xu *et al.*, 2017), thus indicating that the biochar used in this study had more acidic functional groups compared to pyrolysis char, as confirmed by the elemental and FTIR analysis. The point of zero charge of the activated carbon was close to a neutral value of 7,

because it does not contain many functional groups (acidic or basic), as shown by FTIR analysis. The point of zero charge of the activated carbon was similar to that found by Jaria *et al.* (2015).

4.3 Phenol adsorption

The point of zero charge analysis has shown that the point of zero charge of the biochar was close to 8. Since the pH of the industrial wastewater used in this study was also close to 8, pH was not investigated as a variable that influenced the adsorption of phenol and calcium, and therefore all experiments were performed at a fixed pH of 8.

4.3.1 Effect of biochar dosage

Adsorbent dosage is an important factor to consider in adsorption processes, as it will influence the capacity of the adsorbent to reach equilibrium conditions for a fixed adsorbate concentration (Mubarik *et al.*, 2012). The effect of the biochar dosage on phenol adsorption was investigated by varying the biochar dosage between 2 g.L⁻¹ and 12 g.L⁻¹. The results are shown in Figure 4-7.

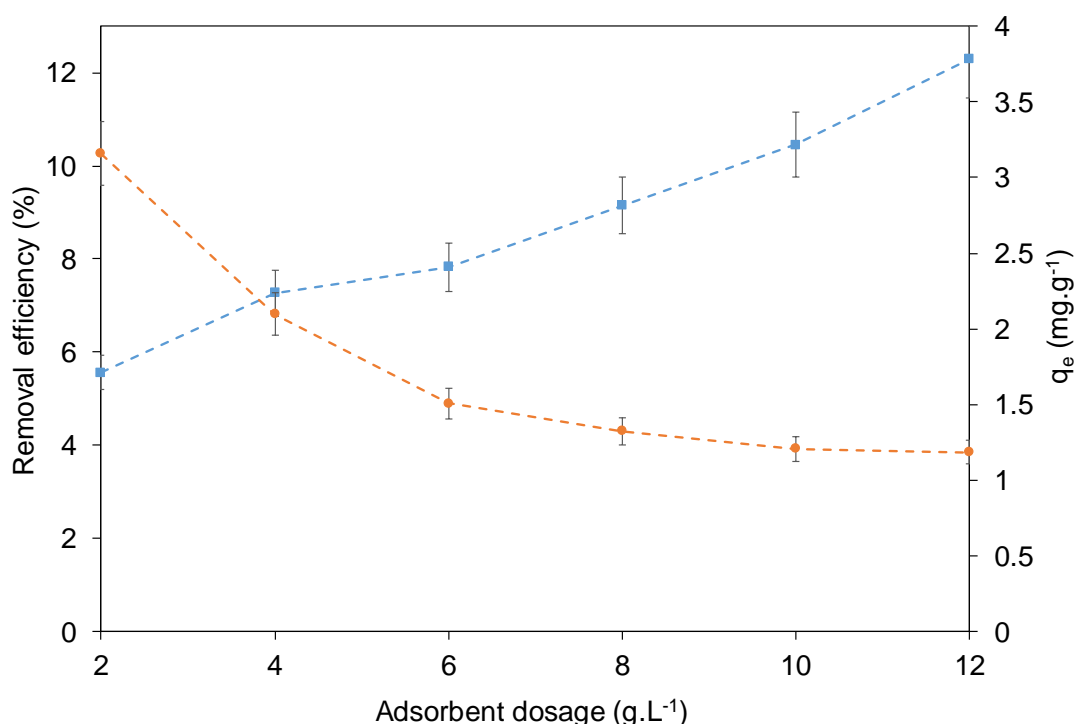


Figure 4-7: Effect of the biochar dosage on phenol removal efficiency (■) and adsorption capacity (●) ($C_i = 150$ ppm, pH 8, contact time = 1440 min, $T = 25^\circ\text{C} \pm 2^\circ\text{C}$)

As seen from Figure 4-7, an increase in the adsorbent dosage from 2 g.L⁻¹ to 12 g.L⁻¹ resulted in an increase in the phenol removal efficiency from 5.56% to 12.30%, with an experimental error of 6.71% based on a 95% confidence level. This can be attributed to an increase in the effective

surface area, and therefore the number of active sites which create more opportunities for the adsorption of phenol molecules (Afsharnia *et al.*, 2016). However, an increase in the adsorbent dosage also resulted in a decrease in the adsorption capacity. Initially, the adsorption capacity decreased from 3.16 mg.g⁻¹ to 1.51 mg.g⁻¹ as the adsorbent dosage was increased from 2 g.L⁻¹ to 6 g.L⁻¹, as a higher dosage resulted in an increase in the amount of unsaturated active sites, while the number of phenol molecules in the solution remained the same (Abbaszadeh *et al.*, 2016). However, increasing the adsorbent dosage beyond 6 g.L⁻¹, resulted in no significant change in the adsorption capacity, as seen from Figure 4-7. This can be attributed to the biochar particles forming agglomerate mixtures, a result of overcrowding, and therefore masking active sites from the phenol molecules for possible adsorption (Gholizadeh *et al.*, 2013; Xu *et al.*, 2013). Thus, the biochar only has a limited number of active sites that can accommodate the adsorption of phenol and adding more biochar to the solution will result in higher removal efficiencies only due to the addition of more, limited active sites.

The highest removal efficiency of 12.30%, with an experimental error of 6.71% based on a 95% confidence level, was achieved with a biochar dosage of 12 g.L⁻¹. The high adsorbent dosage required to achieve the maximum phenol removal efficiency was in agreement with other phenol adsorption studies performed with a variety of adsorbents (Mohammed *et al.*, 2018; Mubarik *et al.*, 2012). Higher adsorbent dosages will also be able to accommodate possible fluctuations in adsorbate concentrations when used in real wastewater environments as well as minimise the experimental error when employed in bench-top scale experiments. Therefore, a dosage of 12 g.L⁻¹ biochar was used for the rest of the adsorption experiments performed in this project.

4.3.2 Effect of initial phenol concentration

The initial phenol concentration is an important parameter to consider as it provides an initial driving force for phenol molecules to overcome mass transfer limitations experienced between the bulk solution and the surface of the adsorbent (Dursun *et al.*, 2005). Also, by changing the initial concentration at a fixed biochar dosage, some insight into the rate-determining mass transfer mechanism can be obtained. The results are given in Figure 4-8.

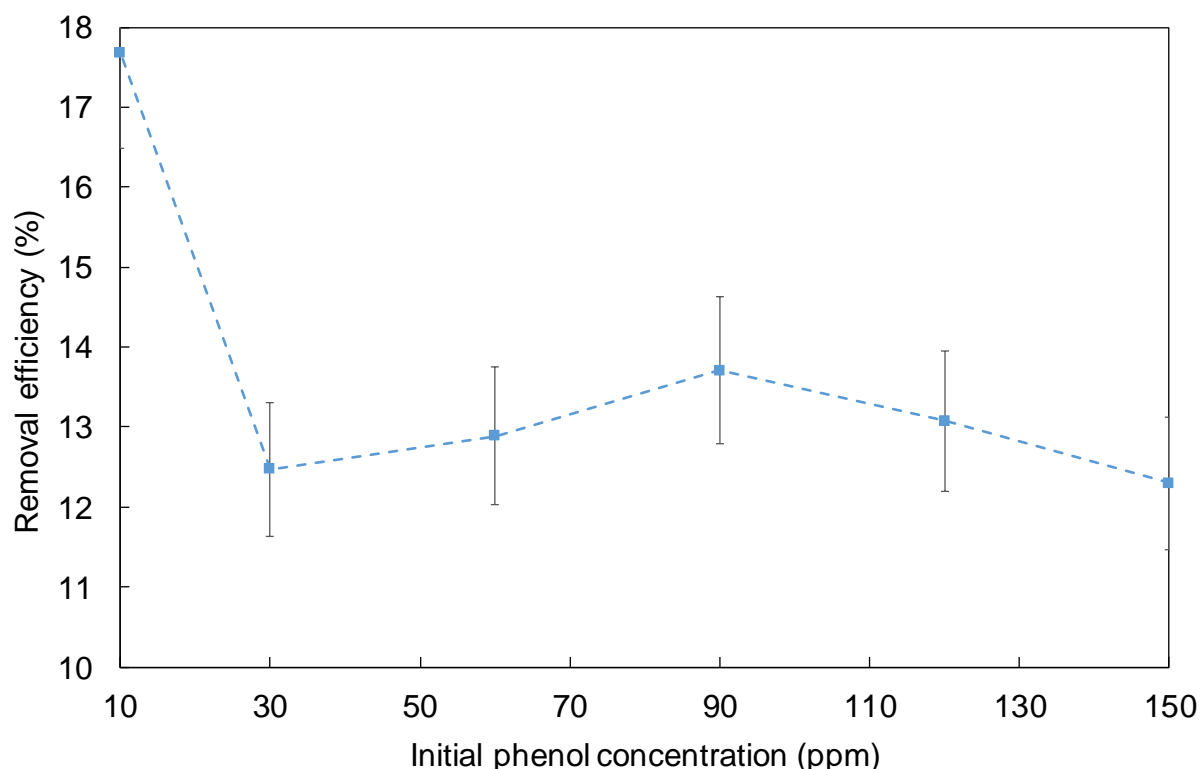


Figure 4-8: Effect of initial concentration on phenol removal (dosage = 12 g.L⁻¹, pH 8, contact time = 1440 min, T= 25°C ± 2°C)

The effect of the initial phenol concentration on the adsorptive performance of the biochar was investigated by varying the initial phenol concentration between 10 ppm and 150 ppm. As seen from Figure 4-8, the highest removal efficiency of 17.67%, with an experimental error of 6.71% based on a 95% confidence level, was obtained at an initial phenol concentration of 10 ppm. However, the removal efficiency decreased as the initial phenol concentration was increased from 10 ppm to 30 ppm. The removal efficiency further remained unchanged as the initial concentration was increased beyond 30 ppm, which can be attributed to the limited surface area and therefore active sites available on the surface of the biochar. Initially, a high removal efficiency was obtained since the limited amount of active sites could accommodate, to some degree, the low concentration of phenol molecules in the solution. However, as the initial concentration was increased beyond 10 ppm phenol, the removal efficiency decreased due to the larger number of phenol molecules in the solution for the same number of active sites on the surface of the biochar. These findings are similar to other authors that performed phenol adsorption studies (Abdel Salam *et al.*, 2011; Dursun *et al.*, 2005; Kilic *et al.*, 2011; Rathore *et al.*, 2016; Singh & Balomajumder, 2016).

The low phenol removal efficiencies can be attributed to the surface characteristics of the biochar, as the adsorption of phenol has been found to be influenced by the surface area and pore sizes of the adsorbent (Purnomo *et al.*, 2012). According to Beker *et al.* (2010), phenol adsorption

occurs mainly in the micropores ($d < 2 \text{ nm}$ or 20 \AA) as the micropores are larger than the diameter of a phenol molecule ($d < 0.62 \text{ nm}$ or 6 \AA). However, the micropore diameter of the biochar used in this study (3.84 \AA) was smaller than the size of a phenol molecule. Therefore, phenol adsorption in the micropores were not expected. The biochar did, however, have a large mesoporous structure with an average pore diameter of 431.39 \AA , larger than the size of phenol molecules. Therefore, adsorption of phenol onto the biochar was only possible by filling mesopores, and since the mesoporous surface area was very low, low removal efficiencies were obtained. Mu'azu *et al.* (2017) also reported that the adsorption of phenol onto sludge-based adsorbents are likely to occur in the mesopores rather than the micropores, resulting in faster diffusion rates, as the larger pores were more accessible to phenol molecules than the smaller micropores. The findings obtained are in agreement with others found in literature (Ferreira *et al.*, 2017).

4.4 Adsorption isotherms

The equilibrium data for the adsorption of phenol onto the biochar produced was used to determine the possible interactions between the phenol molecules in the liquid phase and the surface of the biochar by plotting the adsorption isotherm, as shown in Figure 4-9.

4.4.1 Equilibrium isotherm

As seen from Figure 4-9, a linear relationship existed (adjusted R^2 of 0.991) between the adsorption capacity and the concentration of phenol molecules in the liquid phase at equilibrium. The equilibrium isotherm produced in this study can be classified as a type C (constant partition) isotherm, which indicates that a sufficient number of active sites were available for adsorption (Giles *et al.*, 1960). However, not all the active sites were occupied due to the absence of a well-defined plateau, resulting in the isotherm being further classified as a Subclass 1 isotherm (Bonilla-Petriciolet *et al.*, 2017). Therefore, the adsorption capacity was proportional to the concentration of phenol molecules in the liquid phase, but not all the active sites available were occupied by phenol molecules and therefore, low removal efficiencies were obtained.

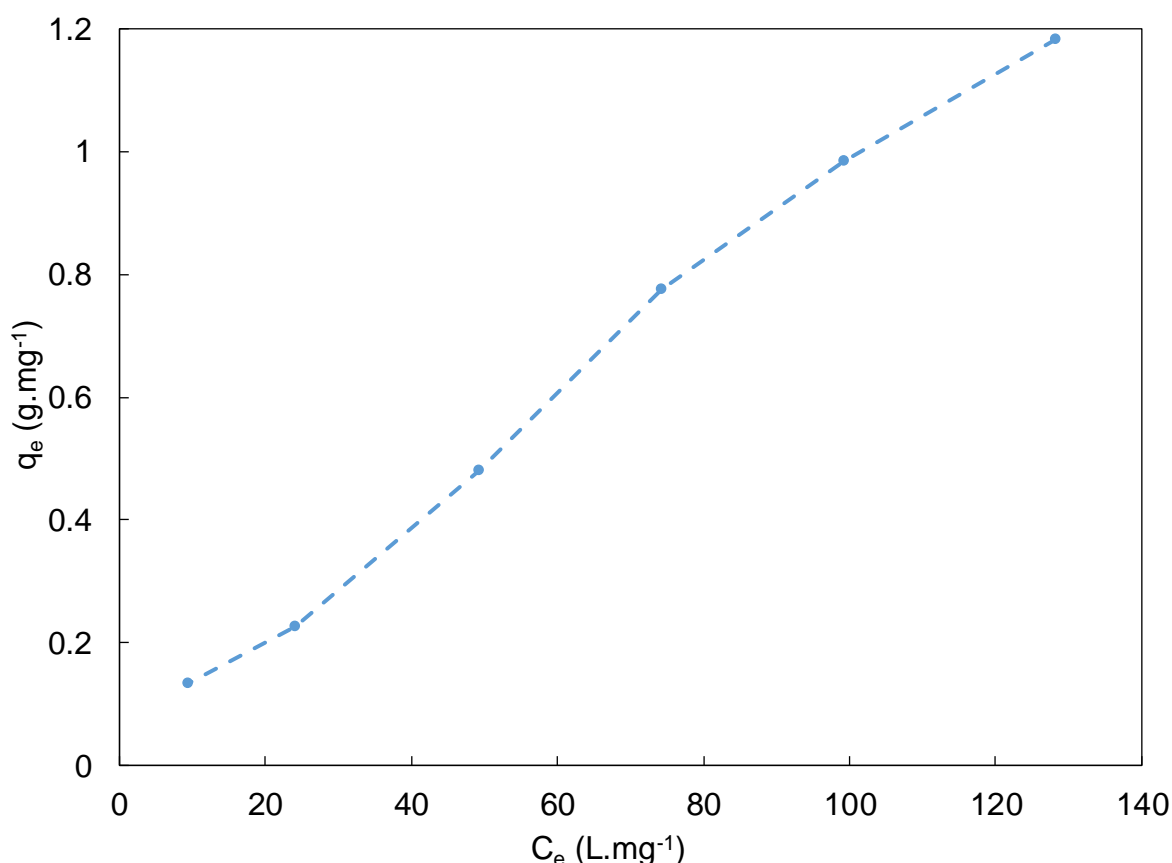


Figure 4-9: Adsorption isotherm of phenol onto biochar (dosage = 12 g.L⁻¹, pH 8, T= 25°C ± 2°C)

The low removal efficiencies can be related to the mineral-rich nature of the biochar, as seen from the XRD and XRF results, that prevented the penetration of phenol molecules deep within the pores of the biochar. Therefore, only a small number of active sites that were not blocked by mineral matter were able to accommodate the adsorption of phenol molecules, whereas the rest of the sites were left inaccessible, as seen by the absence of a plateau in Figure 4-9. These results are in agreement with the low micro- and mesoporous surface area reported for the biochar by BET analysis and also the high ash content calculated by proximate analysis.

4.4.2 Adsorption isotherm models

The equilibrium data was further interpreted by fitting the Langmuir and Freundlich isotherm models as well as Henry's law. The parameters of the Langmuir and Freundlich isotherm models were determined by the linearised forms of each model. The Langmuir parameters were determined from the slope and intercept of the plot of $1/q_e$ versus $1/C_e$, as shown in Figure 4-10. The Freundlich parameters were also determined from the slope and intercept, but by plotting $\ln(q_e)$ versus $\ln(C_e)$ as shown in Figure 4-11. Henry's adsorption constant, K_H , was calculated from the slope by plotting q_e versus C_e , as shown in Figure 4-12. The corresponding parameters calculated for each model was based on a 95% confidence level and is given in Table 4-6.

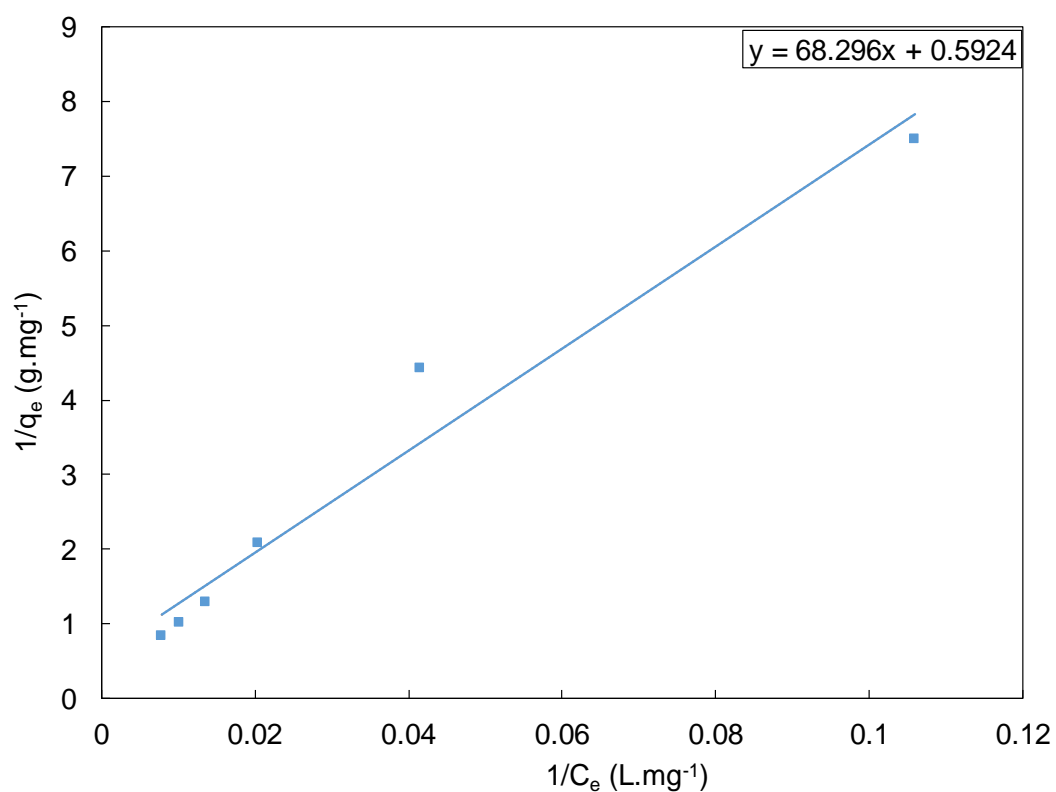


Figure 4-10: Langmuir plot for phenol adsorption onto biochar (dosage = 12 g.L⁻¹, pH 8, T= 25°C ± 2°C)

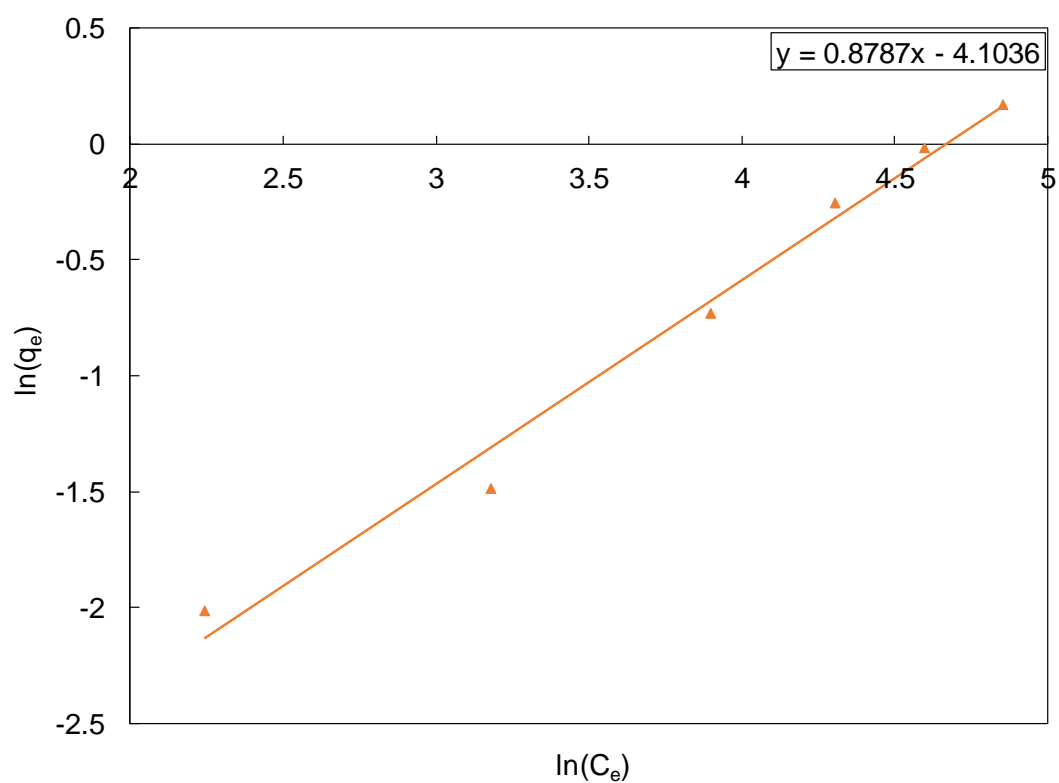


Figure 4-11: Freundlich plot for phenol adsorption onto biochar (dosage = 12 g.L⁻¹, pH 8, T= 25°C ± 2°C)

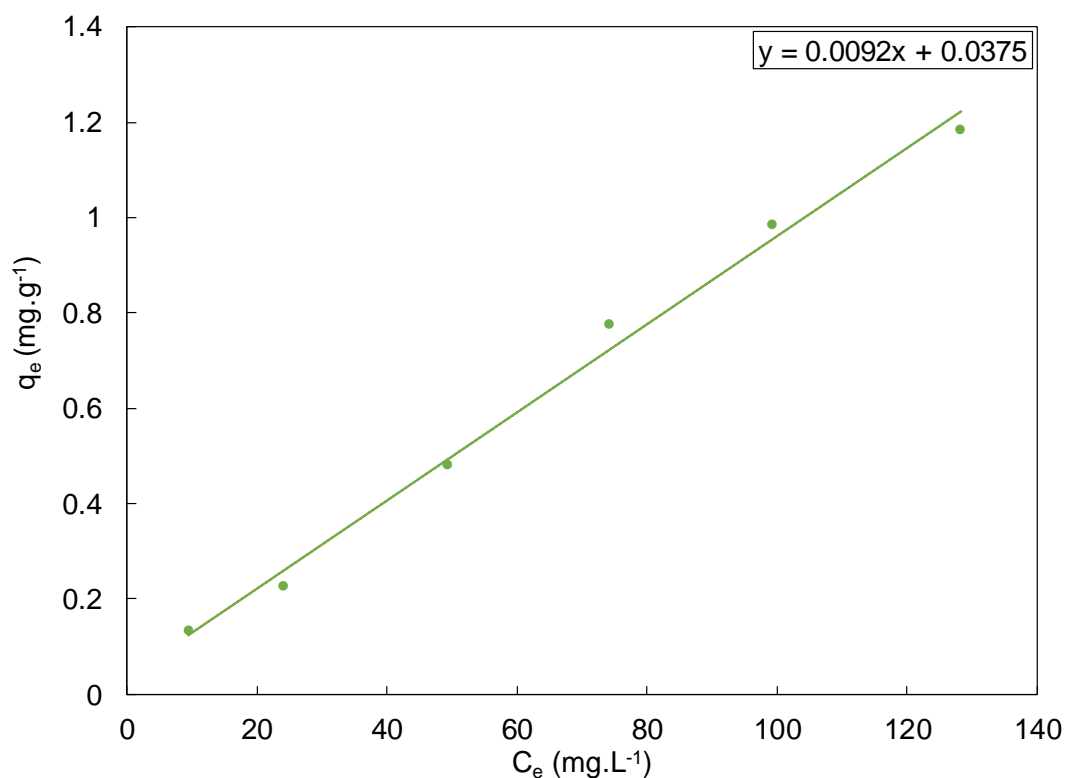


Figure 4-12: Henry's law plot for phenol adsorption onto biochar (dosage = 12 g.L⁻¹, pH 8, T= 25°C ± 2°C)

As seen from Table 4-6 and Figure 4-12, the equilibrium data was best described by Henry's law, as the data points barely deviated from the model and therefore resulted in the highest adjusted R^2 value in comparison with the other two models. Also, the p-value of the parameter, K_H was smaller than 0.05, indicating that its contribution was significant in fitting Henry's law to the experimental data. Thus, the adsorption of phenol onto biochar derived from paper sludge occurred on a uniform surface and the adsorbed phenol molecules did not interact with those adsorbed at adjacent active sites (Ayawei *et al.*, 2017). The suitability of Henry's law to describe the equilibrium data is also related to the linear isotherm shown in Figure 4-9. According to Bonilla-Petriciolet *et al.* (2017), C.1 isotherms are usually described by Henry's law when very low adsorbate concentrations are used.

Table 4-6: Isothermal parameters for phenol adsorption onto biochar at 25°C ± 2°C

Langmuir isotherm					
K_L (L.mg ⁻¹)	P-value	q_{\max} (mg.g ⁻¹)	P-value	Adj.R ²	R_L
0.0087 ± 0.0012	5.59 x 10 ⁻⁰⁴	1.69	0.14	0.95	0.44 – 0.91
Freundlich isotherm					
K_F (mg ^{0.12} .L ^{0.88} .g ⁻¹)	P-value	n	P-value	Adj.R ²	
0.017	4.23 x 10 ⁻⁰⁵	1.14 ± 0.0012	8.20 x 10 ⁻⁰⁵	0.98	
Henry's law					
K_H (L.g ⁻¹)	P-value	C	P-value	Adj.R ²	
0.0092	2.03 x 10 ⁻⁰⁵	0.037	0.28	0.99	

The use of Henry's law to describe equilibrium data of phenol adsorption is rarely reported in literature. Usually, the Freundlich isotherm model is used to describe the equilibrium behaviour of phenol adsorption onto a variety of adsorbents (Afsharnia *et al.*, 2016; Kilic *et al.*, 2011; Miao *et al.*, 2013). However, the adjusted R² values for both the Freundlich isotherm model and Henry's law were quite close to one another, as seen in Table 4-6. This can be attributed to the low phenol concentrations used in this study. According to Tran *et al.* (2017), the Freundlich isotherm reduces to Henry's law at very low adsorbate concentrations as the Freundlich parameter, n, will be equal to one.

The Freundlich parameter, n, is commonly associated with the heterogeneity, and therefore the type and distribution of active sites available on the surface of an adsorbent. According to Girish (2017), values of n greater than one have been found to indicate that an adsorbent has a heterogeneous surface with a non-uniform distribution of the active sites. Therefore, adsorbents with a larger surface area will have more possibilities for the distribution of active sites and a larger value for n will be obtained. Villar da Gama *et al.* (2018) calculated the value of n as 5.03

for the adsorption of phenol onto peanut shell activated carbon with a surface area of $393.80 \text{ m}^2.\text{g}^{-1}$. Giraldo and Moreno-piraján (2014) calculated a lower value for n of 2.60, as the activated carbon produced from eggshells consisted of a lower surface area of $113 \text{ m}^2.\text{g}^{-1}$. In contrast, the biochar used in this study consisted of a low surface area of $1.54 \text{ m}^2.\text{g}^{-1}$ and therefore, a low value of 1.14 was calculated for n . The low value for n also relates to the isotherm classification of C.1 obtained, which indicated that the biochar surface had a low surface area and a limited distribution of active sites was available. Other researchers also calculated low values for n when the adsorbent used consisted of a relatively low surface area. Potgieter *et al.* (2009) used South African coal fly ash with a surface area of $1.29 \text{ m}^2.\text{g}^{-1}$ and calculated the value of n as 1.08, lower than that found for n in this study.

4.4.3 Active sites responsible for phenol adsorption

Although limited active sites were available for adsorption, adsorption of phenol onto the active sites of the biochar still occurred. FTIR analysis was performed on the biochar samples after adsorption with initial phenol concentrations of 10 ppm and 150 ppm, and was compared to that of unused biochar, as shown in Figure 4-13.

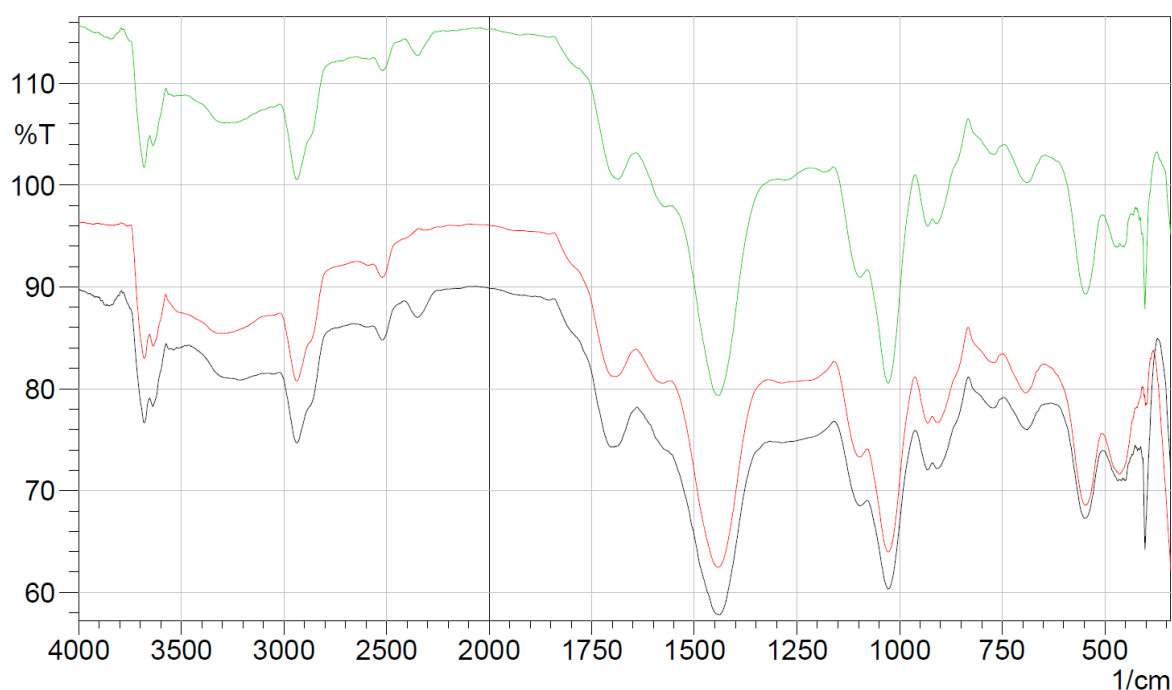


Figure 4-13: FTIR spectra produced for unused biochar (—), biochar after 10 ppm phenol adsorption (—) and biochar after 150 ppm phenol adsorption (—)

As seen from Figure 4-13, the intensity and position of various peaks, as well as the appearance of new peaks, were observed after the adsorption of phenol. The peak at a wavelength of 2345 cm^{-1} changed during the adsorption process as the peak increased in intensity and shifted

to a wavelength of 2350 cm^{-1} for the 10 ppm and 150 ppm biochar samples after adsorption. According to Abdel-Ghani *et al.* (2015), the peaks produced in the wavelength range of 2340 cm^{-1} to 2360 cm^{-1} after the adsorption of phenol onto multiwalled carbon nanotubes were related to the -OH stretching vibration from a strong H-bonded-COOH.

A new peak was also produced at a wavelength of 1220 cm^{-1} for the 150 ppm biochar sample that can be attributed to the -OH bending vibration present in -COOH compounds (Davis *et al.*, 1999). Therefore, the phenol molecules adsorbed onto the surface of the biochar by forming weak hydrogen bonds between the hydrogen atom of the hydroxyl group present in phenol, and the oxygen atom of the hydroxyl group present in the carboxylic compounds available on the surface of the biochar. Lorenc-Grabowska (2016) also noted that hydrogen bonding is expected to occur between the hydrogen of the phenol's hydroxyl group and the hydroxyl groups on the surface of the adsorbent. These results are also in agreement with the isotherm classification, as C.1 type isotherms indicate that bonding forces are weak and depend as such on the concentration in the liquid phase (Bonilla-Petriciolet *et al.*, 2017).

The influence of the phenol concentration on the bonding forces can also be seen from the spectrum produced for the biochar exposed to 10 ppm phenol. As seen at a wavelength of 1590 cm^{-1} , the peak present for both the unused biochar and biochar exposed to 150 ppm phenol were absent in the spectrum produced for the biochar exposed to 10 ppm phenol. The lower concentration of phenol in the liquid phase therefore resulted in the desorption of adsorbed phenol molecules as the adsorption process progressed, as the bonding forces were not strong enough to keep the phenol molecules from leaching into the adsorption medium. Other changes in the FTIR spectra of the unused biochar, compared to the biochar exposed to 10 ppm and 150 ppm phenol, were also observed at wavelengths of 400 cm^{-1} , 466 cm^{-1} and 920 cm^{-1} , which indicated the presence of newly adsorbed phenol molecules.

It can therefore be concluded that oxygenated functional groups such as hydroxyl and carboxylic groups played an important role in the adsorption of phenol onto the biochar produced. Other authors have also noted the importance of oxygenated functional groups in the adsorption of organic contaminants onto various adsorbents (Leng *et al.*, 2015; Zhang *et al.*, 2016).

4.5 Adsorption kinetics

Evolution of the kinetic profile of an adsorption system is an important part of an adsorption process, as it offers insight into the rate of adsorption, the residence time required to reach equilibrium conditions and the effectiveness of the adsorbent used (Bonilla-Petriciolet *et al.*, 2017). The kinetic profile obtained for this study is shown in Figure 4-14.

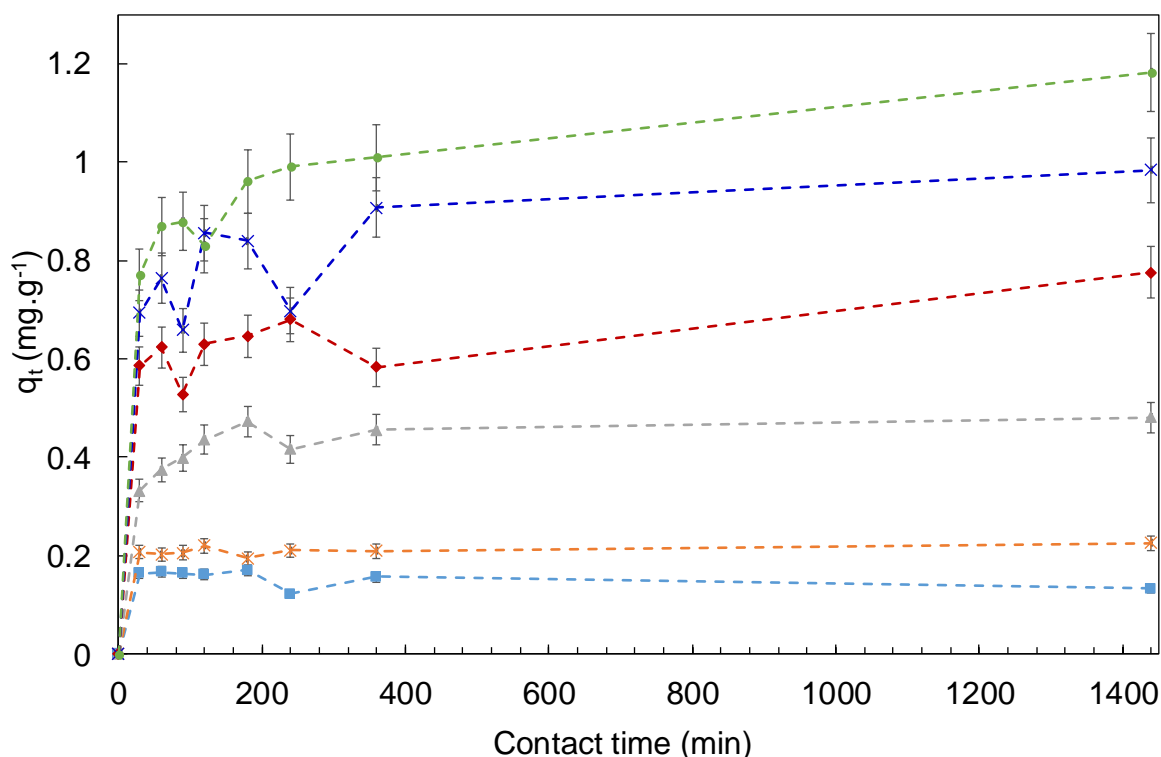


Figure 4-14: Kinetics of phenol adsorption (dosage = 12 g.L⁻¹, pH 8, contact time = 1440 min, T = 25°C ± 2°C) (Phenol concentration: ■, 10 ppm; ✱, 30 ppm; ▲, 60 ppm; ◆, 90 ppm; ✕, 120 ppm; ●, 150 ppm)

The adsorption of phenol onto the biochar produced required between 30 minutes and 360 minutes to reach equilibrium conditions, depending on the initial phenol concentration used. The contact time required to reach equilibrium conditions were in agreement with the time expected for phenol adsorption studies. According to Sobiesiak (2017), the contact time required for the adsorption of phenol to reach equilibrium conditions ranges between one and 24 hours, where rapid uptake is expected within the first 30 minutes of the adsorption process as all the active sites are still accessible.

As seen from Figure 4-14, the lower phenol concentrations of 10 ppm, 30 ppm and 60 ppm reached equilibrium conditions within the first 30 minutes of the adsorption process. The higher phenol concentration of 90 ppm, 120 ppm and 150 ppm required more time (120 min – 360 min) to reach equilibrium. This can be attributed to the mass transfer effects existing in the adsorption medium. At the start of the adsorption process, all the active sites were available for the adsorption of phenol molecules. High initial phenol concentrations, however, provide a large driving force for mass transfer from the solution to the surface of the biochar, and thus obtained the fastest initial rate of adsorption, as shown by the steeper slopes produced for the 90 ppm to 150 ppm experiments shown in Figure 4-14. However, as the adsorption process progresses, it will require more time to reach equilibrium conditions as the driving force for mass transfer is decreased with increased occupation of active sites. The phenol molecules occupying active sites will also

hinder/repulse other phenol molecules from occupying the adjacent active sites, which slows down the adsorption with time (Yousef *et al.*, 2011). Once all available and accessible adsorption sites are occupied, the biochar is saturated and equilibrium conditions are reached where no further additional active sites can be occupied by phenol molecules. Lower initial phenol concentrations reached equilibrium conditions much faster, as only a limited number of phenol molecules were present in the solution and therefore the mass transfer and repulsion effects were not as significant as seen with the higher phenol concentrations. These results correspond to other phenol adsorption studies performed in literature (Abdelkreem, 2013; Dursun *et al.*, 2005; El-Naas *et al.*, 2010; Kumar & Jena, 2016; Zhou *et al.*, 2017).

The presence of different adsorption mechanisms was also observed from the kinetic profile. As seen from Figure 4-14, the curves for the 90 ppm and 120 ppm initial phenol concentrations had data points that dipped at different time intervals, reaching the same adsorption capacity thereafter. The random decreasing data points can be attributed to the adsorption of phenol molecules to active sites with different compounds present, such as carboxylic or alcohols, which both provided the phenol molecules with the opportunity to adsorb. The curve produced for the initial phenol concentration of 10 ppm also showed a dip in the adsorption capacity (240 minutes). However, the 10 ppm phenol experiment reached equilibrium for a second time after 360 minutes but obtained a lower adsorption capacity than that obtained initially after 30 minutes. This can be attributed to the desorption of phenol due to the weak forces produced at the low phenol concentration of 10 ppm and not re-adsorbing afterwards. The desorption of phenol was also evident from the FTIR spectrum produced by the 10 ppm biochar sample after 1440 minutes, shown in Figure 4-13.

In order to determine the rate of adsorption of phenol onto the biochar produced, the pseudo-first-order and pseudo-second-order rate models were fitted to the experimental data. However, only the results of the fitting of pseudo-second-order model is given here, because the data did not fit the pseudo first-order model ($R^2 \leq 0$). Others also found that the pseudo-first-order was not a good fit to experimental data (Abdel-Ghani *et al.*, 2015; El-Naas *et al.*, 2010; Tancredi *et al.*, 2004).

4.5.1 Pseudo-second-order model

The kinetic parameters of the pseudo-second-order kinetic model were calculated from plotting the linearised form of the model, as shown in Equation 4-1, to the experimental data and calculating the slope and intercept for each phenol concentration, as shown in Figure 4-15. The parameters and the coefficients of determination are given in Table 4-7.

$$\frac{t}{q_t} = \frac{1}{k_2 q_e^2} + \frac{t}{q_e} \quad (4-1)$$

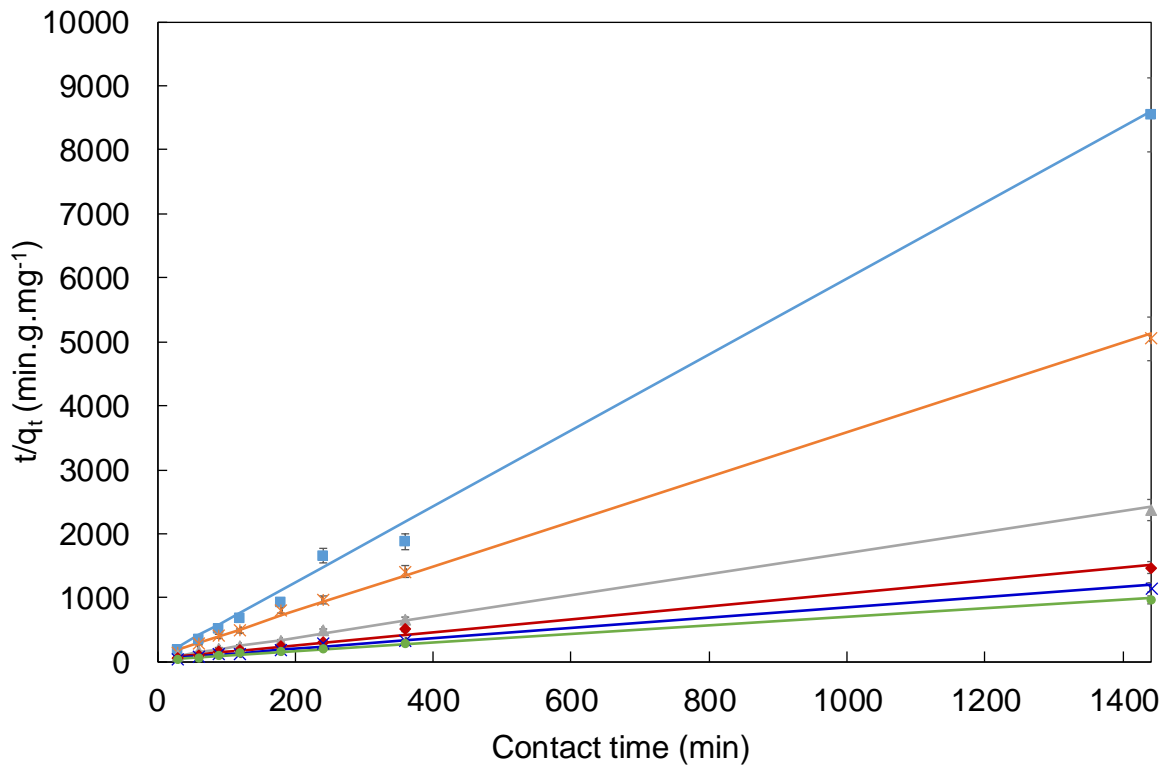


Figure 4-15: t/q_t versus contact time fit for the pseudo second-order rate expression (dosage = 12 g.L⁻¹, pH 8, T= 25°C ± 2°C) (Phenol concentration: ■, 10 ppm; *, 30 ppm; ▲, 60 ppm; ◆, 90 ppm; ×, 120 ppm; ●, 150 ppm)

The pseudo-second-order rate expression was found to fit the kinetic data very well for initial phenol concentrations higher than 10 ppm, as seen by the linear plots shown in Figure 4-15 and the high adjusted R² values given in Table 4-7. The equilibrium adsorption capacities predicted by the model correlated well with the experimental values obtained at a 95% confidence level. Other authors also found that the pseudo-second-order kinetic model best described phenol adsorption onto various adsorbents (Abdel-Ghani *et al.*, 2015; El-Naas *et al.*, 2010; Gholizadeh *et al.*, 2013).

Table 4-7: Pseudo-second-order parameters for phenol adsorption onto biochar at 25°C ± 2°C

C_i (ppm)	q_{e,exp} (mg.g⁻¹)	q_{e,cal} (mg.g⁻¹)	P-value	k₂ (g.mg⁻¹ min⁻¹)	P-value	h_o (mg.g⁻¹.min⁻¹)	Adj.R²
10	0.13	0.13	3.91 x 10 ⁻⁰⁹	<0.00	0.13	<0.00	0.997
30	0.23	0.23	6.10 x 10 ⁻¹¹	0.32±0.074	0.039	0.016	0.999
60	0.48	0.49	3.27 x 10 ⁻¹¹	0.11±0.011	0.0076	0.026	0.999
90	0.78	0.79	6.94 x 10 ⁻⁰⁸	0.03±0.070	0.044	0.019	0.993
120	0.98	1.01	1.89 x 10 ⁻⁰⁸	0.03±0.004	0.030	0.026	0.995
150	1.18	1.21	1.07 x 10 ⁻⁰⁹	0.02±0.0014	0.0028	0.029	0.998

As seen from Table 4-7, changing the initial phenol concentration influenced the pseudo-second-order rate constant, k_2 , and therefore the initial rate of adsorption, h_o . Initially, an increase in the phenol concentration from 10 ppm to 60 ppm resulted in an increase in the initial rate of adsorption as the effects of mass transfer were not as significant in the liquid phase, as a low concentration of phenol molecules were present. However, increasing the initial phenol concentration from 60 ppm to 90 ppm resulted in a decrease in the initial adsorption rate due to transport difficulties experienced in the liquid phase, and also within the pores of the biochar as more molecules were present in the adsorption medium. A further increase in the initial phenol concentration beyond 90 ppm resulted in an increase in the initial rate of adsorption, as a larger concentration of phenol molecules in the liquid phase provided a large enough driving force to overcome the mass transfer limitations experienced.

The highest initial rate of adsorption was achieved with an initial phenol concentration of 150 ppm, corresponding to the kinetic profile that showed that an initial phenol concentration of 150 ppm obtained the steepest slope. However, the lowest value for k_2 calculated for an initial phenol concentration of 150 ppm indicated that equilibrium conditions were approached very slowly due to inaccessibility of pores as caused by the repulsion of adsorbed molecules and the limited surface area of the biochar. The pseudo-second-order rate constant for an initial phenol concentration of 10 ppm could not be estimated with the pseudo-second-order rate expression, as desorption of adsorbed phenol molecules occurred which influenced the rate of adsorption of phenol molecules onto the surface of the biochar, as shown by the value of k_2 below zero.

The rate constants for the adsorption of phenol onto the biochar produced for different initial phenol concentrations were higher than those found in literature, but the equilibrium adsorption capacities were much lower. Mohammed *et al.* (2018) calculated the value of k_2 as 0.029 g.mg⁻¹ min⁻¹, q_e as 88.92 mg.g⁻¹ and an initial rate of adsorption of 229.30 mg.g⁻¹.min⁻¹ with

an initial phenol concentration of 50 ppm by using biochar derived from pine fruit shell through pyrolysis as adsorbent at 25°C. Mubarik *et al.* (2012) calculated the pseudo-second-order rate constant to be 0.018 g.mg⁻¹ min⁻¹, q_e as 24.10 mg.g⁻¹ and an initial rate of adsorption of 10.45 mg.g⁻¹.min⁻¹ with an initial concentration of 25 ppm phenol, by using biochar derived from sawdust as adsorbent at 25°C ± 2°C. However, both the pine fruit shell derived activated carbon and the sawdust biochar had faster initial rates of adsorption, as they consisted of larger surface areas and therefore more active sites that could accommodate the adsorption of more phenol molecules much faster. However, the biochar produced in this study reached equilibrium conditions much faster as the limited amount of active sites could be filled more rapidly compared to adsorbents that have more active sites which takes time to be reached by adsorbate species.

The classification of the isotherm showed that a sufficient number of active sites were available for the adsorption of phenol onto the biochar produced. However, not all the sites were occupied as mineral matter prevented transport deep within the pores of the biochar. Also, the kinetic profile showed that other mechanisms were influencing the rate of adsorption. Therefore, adsorption diffusion models were fitted to the experimental data in order to determine the rate-limiting step influencing the overall rate of adsorption. The adsorption kinetic models such as the pseudo-second-order model cannot be used to determine the rate-limiting step, as they are based on chemical reaction kinetics and therefore not taking the actual movement of the adsorbate through the boundary layer, within the pores and to the surface of the adsorbent into account (Bonilla-Petriciolet *et al.*, 2017). Adsorption processes can mainly be controlled by liquid film diffusion and/or intra-particle diffusion. The reaction step of the adsorbate with the surface of the adsorbent is very rapid and therefore negligible (Qiu *et al.*, 2009).

4.5.2 Intra-particle diffusion model

The kinetic parameters for the intra-particle diffusion model were calculated from plotting the linearised form of the model, as shown in Equation 4-2, to the experimental data and calculating the slope and intercept for each phenol concentration, as shown in Figure 4-16. The parameters and the regression coefficients are shown in Table 4-8.

$$q_t = k_{id} t^{0.5} + C \quad (4-2)$$

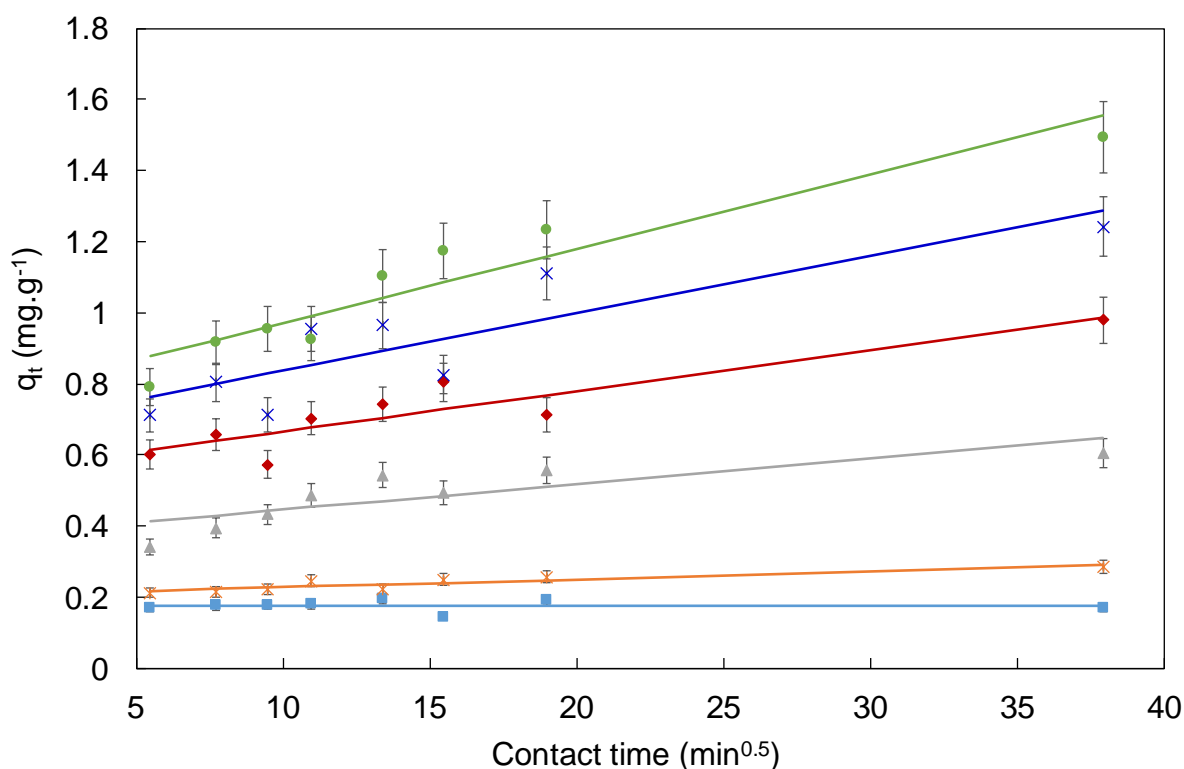


Figure 4-16: Effect of contact time on the intra-particle diffusion of phenol onto PSBC (dosage = 12 g.L⁻¹, pH 8, T= 25°C ± 2°C) (Phenol concentration: ■, 10 ppm; *, 30 ppm; ▲, 60 ppm; ◆, 90 ppm; ×, 120 ppm; ●, 150 ppm)

The linear correlations observed in Figure 4-16 is an indication that intra-particle diffusion plays a role in the adsorption process. Intra-particle diffusion limitations were expected because of the many small micropores of the biochar that were too small to accommodate phenol molecules, as well as the small number of large mesopores where phenol adsorption was likely to occur. Also, the presence of mineral matter further prevented the successful transport of phenol molecules within the pores. However, intra-particle diffusion was not the only rate-limiting step as the straight line plots do not pass through the origin, indicating that other mass transfer phenomena also influenced the overall rate of mass transfer (Kilic *et al.*, 2011). Other authors also found that intra-particle diffusion was applicable and that it was not the only rate-limiting step when adsorbing phenol (Hameed & Rahman, 2008; Kilic *et al.*, 2011; Kumar & Jena, 2016).

Table 4-8: Intra-particle diffusion parameters for phenol adsorption onto biochar at 252°C ± 2°C

C_i (ppm)	k_{id} (mg.g⁻¹.time^{0.5})	P-value	C	P-value	Adj.R²
10	<0.00	0.13	0.16	3.10 x 10 ⁻⁰⁷	0.22
30	1.40 x 10 ⁻⁰⁵	0.07	0.21	1.50 x 10 ⁻⁰⁹	0.35
60	6.63 x 10 ⁻⁰⁵	0.11	0.40	7.73 x 10 ⁻⁰⁷	0.26
90	1.27 x 10 ⁻⁰⁴	0.02	0.59	1.37 x 10 ⁻⁰⁷	0.57
120	1.80 x 10 ⁻⁰⁴	0.04	0.74	1.05 x 10 ⁻⁰⁶	0.45
150	2.43 x 10 ⁻⁰⁴	0.00	0.86	9.04 x 10 ⁻⁰⁸	0.74

As seen from Table 4-8, the boundary layer thickness (C) increased as the initial phenol concentration was increased. The thickening of the boundary layer can be related to the larger concentration of phenol molecules in the solution and therefore more phenol molecules around the biochar particles resulting in film diffusional effects in the liquid phase (Sobiesiak, 2017; Tran *et al.*, 2017).

Intra-particle diffusion did not play a role at all in the mass transfer at an initial phenol concentration of 10 ppm. According to Gholizadeh *et al.* (2013), the adsorption of phenolics at initial low concentrations are expected to occur at the external active sites, whereas higher concentrations will result in pore diffusion and further adsorption. The results of the study therefore indicate that adsorption of phenol onto biochar proceeded by the outer surface adsorption first, followed by pore diffusion in the mesopores and adsorption of phenol onto the internal surface of the biochar particles. At phenol concentrations of 10 ppm and lower, the phenol molecules are adsorbed only onto the outer surface of the biochar and therefore intra-particle diffusion effects were negligible. This is also confirmed by the kinetic profile of the adsorption process where the 10 ppm phenol concentration reached equilibrium much faster than the higher phenol concentrations where intra-particle was more significant. In contrast, higher initial concentrations provided a larger driving force to overcome mass transfer limitations caused by film and intra-particle diffusion. Therefore, at higher phenol concentrations, higher specific rates of adsorption are observed due to an increase in the mass transfer driving force, but more time is required to reach equilibrium due to the rate-limiting effect of intra-particle diffusion and to some degree, film diffusion. In order to determine to what extent film and intra-particle diffusion influenced the adsorption process, the diffusion coefficients for each were determined.

4.5.3 Rate-limiting mass transfer mechanism

The diffusion coefficients for each mass transfer mechanism was calculated based on an average particle radius, r_p of 6.73×10^{-3} cm for the biochar produced. The film diffusion coefficient, D_{film} , were calculated from the slope, as shown in Equation (4-3), by plotting F , the fractional attainment, against $t^{0.5}$. The intra-particle diffusion coefficient, D_{intra} , was calculated from the slope, as shown in Equation (4-4), by plotting $-\ln(1-F^2)$ against t . The diffusion coefficients for each mass transfer mechanism and their regression coefficients are given in Table 4-9. The contributions (%) of each of the two mass transfer mechanisms to the mass transfer limitations experienced during the adsorption process are summarised in Table 4-10.

$$F = 6 \left(\frac{D_{film}}{\pi r_p^2} \right)^{0.5} t^{0.5} \quad (4-3)$$

$$\ln \left(\frac{1}{1-F(t)^2} \right) = \left(\frac{\pi D_{intra}}{r_p^2} \right) t \quad (4-4)$$

As seen in Table 4-9 and Table 4-10, intra-particle diffusion was the main mass transfer mechanism that influenced the adsorption process. According to Doke and Khan (2017), adsorption processes are controlled by pore diffusion if pore diffusion coefficients are in the range of 10^{-11} to 10^{-13} , whereas film diffusion coefficients in the range of 10^{-6} to 10^{-8} indicate that film diffusion was the rate-controlling step. As seen from Table 4-9, the magnitude of the intra-particle diffusion coefficients was within the range of 10^{-11} to 10^{-13} and also larger than the magnitude of the film diffusion coefficients. Therefore, intra-particle diffusion had the largest influence on the adsorption of phenol onto the biochar produced. These results are also in agreement with those found in the previous section.

Table 4-9: Film and intra-particle diffusion coefficients calculated at a temperature of $25^\circ\text{C} \pm 2^\circ\text{C}$

C_i (ppm)	F	D_{film} ($\text{cm}^2.\text{s}^{-1}$)	P-value	Adj.R ²	D_{intra} ($\text{cm}^2.\text{s}^{-1}$)	P-value	Adj.R ²
30	0.86 – 0.98	2.65×10^{-14}	0.86	<0.00	1.12×10^{-11}	0.95	<0.00
60	0.69 – 0.98	2.04×10^{-11}	0.029	0.58	3.61×10^{-10}	0.19	0.18
90	0.68 – 0.88	1.04×10^{-12}	0.53	<0.00	4.55×10^{-11}	0.59	<0.00
120	0.67 – 0.92	9.54×10^{-12}	0.17	0.20	2.17×10^{-10}	0.095	0.35
150	0.65 – 0.85	1.44×10^{-11}	0.0034	0.81	1.74×10^{-10}	0.0025	0.84

The contribution of film diffusion for initial phenol concentrations of 30 ppm – 120 ppm were not significant (p-value > 0.05), except for an initial phenol concentration of 150 ppm (p-value < 0.05) as seen from Table 4-9 and Table 4-10. Therefore, the rotary speed of 150 ppm chosen for the adsorption experiments were sufficient (Karthikeyan *et al.*, 2010). The significant, but still small contribution of film diffusion at an initial phenol concentration of 150 ppm can be attributed to the larger concentration of phenol molecules that had to penetrate the boundary layer around the biochar particles, and therefore more time was spent by the phenol molecules to pass through the boundary layer in order to reach the surface of the biochar, as compared to the lower phenol concentrations used.

Table 4-10: Overall diffusion coefficients for different initial phenol concentrations at 25°C ± 2°C

C_i (ppm)	D_{overall} (cm².s⁻¹)	Contribution of intra-particle diffusion (%)	Contribution of film diffusion (%)
30	1.12 x 10 ⁻¹¹	99.76	0.24
60	3.81 x 10 ⁻¹⁰	94.66	5.34
90	4.65 x 10 ⁻¹¹	97.77	2.23
120	2.26 x 10 ⁻¹⁰	95.79	4.21
150	1.89 x 10 ⁻¹⁰	92.40	7.60

The small contribution of film diffusion (< 8.00%) was also evident from the intra-particle diffusion plots shown in Figure 4-16. The linear plots for the different phenol concentrations started at approximately 5 min⁻¹ or 30 minutes. A half an hour represents only a small fraction of the 24-hour period required for the different experiments to have reached equilibrium conditions. Therefore, the rate-limiting effects were experienced during the first 30 minutes of the adsorption process where intra-particle diffusion was controlling the adsorption rate for the rest of the process. Other authors also found that film diffusion is usually experienced that the start of the adsorption process where intra-particle diffusion limited the adsorption rate thereafter (Abdel-Ghani *et al.*, 2015; Itodo *et al.*, 2010).

The limitations of intra-particle diffusion were expected due to the low surface area and high ash content calculated for the biochar, although the biochar consisted of attractive active sites that were favourable for phenol adsorption. Unfortunately, the presence of mineral matter such as calcite prevented the effective movement of the phenol molecules within the pores and therefore low removal efficiencies were obtained. The biochar produced was however capable of adsorbing

phenol (type C isotherm) but the blockage of the pores by mineral matter resulted in most of the sites being left unoccupied (subclass one isotherm) by the time equilibrium conditions were reached.

4.6 Calcium adsorption

The adsorption of calcium onto biochar was studied at different adsorbent dosages (2 g.L^{-1} – 12 g.L^{-1}) and initial calcium concentrations (600 ppm - 1000 ppm). The results generated revealed that calcium did not adsorb onto the biochar. No significant change in the calcium ion concentration was observed for longer than 24 hours, irrespective of the adsorbent dosage or initial calcium concentration used. This can be attributed to the chemical characteristics of the biochar. As seen from the characterisation results in Section 4.2, the biochar contained significant amounts of calcite, which limited the driving force for mass transport to the surface of the biochar.

The biochar was washed with 1 M hydrochloric acid (HCl) solution in water in an effort to remove the calcite from the pores of the biochar. Subsequent proximate analysis showed only a 12.09 wt.% reduction in the ash content of the biochar, indicating that only some of the calcium was removed from the pore matrix of the biochar. Adsorption of calcium onto the surface of the washed biochar was again attempted with both low and high concentrations (600 ppm, 1000 ppm) of calcium but no adsorption was observed.

Fosso-Kankeu *et al.* (2011) reported that the removal of calcium from wastewater through adsorption is difficult and very limited. However, some other studies did report on the successful adsorption of calcium ions onto mineral-based adsorbents. Cherian *et al.* (2018) who tested the adsorption capabilities of different clays, such as kaolin, bentonite and raw clay, found that calcium adsorption occurred mainly due to the presence of active exchangeable sites available on the clay surfaces. This can be attributed to the high concentration of SiO_2 (> 60%) present in the clay samples that allowed cation exchange reactions to take place, as calcium has been found to have a strong affinity for quartz (Han *et al.*, 2018). Similarly, Sepehr *et al.* (2013) found that removal efficiencies of 83% and 94% for calcium adsorption onto natural (63.45% SiO_2) and modified pumice stones (66.34% SiO_2) were achieved due to ion exchange reactions. Therefore, the adsorption of calcium is expected to take place only due to ion exchange and electrostatic interactions. However, the biochar used in this study contained only a few suitable mineral sites (quartz) to enable ion exchange mechanisms and therefore affected the adsorption of calcium ions negatively.

The limitations of the biochar surface were not the only factor that contributed to calcium not adsorbing. As seen from the FTIR spectra in Figure 4-17, presence of a high concentration of

calcium ions in the adsorption medium resulted in significant changes occurring at mainly the peaks attributed to mineral-based compounds such as kaolinite and calcite.

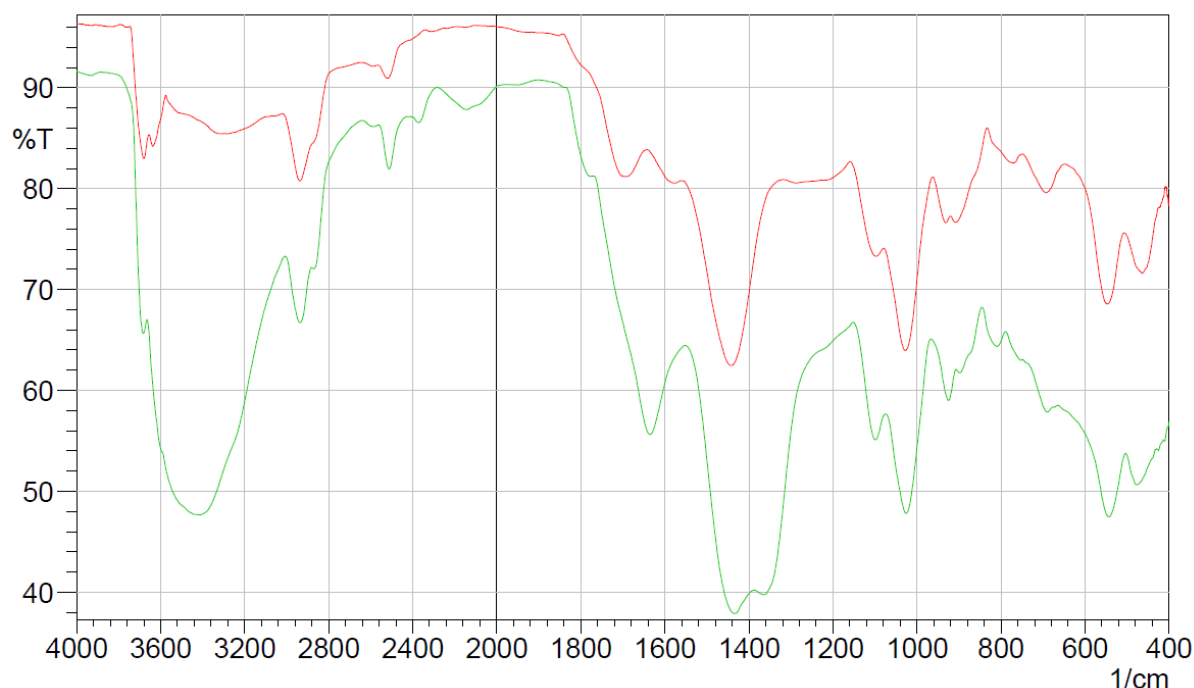


Figure 4-17: FTIR spectra produced for unused biochar (—) and biochar after being exposed to 600 ppm calcium (—)

The two characteristic peaks of kaolinite observed at a wavelength of 3619 cm^{-1} and 3694 cm^{-1} were replaced by a broad and intensified peak at a wavelength of 3434 cm^{-1} . The change observed in the kaolinite peaks can be attributed to the interaction of calcium and hydroxyl ions with the structure of kaolinite. Kaolinite is composed of an octahedral layer of alumina ($\text{Al}_2(\text{OH})_4$) that is sandwiched between two tetrahedral silica surfaces (Si-O_5) (Konan *et al.*, 2007). The presence of the hydroxyl groups can be observed at a wavelength of 3694 cm^{-1} attributed to the stretching vibrations of surface hydroxyl groups and at a wavelength of 3620 cm^{-1} due to inner hydroxyl group vibrations (Chen & Lu, 2015).

At a pH of 8, a considerable number of hydroxyl ions were present in the adsorption medium. The high concentration of calcium ions was free to interact with species such as the hydroxyl ions in the solution, which resulted in the formation of calcium hydroxide ($\text{Ca}(\text{OH})_2$) molecules, a strong base. The free calcium hydroxide ions then interacted with the mineral-based species on the surface of the biochar, thus resulting in changes occurring to the structure of mineral-based species such as kaolinite. According to Frost and Kristóf (2004), modification of kaolinite occurs when an acid or base reacts with the layers within kaolinite. An acid or base species will disrupt the stacking of layers within the structure of kaolinite and therefore produce a disordered structure with structural defects. Thus, the calcium hydroxide in the solution reacted with or attacked the

layers of the kaolinite which resulted in its structure changing from an ordered to a disordered arrangement, as seen by the doublet peaks being replaced by a single peak. According to Ramasamy *et al.* (2009), replacement of the doublet peaks of kaolinite with a single peak indicates that the kaolinite has a disordered structure which resulted from either an acid or a base reacting with the layers of kaolinite. The disordered arrangement of layers within kaolinite also resulted in the exposure of inner hydroxyl groups to the adsorption medium, as seen by the disappearance of the peak at 3620 cm^{-1} , and therefore producing a broad and intensified peak at 3434 cm^{-1} that corresponds to hydroxyl group vibrations.

The introduction of calcium ions into the solution also influenced the structure of the calcite, as the characteristic peak observed at a wavelength of 1437 cm^{-1} split into two smaller peaks observed at wavelengths of 1436 cm^{-1} and 1362 cm^{-1} . According to Cai *et al.* (2010), the splitting of the calcite peak observed at a wavelength of 1425 cm^{-1} have been found to be characteristic of amorphous calcium carbonate. Therefore, the introduction of a high concentration of calcium ions into the adsorption medium resulted in the disruption of the kaolinite and calcite structure, rather than adsorbing onto the surface of the biochar.

4.7 Binary adsorption studies

Although the adsorption of calcium onto biochar was not successful, the presence of calcium ions in the industrial wastewater could have a significant effect on the adsorption of phenol onto the biochar (Tabassi *et al.*, 2017). The adsorption of phenol in the presence of calcium was thus studied, and the effect on the phenol removal efficiency with and without the presence of calcium ions are compared in Figure 4-18. The removal efficiency of phenol decreased by 15.76% with an experimental error of 6.71% based on a 95% confidence level when calcium was added to the adsorption medium.

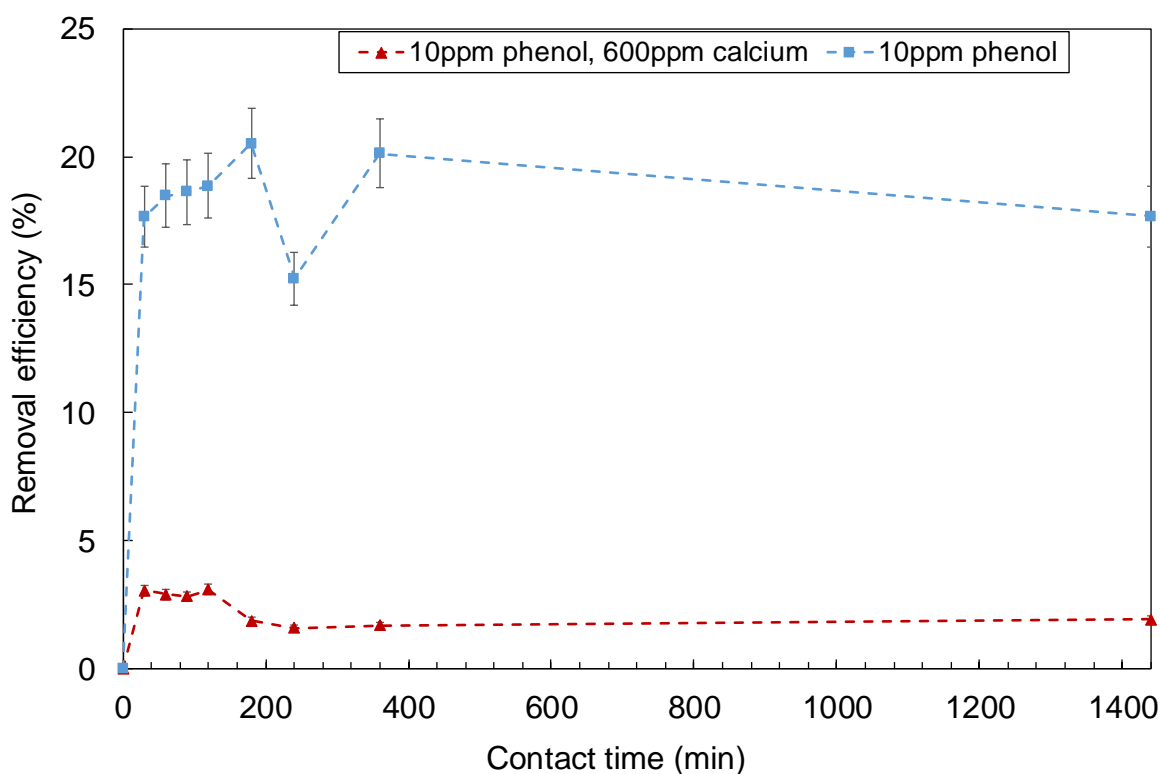


Figure 4-18: Phenol removal efficiency with (▲) and without (■) the presence of 600 ppm calcium (dosage = 12 g.L⁻¹, pH 8, contact time = 1440 min, T= 25°C ± 2°C)

According to Rathore *et al.* (2016), a mixture of adsorbates can result in synergism, antagonism or non-interaction effects between adsorbates. In this case, the addition of calcium into the solution resulted in antagonistic behaviour as the removal efficiency of phenol decreased with 15.76%. The decrease in the phenol removal efficiency can be attributed to the mass transfer limitations experienced in the medium. As seen from the FTIR spectrum in Figure 4-17, the introduction of calcium ions into the solution resulted in the peaks of kaolinite and calcite changing due to the attack of calcium hydroxide molecules. The same can be seen from the FTIR spectrum produced for the binary adsorption of both phenol and calcium shown in Figure 4-19. Therefore, although calcium was not adsorbing to the surface of the biochar, it still moved from the bulk solution, through the boundary layer and to the surface of the biochar while the phenol molecules were trying to do the same. However, the movement of phenol molecules was influenced more than the movement of calcium hydroxide molecules, as the larger concentration of calcium, and therefore calcium hydroxide molecules outweighed the low phenol concentration of 10 ppm. The obstruction of phenol molecules then resulted in the lower removal efficiency obtained compared to the removal efficiency obtained in the absence of calcium.

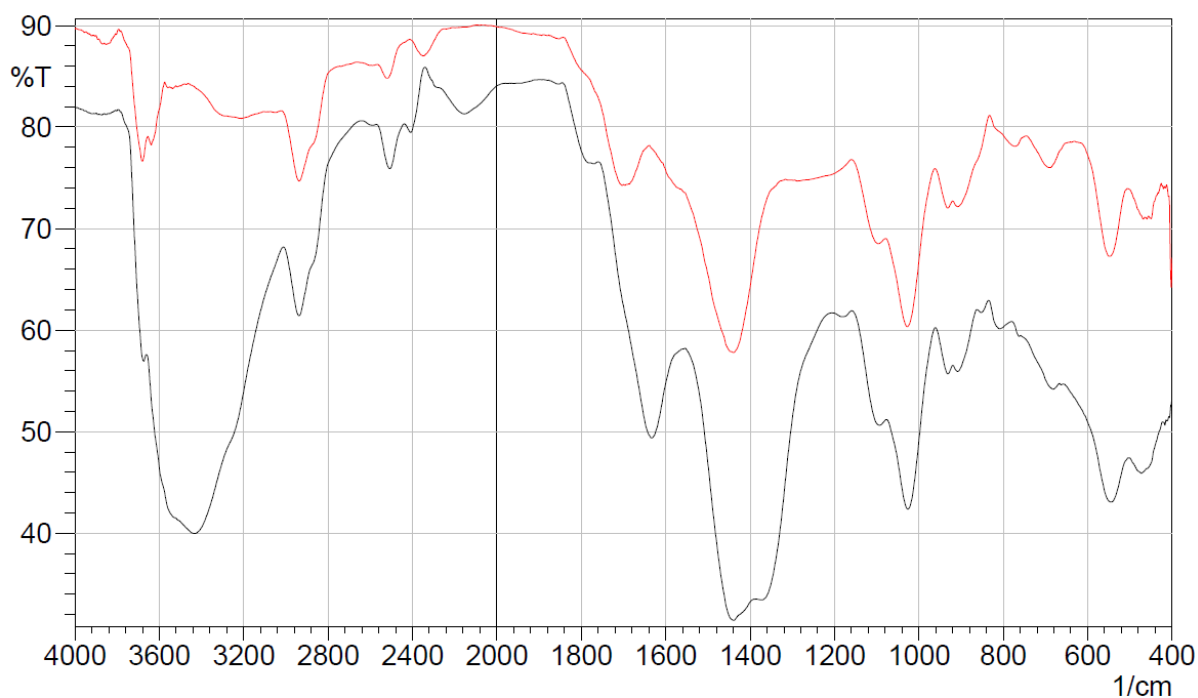


Figure 4-19: FTIR spectra of biochar after 10 ppm phenol adsorption (–) and after binary adsorption with 10 ppm phenol and 600 ppm calcium (–)

The high concentration of calcium did not only change the surface of the biochar but also influenced the adsorbed phenol molecules that successfully reached the surface of the biochar. As seen from Figure 4-18, the biochar after 10 ppm phenol adsorption showed a decrease in the removal efficiency at 240 minutes due to the weak forces between the adsorbed phenol molecules and the surface of the biochar, as discussed in Section 4.5.3. The binary adsorption of phenol in the presence of calcium also showed a similar decrease in the removal efficiency, but after 180 minutes, approximately 60 minutes sooner than in the absence of calcium. Therefore, the introduction of calcium into the solution with phenol resulted in the weakening of already weakly bonded phenol molecules to the surface of the biochar and thus obtained a much lower removal efficiency being at equilibrium conditions as compared to that obtained in the absence of calcium. Also, the binary adsorption of phenol in the presence of calcium reached equilibrium conditions after 180 minutes, faster than the single adsorption of phenol due to the larger degree of mass transfer limitations experienced in the medium. Other authors have also reported that the presence of dissolved salts results in the weakening of forces between phenol and the adsorbent, and therefore producing lower removal efficiencies (Sobiesiak, 2017).

4.8 Wastewater adsorption studies

The adsorptive performance of biochar was tested in both single and binary environments. However, in order to meet the last objective of the project, the adsorptive performance of the biochar was tested in real industrial wastewater as collected from the paper mill. Section 4.8.1

reports the characterisation results obtained for the collected wastewater. Sections 4.8.2 and 4.8.3 discuss the COD and phenolic removal efficiencies of the biochar compared to commercial activated carbon in real industrial wastewater.

4.8.1 Characterisation of wastewater

The collected wastewater was characterised by various methods. As seen from Table 4-11, the wastewater had an alkaline pH and a relatively high total suspended solids (TSS) concentration, as expected for recycling paper mill wastewater (Pokhrel & Viraraghavan, 2004; Rahman & Kabir, 2010). The TSS concentration of 320 ppm was high, as was expected for wastewater that has only been subjected to primary treatment steps, since the primary treatment steps do not remove all the suspended solids (Möbius, 2006). The COD concentration of 2720 ppm was also within the COD concentration range, as expected for typical recycling paper mills (Möbius, 2006). The lower BOD₅ concentration than expected resulted in a BOD₅/COD ratio lower than 0.40. Therefore, tertiary treatment steps such as adsorption are required to treat the wastewater collected, as the wastewater is not readily biodegradable.

The total phenolic concentration, $T_{\text{phenolics}}$, was lower compared to the phenolic content expected in the wastewater produced by the pulp and paper industry. According to Polat *et al.* (2006), phenolic concentrations as high as 22 ppm have been reported for pulp and paper wastewater. However, the concentration of phenol present in the wastewater produced depends on the processes employed during the paper manufacturing process. Mpact's Springs mill is a fibre recycling mill that only re-pulps the feedstock before it is used for the rest of the manufacturing steps. Therefore, low phenol concentrations are expected in the wastewater produced, as no pulping operations are employed during the manufacturing process.

Table 4-11: Characteristic properties of collected industrial wastewater

pH	COD (ppm)	BOD ₅ (ppm)	BOD ₅ /COD	$T_{\text{phenolics}}$ (ppm)	T_{calcium} (ppm)	TDS (ppm)	TSS (ppm)	Conductivity (mS.cm ⁻¹)
7.8	2720	694.40	0.26	8.00	579.12	3794	320	3.045

The calcium concentration in the wastewater was very high, as seen from Table 4-11. The high calcium concentration therefore results in a high calcium carbonate concentration > 300 ppm, indicating that the collected wastewater is very hard water (Kotzé *et al.*, 2014). The high calcium concentrations in the wastewater also agree with the characterisation results of the paper sludge.

Relatively high concentrations of other salt ions such as sodium (381.22 ppm), magnesium (38.50 ppm) and potassium (19.65 ppm) were also found in the wastewater. Furthermore, the

wastewater had a relatively high conductivity owing to the high concentration of dissolved ions, and therefore a high corresponding total dissolved solid (TDS) concentration.

4.8.2 COD removal results

The complex composition of the wastewater and the low concentration of some compounds made qualitative analysis of individual components difficult, and therefore the efficiency of the biochar to lower the COD of the wastewater stream was used as a quantitative measure to follow the removal efficiency. The COD removal efficiencies of the biochar and the activated carbon were measured over a period of 1440 minutes or 24 hours, as shown in Figure 4-20.

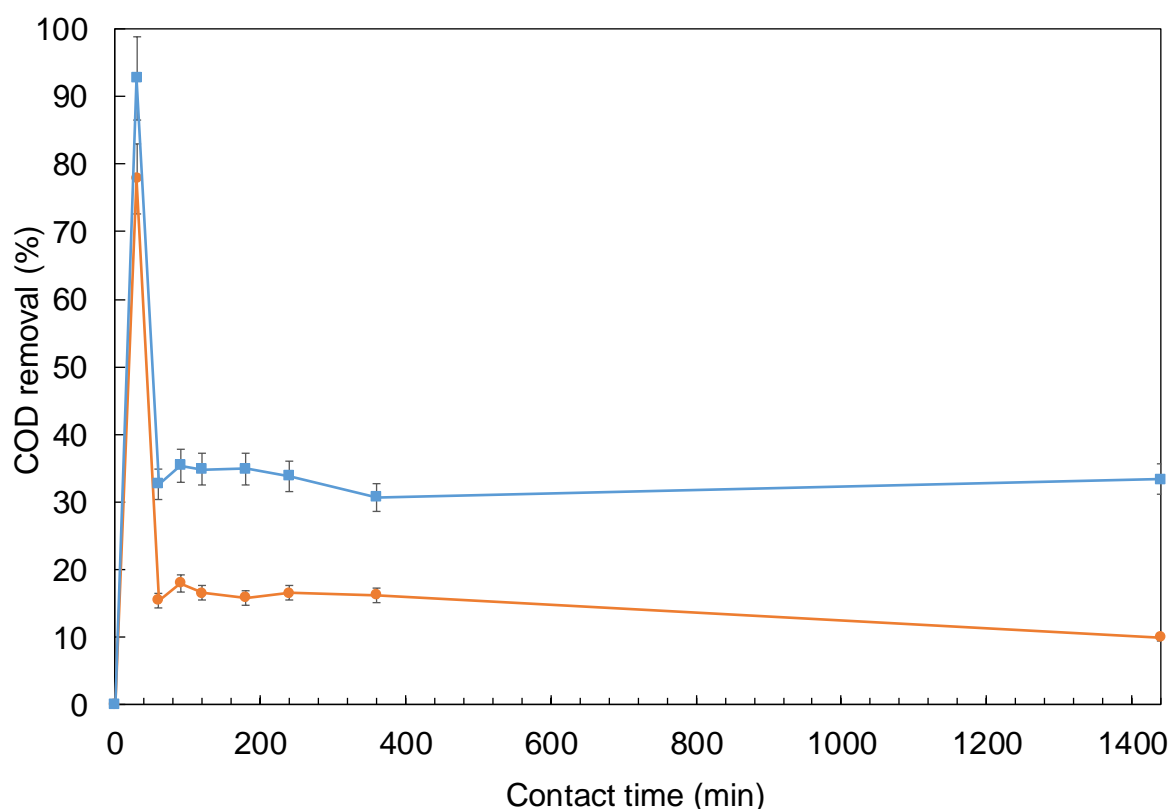


Figure 4-20: COD removal efficiency of biochar (●) compared with activated carbon (■) (dosage = 12 g.L⁻¹, pH 8, contact time = 1440 min, T= 25°C ± 2°C)

As seen from Figure 4-20, both adsorbents achieved their highest COD removal efficiencies within the first 30 minutes of the experiments. Approximately 92.72% ± 6.22% of the COD could be removed by the activated carbon and 77.83 ± 5.22% by the biochar. The process reached equilibrium conditions after 60 minutes, as no significant change in the COD removal efficiency was observed thereafter. In comparison with the single (10 ppm phenol) and binary adsorption (10 ppm phenol, 600 ppm calcium) equilibrium times obtained, more time was required by the biochar to reach equilibrium conditions, as the high concentration of suspended and dissolved matter influenced the movement of phenolics to the surface of the biochar, as seen from Table

4-11. The COD removal efficiency obtained by the activated carbon was in agreement with those found in literature (Huggins *et al.*, 2016). The biochar can be considered as a suitable and inexpensive adsorbent for continuous practical wastewater treatment applications since it removed most of the COD within the first 30 minutes of the process (Zhou *et al.*, 2018). Lastly, the COD removal efficiencies obtained for the biochar by adsorption was higher than other wastewater treatment methods such as ozonation (approximately 20%) and aerobic treatment technologies such as aerated stabilisation basins (67%) and biofilters (52%) (Amat *et al.*, 2005; Ashrafi *et al.*, 2015).

4.8.3 Total phenolic adsorptive performance

The performance of the biochar improved when the adsorbent was subjected to a real wastewater medium. As seen from Table 4-12, the biochar removed almost all of the phenolics out of the wastewater medium within the first 30 minutes of the experiment. The concentration of phenolics still left in the wastewater after a contact time of 30 minutes was well below the allowed limit of 1 ppm for phenolic compounds present in industrial effluents (Tabassi *et al.*, 2017).

Table 4-12: Total phenolic concentration comparison

Adsorbent	Total phenolic concentration (ppm)	
	After 30 min	After 1440 min
Biochar	< 0.20	8.00
Activated carbon	< 0.20	0.80

The performance of the biochar was comparable with the performance of the activated carbon in removing phenolic compounds from the wastewater within the first 30 minutes of the adsorption process. However, the initial total phenol concentration was obtained for the biochar when the adsorption process was left to continue for longer than 30 minutes, as seen in Table 4-12. The activated carbon, on the other hand, also ended with a higher phenolic concentration than obtained after 30 minutes, but much lower in comparison with the phenolic concentration obtained at the end by the biochar. The decrease in the phenolic concentration after 30 minutes can be attributed to the weakening of the forces between the adsorbed phenolics and the surface of each adsorbent, due to the high concentration of dissolved salt species in the wastewater, as seen by the binary adsorption results. However, the high salt concentration did not affect the activated carbon as much as the biochar, since the bonding forces between the phenolics and the surface of the activated carbon was stronger in comparison with the weak intermolecular forces present with the biochar. According to Dąbrowski *et al.* (2005), the adsorption of phenol and phenol derivatives have been found to mainly take place through the formation of electron donor-acceptor complexes and π - π interactions between the surface of the activated carbon and the aromatic

ring of the phenolic compounds. Therefore, the adsorption onto the activated carbon was by the exchange of electrons and thus stronger bonds that are harder to break.

The removal efficiency obtained by the biochar in real industrial wastewater was higher than in a synthetic wastewater environment. That is in contrast with the results reported in literature. According to Rengaraj *et al.* (2002), the removal efficiencies of phenolic compounds from real industrial wastewater is expected to be lower in comparison with the removal efficiencies obtained in synthetic wastewater. This can be attributed to the presence of impurities in the real wastewater that can interfere and also compete in the adsorption process (Ferreira *et al.*, 2017). However, the total phenolic measurements for the real wastewater experiment showed that almost all the phenolic compounds were removed from the wastewater within the first 30 minutes of the experiment, in contrast with the synthetic single and binary results obtained in previous sections. The higher removal efficiency in real wastewater compared with synthetic wastewater can be attributed to the type of phenolics present in the different scenarios. The synthetic single and binary experiments were conducted with the parent compound of the phenolics, phenol. However, the real industrial wastewater did not only contain phenol but a variety of different phenolic compounds, as indicated by the total phenolic concentration, $T_{\text{phenolics}}$, given in Table 4-11.

Different types of phenolic compounds have different adsorption performances due to a difference in water solubility. According to Calace *et al.* (2002), the adsorption of substituted phenolics with a more hydrophobic nature (due to having low pKa values) will adsorb more easily than phenol with a higher solubility and therefore a higher pKa value. The adsorption capacity of substituted phenolics have been found in literature to be higher than that of phenol. According to Mu'azu *et al.* (2017), the adsorption affinity of sludge-based adsorbents was higher for chlorinated and nitrogen-based phenolics, as these groups contained electron-drawing groups that promote adsorption activities. The presence of nitrogen and chlorine-based phenolics/aromatics have been reported to be present in the wastewater produced by the pulp and paper industry (Gholizadeh *et al.*, 2013; Liu *et al.*, 2010; Saleh *et al.*, 2016).

Furthermore, an increase in the ionic strength due to the addition of inorganic salt species like divalent calcium, magnesium, sodium and potassium have been found to promote the adsorption of organic contaminants that are more hydrophobic than phenol, such as phenolics substituted with additional chlorine and nitrogen-based groups. According to Zhang *et al.* (2019), an increase in the ionic strength will promote the adsorption of organic species due to a decrease in component solubility caused by the salting-out effect created by the salt species. This can be attributed to the salt species reducing or destroying the hydration layer around the organic compounds, resulting in decreased solubility (Sobiesiak, 2017). In conclusion, the results obtained for the biochar in a real wastewater environment indicated that biochar could be a

possible replacement for conventional adsorbents, such as activated carbon, for the treatment of industrial wastewater streams when low contact times of 30 minutes are used in the process.

4.9 Concluding remarks

The biochar had unique characteristics that influenced its adsorptive performance to a large extent. The production method selected, HTL mainly influenced the surface characteristics of the biochar, including the surface area, pore size and the surface functional groups. The ash content in the paper sludge contributed to the limited surface area produced during the HTL process since the ash components interfered with effective pore formation.

The biochar succeeded in the removal of phenol from a synthetic solution. Phenol molecules were adsorbed onto the surface of the biochar by forming weak hydrogen bonds between the hydrogen atom of the hydroxyl group present in phenol, and the oxygen atom of the hydroxyl group present in the carboxylic compounds available on the surface of the biochar. The experimental data were therefore well described by a C.1 type adsorption isotherm. However, relatively low removal efficiencies were obtained due to the limited surface area available on the surface of the biochar. The presence of mineral-based species in the biochar prevented the phenol molecules of occupying all the available active sites on the surface of the biochar.

The biochar could not adsorb calcium from a synthetic solution due to the unfavourable chemical composition of the biochar, as well as the disruption of the mineral-based groups on the surface of the biochar by the calcium, rather than adsorbing onto the surface of the biochar. The addition of calcium to the synthetic phenol solution had a negative effect on the adsorption of phenol, and therefore a lower removal efficiency was obtained. However, the biochar succeeded in almost complete removal of the phenolic species present in the real wastewater medium after only 30 minutes due to the presence of other less-soluble substituted phenolic species. High COD removal efficiencies were obtained that were comparable with other tertiary wastewater treatment methods employed in literature. The performance of the biochar was close to that of the activated carbon when a low contact time of 30 minutes was used, indicating the feasibility of biochar as adsorbent for the treatment of contaminant industrial wastewater.

REFERENCES

- Abbaszadeh, S., Alwi, S.R.W., Webb, C., Ghasemi, N. & Muhamad, I.I. 2016. Treatment of lead-contaminated water using activated carbon adsorbent from locally available papaya peel biowaste. *Journal of Cleaner Production*, 118:210-222.
- Abdel-Ghani, N.T., El-Chaghaby, G.A. & Helal, F.S. 2015. Individual and competitive adsorption of phenol and nickel onto multiwalled carbon nanotubes. *Journal of Advanced Research*, 6:405-415.
- Abdel Salam, O.E., Reiad, N.A. & ElShafei, M.M. 2011. A study of the removal characteristics of heavy metals from wastewater by low-cost adsorbents. *Journal of Advanced Research*, 2:297-303.
- Abdelkreem, M. 2013. Adsorption of phenol from industrial wastewater using olive mill waste. *APCBEE Procedia*, 5:349-357.
- Afsharnia, M., Saeidi, M., Zarei, A., Narooie, M.R. & Biglari, H. 2016. Phenol removal from aqueous environment by adsorption onto pomegranate peel carbon. *Electronic Physician*, 8(11):3248-3256.
- Al-Malack, M.H. & Dauda, M. 2017. Competitive adsorption of cadmium and phenol on activated carbon produced from municipal sludge. *Journal of Environmental Chemical Engineering*, 5:2718-2729.
- Amat, A.M., Arques, A., Miranda, M.A. & López, F. 2005. Use of ozone and/or UV in the treatment of effluents from board paper industry. *Chemosphere*, 60:1111-1117.
- Antonides, F. 2000. Simultaneous neutral sulphite semichemical pulping of hardwood and softwood. Durban: University of Natal. (Dissertation: MSc).
- Areeprasert, C., Coppola, A., Urciuolo, M., Chirone, R., Yoshikawa, K., & Scala, F. 2015. The effect of hydrothermal treatment on attrition during the fluidized bed combustion of paper sludge. *Fuel Processing Technology*, 140:57-66.
- Ashrafi, O., Yerushalmi, L. & Haghighat, F. 2015. Wastewater treatment in the pulp-and-paper industry: A review of treatment processes and the associated greenhouse gas emission. *Journal of environmental management*, 158:146-157.
- Ayawei, N., Ebelegi, A.N. & Wankasi, D. 2017. Modelling and Interpretation of Adsorption Isotherms. *Journal of Chemistry*, 2017:1-11.

- Bajpai, P. 2015. Composition of waste. (*In Management of Pulp and Paper Mill Waste*. Switzerland: Springer International Publishing. p. 19-28).
- Beker, U., Ganbold, B., Dertli, H., Gülbayir, D.D. & Duranog, D. 2010. Adsorption of phenol by activated carbon: Influence of activation methods and solution pH. *Energy Conversion and Management*, 51:235-240.
- Bonilla-Petriciolet, A., Mendoza-Castillo, D.I. & Reynel-Ávila, H.E. 2017. Adsorption processes for water treatment and purification. Switzerland: Springer International Publishing.
- Cai, G., Bin, Chen, S.F., Liu, L., Jiang, J., Yao, H., Bin, Xu, A.W. & Yu, S.H. 2010. 1,3-Diamino-2-hydroxypropane-N,N,N',N'-tetraacetic acid stabilized amorphous calcium carbonate: Nucleation, transformation and crystal growth. *CrystEngComm*, 12:234-241.
- Calace, N., Nardi, E., Petronio, B.M. & Pietroletti, M. 2002. Adsorption of phenols by papermill sludges. *Environmental Pollution*, 118(3):315-319.
- Calisto, V., Ferreira, C.I.A., Santos, S.M., Gil, M.V., Otero, M. & Esteves, V.I. 2014. Production of adsorbents by pyrolysis of paper mill sludge and application on the removal of citalopram from water. *Bioresource Technology*, 166:335-344.
- Chen, Y.H. & Lu, D.L. 2015. CO₂ capture by kaolinite and its adsorption mechanism. *Applied Clay Science*, 104:221-228.
- Cherian, C., Kollannur, N.J., Bandipally, S. & Arnepalli, D.N. 2018. Calcium adsorption on clays: effects of mineralogy, pore fluid chemistry and temperature. *Applied Clay Science*, 160:282-289.
- Choat, B., Cobb, A.R. & Jansen, S. 2008. Structure and function of bordered pits: new discoveries and impacts on whole-plant hydraulic function. *New Phytologist*, (177):608-626.
- Dąbrowski, A., Podkościelny, P., Hubicki, Z. & Barczak, M. 2005. Adsorption of phenolic compounds by activated carbon – A critical review. *Chemosphere*, 58(8):1049-1070.
- Davis, W., Erickson, C., Johnston, C., Delfino, J. & Porter, J. 1999. Quantitative fourier transform infrared spectroscopic investigation of humic substance functional group composition. *Chemosphere*, 38(12):2913-2928.
- Devi, P. & Saroha, A.K. 2015. Effect of pyrolysis temperature on polycyclic aromatic hydrocarbons toxicity and sorption behaviour of biochars prepared by pyrolysis of paper mill effluent treatment plant sludge. *Bioresource Technology*, 192:312-320.

Doke, K.M. & Khan, E.M. 2017. Equilibrium, kinetic and diffusion mechanism of Cr(VI) adsorption onto activated carbon derived from wood apple shell. *Arabian Journal of Chemistry*, 10:S252-S260.

Dursun, G., Çiçek, H., Dursun, A.Y. & Handan, C. 2005. Adsorption of phenol from aqueous solution by using carbonised beet pulp. *Journal of Hazardous Materials*, B125:175-182.

El-Naas, M.H., Al-Zuhair, S. & Alhaija, M.A. 2010. Removal of phenol from petroleum refinery wastewater through adsorption on date-pit activated carbon. *Chemical Engineering Journal*, 162:997-1005.

Ferreira, C.I.A., Calisto, V., Otero, M., Nadais, H. & Esteves, V.I. 2017. Removal of tricaine methanesulfonate from aquaculture wastewater by adsorption onto pyrolysed paper mill sludge. *Chemosphere*, 168:139-146.

Fosso-Kankeu, E., Mulaba-Bafubiandi, A.F., Mamba, B.B. & Barnard, T.G. 2011. Prediction of metal-adsorption behaviour in the remediation of water contamination using indigenous microorganisms. *Journal of Environmental Management*, 92(10):2786-2793.

Frost, R. & Kristóf, J. 2004. Raman and infrared spectroscopic studies of kaolinite surfaces modified by intercalation. *Interface Science and Technology*, 1:1-36.

Gascó, G., Paz-Ferreiro, J., Álvarez, M.L., Saa, A. & Méndez, A. 2018. Biochars and hydrochars prepared by pyrolysis and hydrothermal carbonisation of pig manure. *Waste Management*, 79:395-403.

Gholizadeh, A., Kermani, M., Gholami, M. & Farzadkia, M. 2013. Kinetic and isotherm studies of adsorption and biosorption processes in the removal of phenolic compounds from aqueous solutions: comparative study. *Journal of Environmental Health Science and Engineering*, 11(29):1-10.

Giles, C., MacEwan, T., Nakhwa, S. & Smith, D. 1960. Studies in adsorption. Part XI. A system of classification of solution adsorption isotherms, and its use in diagnosis of adsorption mechanisms and in measurement of specific surface areas of solids. *Journal of Chemical Society*, 3973-3993.

Giraldo, L. & Moreno-piraján, J.C. 2014. Study of adsorption of phenol on activated carbons obtained from eggshells. *Journal of Analytical and Applied Pyrolysis*, 106:41-47.

Girish, C.R. 2017. Various isotherm models for multicomponent adsorption: A review. *International Journal of Civil Engineering and Technology*, 8(10):80-86.

- Hameed, B.H. & Rahman, A.A. 2008. Removal of phenol from aqueous solutions by adsorption onto activated carbon prepared from biomass material. *Journal of Hazardous Materials*, 160:576-581.
- Han, C., Liu, W., Wang, X., Duan, H., Wei, D. & Wang, B. 2018. The adsorption mechanism of calcium ion on quartz (101) surface: A DFT study. *Powder Technology*, 329:158-166.
- Hojamberdiev, M., Kameshima, Y., Nakajima, A., Okada, K. & Kadirova, Z. 2008. Preparation and sorption properties of materials from paper sludge. *Journal of Hazardous Materials*, 151:710-719.
- Huggins, T.M., Haeger, A., Biffinger, J.C. & Ren, Z.J. 2016. Granular biochar compared with activated carbon for wastewater treatment and resource recovery. *Water Research*, 94:225-232.
- Ichiura, H., Nakatani, T. & Ohtani, Y. 2011. Separation of pulp and inorganic materials from paper sludge using ionic liquid and centrifugation. *Chemical Engineering Journal*, 173:129-134.
- Itodo, A., Abdulrahman, F., Hassan, L., Maigandi, S.A. & Itodo, H. 2010. Intraparticle diffusion and intraparticulate diffusivities of herbicide on derived activated carbon. *Researcher*, 2(2):74-86.
- Jaria, G., Calisto, V., Gil, M.V., Otero, M. & Esteves, V.I. 2015. Removal of fluoxetine from water by adsorbent materials produced from paper mill sludge. *Journal of Colloid and Interface Science*, 448:32-40.
- Kang, S., Li, X., Fan, J. & Chang, J. 2013. Hydrothermal conversion of lignin: A review. *Renewable and Sustainable Energy Reviews*, 27:546-558.
- Karthikeyan, S., Sivakumar, B. & Sivakumar, N. 2010. Film and pore diffusion modelling for adsorption of reactive red 2 from aqueous solution on to activated carbon prepared from bio-diesel industrial waste. *E-Journal of Chemistry*, 7(S1):175-185.
- Khalili, N.R., Vyas, J.D., Weangkaew, W., Westfall, S.J., Parulekar, S.J. & Sherwood, R. 2002. Synthesis and characterization of activated carbon and bioactive adsorbent produced from paper mill sludge. *Separation and Purification Technology*, 26:295-304.
- Kilic, M., Apaydin-varol, E. & Pütün, E. 2011. Adsorptive removal of phenol from aqueous solutions on activated carbon prepared from tobacco residues: Equilibrium, kinetics and thermodynamics. *Journal of Hazardous Materials*, 189:397-403.

- Kizinievič, O., Kizinievič, V. & Malaiškienė, J. 2018. Analysis of the effect of paper sludge on the properties, microstructure and frost resistance of clay bricks. *Construction and Building Materials*, 169:689-696.
- Konan, K.L., Peyratout, C., Bonnet, J.P., Smith, A., Jacquet, A., Magnoux, P. & Ayrault, P. 2007. Surface properties of kaolin and illite suspensions in concentrated calcium hydroxide medium. *Journal of Colloid and Interface Science*, 307(1):101-108.
- Kotzé, N., Johnston, S., Harper, C.L., Masters, G.M. & Maier, P. 2014. The impact of engineering on society. Second ed. Harlow: Pearson.
- Kumar, A. & Jena, H.M. 2016. Removal of methylene blue and phenol onto prepared activated carbon from Fox nutshell by chemical activation in batch and fixed-bed column. *Journal of Cleaner Production*, 137:1246-1259.
- Kuokkanen, T., Nurmesniemi, H., Pöykiö, R., Kujala, K., Kaakinen, J. & Kuokkanen, M. 2008. Chemical and leaching properties of paper mill sludge. *Chemical Speciation and Bioavailability*, 20(2):111-122.
- Leng, L.J., Yuan, X.Z., Huang, H.J., Wang, H., Wu, Z., Bin, Fu, L.H., Peng, X., Chen, X.H. & Zeng, G.M. 2015. Characterization and application of bio-chars from liquefaction of microalgae, lignocellulosic biomass and sewage sludge. *Fuel Processing Technology*, 129:8-14.
- Lin, Y., Ma, X., Peng, X.X., Hu, S., Yu, Z. & Fang, S. 2015. Effect of hydrothermal carbonization temperature on combustion behavior of hydrochar fuel from paper sludge. *Applied Thermal Engineering*, 91:574-582.
- Liu, Z., Quek, A., Hoekman, S.K. & Balasubramanian, R. 2013. Production of solid biochar fuel from waste biomass by hydrothermal carbonization. *Fuel*, 103:943-949.
- Liu, Z., Zhang, F.S. & Wu, J. 2010. Characterization and application of chars produced from pinewood pyrolysis and hydrothermal treatment. *Fuel*, 89:510-514.
- Lorenc-Grabowska, E. 2016. Effect of micropore size distribution on phenol adsorption on steam activated carbons. *Adsorption*, 22:599-607.
- Lupoi, J.S., Singh, S., Parthasarathi, R., Simmons, B.A. & Henry, R.J. 2015. Recent innovations in analytical methods for the qualitative and quantitative assessment of lignin. *Renewable and Sustainable Energy Reviews*, 49:871-906.

- Mäkelä, M., Fullana, A. & Yoshikawa, K. 2016. Ash behavior during hydrothermal treatment for solid fuel applications. Part 1: Overview of different feedstock. *Energy Conversion and Management*, 121:402-408.
- Méndez, A., Barriga, S., Fidalgo, J.M. & Gascó, G. 2009. Adsorbent materials from paper industry waste materials and their use in Cu(II) removal from water. *Journal of Hazardous Materials*, 165:736-743.
- Miao, Q., Tang, Y., Xu, J., Liu, X., Xiao, L. & Chen, Q. 2013. Activated carbon prepared from soybean straw for phenol adsorption. *Journal of the Taiwan Institute of Chemical Engineers*, 44:458-465.
- Möbius, C.H. 2006. Water use and wastewater treatment in papermills. Norderstedt: Books on Demand GmbH.
- Mohammed, N.A.S., Abu-zurayk, R.A., Hamadneh, I. & Al-Dujaili, A.H. 2018. Phenol adsorption on biochar prepared from the pine fruit shells: Equilibrium, kinetic and thermodynamics studies. *Journal of Environmental Management*, 226:377-385.
- Mohan, D., Sarswat, A., Ok, Y.S., & Pittman, C.U. 2014. Organic and inorganic contaminants removal from water with biochar, a renewable, low cost and sustainable adsorbent – A critical review. *Bioresource technology*, 160:191-202.
- Mu'azu, N.D., Jarrah, N., Zubair, M., & Alagha, O. 2017. Removal of phenolic compounds from water using sewage sludge-based activated carbon adsorption: A review. *International Journal of Environmental Research and Public Health*, 14(10):1-34.
- Mubarik, S., Saeed, A., Mehmood, Z. & Iqbal, M. 2012. Phenol adsorption by charred sawdust of sheesham (Indian rosewood; *Dalbergia sissoo*) from single, binary and ternary contaminated solutions. *Journal of the Taiwan Institute of Chemical Engineers*, 43:926-933.
- Okada, K., Yamamoto, N., Kameshima, Y. & Yasumori, A. 2003. Porous properties of activated carbons from waste newspaper prepared by chemical and physical activation. *Journal of Colloid and Interface Science*, 262:179-193.
- Oliveira, G., Calisto, V., Santos, S.M., Otero, M. & Esteves, V.I. 2018. Paper pulp-based adsorbents for the removal of pharmaceuticals from wastewater: A novel approach towards diversification. *Science of the Total Environment*, 631-632:1018-1028.

- Ouallal, H., Dehmani, Y., Moussout, H., Messaoudi, L. & Azrour, M. 2019. Kinetic, isotherm and mechanism investigations of the removal of phenols from water by raw and calcined clays. *Heliyon*, 5(5).
- Pokhrel, D. & Viraraghavan, T. 2004. Treatment of pulp and paper mill wastewater – A review. *Science of the Total Environment*, 333(1-3):37-58.
- Polat, H., Molva, M. & Polat, M. 2006. Capacity and mechanism of phenol adsorption on lignite. *International Journal of Mineral Processing*, 79:264-273.
- Potgieter, J., Bada, S. & Potgieter-Vermaak, S. 2009. Adsorptive removal of various phenols from water by South African coal fly ash. *Water SA*, 35:89-96.
- Purnomo, C.W., Salim, C. & Hinode, H. 2012. Effect of the activation method on the properties and adsorption behavior of bagasse fly ash-based activated carbon. *Fuel Processing Technology*, 102:132-139.
- Qiu, H., Lv, L., Pan, B.C., Zhang, Q.J., Zhang, W.M. & Zhang, Q.X. 2009. Critical review in adsorption kinetic models. *Journal of Zhejiang University: Science A*, 10(5):716-724.
- Rahman, M.M. & Kabir, K.B. 2010. Wastewater treatment options for paper mills using recycled paper/imported pulps as raw materials: Bangladesh perspective. *Chemical Engineering Research Bulletin*, 14:65-68.
- Ramasamy, V., Rajkumar, P. & Ponnusamy, V. 2009. Depth wise analysis of recently excavated Vellar river sediments through FTIR and XRD studies. *Indian Journal of Physics*, 83(9):1295-1308.
- Rathore, V.K., Dohare, D.K. & Mondal, P. 2016. Competitive adsorption between arsenic and fluoride from binary mixture on chemically treated laterite. *Journal of Environmental Chemical Engineering*, 4:2417-2430.
- Rengaraj, S., Moon, S.H., Sivabalan, R., Arabindoo, B. & Murugesan, V. 2002. Agricultural solid waste for the removal of organics: Adsorption of phenol from water and wastewater by palm seed coat activated carbon. *Waste Management*, 22:543-548.
- Saleh, S., Kamarudin, K.B., Ghani, W.A.W.A.K. & Kheang, L.S. 2016. Removal of organic contaminant from aqueous solution using magnetic biochar. *Procedia Engineering*, 148:228-235.
- Sepehr, M., Mansur, Z., Hossein, K., Abdeltif, A., Kamiar, Y. & Hamid, R.G. 2013. Removal of hardness agents, calcium and magnesium, by natural and alkaline modified pumice stones in single and binary systems. *Applied surface science*, 274:295-305.

Singh, N. & Balomajumder, C. 2016. Simultaneous removal of phenol and cyanide from aqueous solution by adsorption onto surface modified activated carbon prepared from coconut shell. *Journal of Water Process Engineering*, 9:233-245.

Sobiesiak, M. 2017. Chemical structure of phenols and its consequence for sorption processes. (In Soto-Hernández, M., Tenango, M.P., García-Mateos, R. (Eds.), Phenolic compounds natural sources, importance and applications. IntechOpen, pp. 3-28.).

Tabassi, D., Harbi, S., Louati, I. & Hamrouni, B. 2017. Response surface methodology for optimization of phenol adsorption by activated carbon: Isotherm and kinetics study. *Indian Journal of Chemical Technology*, 24:239-255.

Tancredi, N., Medero, N., Möller, F., Píriz, J., Plada, C. & Cordero, T. 2004. Phenol adsorption onto powdered and granular activated carbon, prepared from Eucalyptus wood. *Journal of Colloid and Interface Science*, 279:357-363.

Tran, H.N., You, S.J., Hosseini-Bandegharai, A. & Chao, H.P. 2017. Mistakes and inconsistencies regarding adsorption of contaminants from aqueous solutions: A critical review. *Water Research*, 120:88-116.

Veluchamy, C. & Kalamdhad, A.S. 2017. Enhancement of hydrolysis of lignocellulose waste pulp and paper mill sludge through different heating processes on thermal pretreatment. *Journal of Cleaner Production*, 168:219-226.

Villar da Gama, B.M., Elisandra do Nascimento, G., Silva Sales, D.C., Rodríguez-Díaz, J.M., Bezerra de Menezes Barbosa, C.M. & Menezes Bezerra Duarte, M.M. 2018. Mono and binary component adsorption of phenol and cadmium using adsorbent derived from peanut shells. *Journal of Cleaner Production*, 201:219-228.

Wong, S., Ngadi, N., Inuwa, I.M. & Hassan, O. 2018. Recent advances in applications of activated carbon from biowaste for wastewater treatment: A short review. *Journal of Cleaner Production*, 175:361-375.

Xu, X., Hu, X., Ding, Z., Chen, Y. & Gao, B. 2017. Waste-art-paper biochar as an effective sorbent for recovery of aqueous Pb(II) into value-added PbO nanoparticles. *Chemical Engineering Journal*, 308:863-871.

Yao, Z., Ma, X., Wu, Z. & Yao, T. 2017. TGA–FTIR analysis of co-pyrolysis characteristics of hydrochar and paper sludge. *Journal of Analytical and Applied Pyrolysis*, 123:40-48.

- Yoon, K., Cho, D.W., Tsang, D.C.W.W., Bolan, N., Rinklebe, J. & Song, H. 2017. Fabrication of engineered biochar from paper mill sludge and its application into removal of arsenic and cadmium in acidic water. *Bioresource Technology*, 246:69-75.
- Yousef, R.I., El-Eswed, B. & Al-Muhtaseb, A.H. 2011. Adsorption characteristics of natural zeolites as solid adsorbents for phenol removal from aqueous solutions: Kinetics, mechanism, and thermodynamics studies. *Chemical Engineering Journal*, 171:1143-1149.
- Zhang, D., Huo, P. & Liu, W. 2016. Behavior of phenol adsorption on thermal modified activated carbon. *Chinese Journal of Chemical Engineering*, 24:446-452.
- Zhang, J., Shao, J., Jin, Q., Li, Z., Zhang, X., Chen, Y., Zhang, S. & Chen, H. 2019. Sludge-based biochar activation to enhance Pb(II) adsorption. *Fuel*, 252:101-108.
- Zhang, M., Gao, B., Yao, Y., Xue, Y. & Inyang, M. 2012. Synthesis of porous MgO-biochar nanocomposites for removal of phosphate and nitrate from aqueous solutions. *Chemical Engineering Journal*, 210:26-32.
- Zhou, H., Wei, C., Zhang, F., Liao, J., Hu, Y. & Wu, H. 2018. Energy-saving optimization of coking wastewater treated by aerobic bio-treatment integrating two-stage activated carbon adsorption. *Journal of Cleaner Production*, 175:467-476.
- Zhou, Y., Liu, X., Xiang, Y., Wang, P., Zhang, J., Zhang, F., Wei, J., Luo, L., Lei, M. & Tang, L. 2017. Modification of biochar derived from sawdust and its application in removal of tetracycline and copper from aqueous solution: Adsorption mechanism and modelling. *Bioresource Technology*, 245:266-273.
- Zhuang, X., Zhan, H., Song, Y., He, C., Huang, Y., Yin, X. & Wu, C. 2019. Insights into the evolution of chemical structures in lignocellulose and non-lignocellulose biowastes during hydrothermal carbonization (HTC). *Fuel*, 236:960-974.

CHAPTER 5 – CONCLUSIONS AND RECOMMENDATIONS

In this chapter, the main outcomes achieved for the usage of biochar derived from paper sludge as adsorbent for the co-adsorption of phenol and calcium for an industrial wastewater stream are summarised. The main conclusions are given in Section 5.1, followed by possible recommendations for future studies in Section 5.2.

5.1 Conclusions

In this study, it was evident that biochar derived from paper sludge can be used as an adsorbent to remove hazardous organic pollutants such as phenol and/or phenol derivatives from both synthetic and real industrial wastewater streams. However, low phenol removal efficiencies were obtained in synthetic phenol solutions due to the low surface area and therefore the limited number of active sites available on the surface of the produced biochar. The low surface area was largely contributed to the blockage of pores by mineral based compounds such as calcite and kaolinite.

The produced biochar is not an appropriate adsorbent to remove calcium from both synthetic and real wastewater streams, due to its inherent chemical nature that was unfavourable for calcium adsorption. Also, it was shown that calcium, in co-operation with the hydroxyl ions in the solution, resulted in structural changes occurring of the mineral-based groups such as kaolinite and calcite located on the surface of the biochar. Therefore, the calcium in the solution did not adsorb but rather altered the structure of some of the surface functional groups present on the surface of the biochar.

The presence of calcium in a binary setting of both phenol and calcium influenced the adsorption of phenol negatively. The phenol removal efficiency decreased with $15.76\% \pm 1.06\%$ when calcium was added to the solution. This can be attributed to the mass transfer limitations experienced in the medium due to the high concentration of calcium hydroxide molecules diffusing to the surface of the biochar and therefore constricting the movement of the limited number of phenol molecules in the solution.

The adsorption experiments in the real industrial wastewater medium was much more successful than the synthetic adsorption experiments due to presence of less-soluble phenolics other than phenol. The biochar achieved a COD removal efficiency of $77.83\% \pm 5.22\%$, close to the COD removal efficiency of $92.72\% \pm 6.22\%$ obtained by the commercial activated carbon. Therefore, biochar derived from paper sludge has the potential to replace expensive adsorbents such as activated carbon to remove harmful organic pollutants from real industrial wastewater streams.

The impact of the pulp and paper industry will also be reduced by the usage of paper sludge for adsorbent production and applications. Firstly, the direct usage of wet biomass such as paper

sludge for HTL purposes offers cost-effective waste management solutions that can be used as an alternative to the current disposal methods employed. And secondly, pulp and paper mills can now utilise their own waste products such as paper sludge to clean the wastewater produced during the paper manufacturing activities. This will then result in the production of cleaner water that can be re-circulated back into the system and therefore the demand for freshwater resources by the pulp and paper industry can be reduced.

5.2 Recommendations

The characterisation results showed that the paper sludge, and therefore the produced biochar, was rich in mineral-based species such as calcite and kaolinite. From the phenol adsorption results, it was evident that the presence of these mineral-based species prevented the movement of phenol molecules within pores of the biochar as intra-particle diffusion limited the adsorption process. Therefore, the removal of ash compounds from the paper sludge before the production of the biochar should be considered to ensure that pore development is not limited during the HTL process, producing biochar with more favourable adsorption characteristics.

The calcium adsorption studies showed that with or without ash compounds present, adsorption of calcium onto the paper sludge-based biochar was not possible. Also, the removal of calcium by adsorption treatment methods are hardly employed in literature due to the challenges involved with the process. Therefore, alternative treatment methods such as chemical precipitation should be considered to remove calcium from industrial wastewater streams, followed by adsorption treatment steps to remove the phenolics present in the received wastewater.

APPENDIX A

A.1 Batch hydrothermal liquefaction: standard operating procedure

1. Place biomass and solvent into the reactor sleeve.
2. Load the sleeve into the reactor.
3. Fit the top of the reactor to the bottom, ensuring a good seal along the gasket.
4. Rotate the top to align the markings on the top and bottom, this will correctly align the bolt holes.
5. Lubricate the bolts with copper slip and insert into holes.
6. Tighten the bolts in a crisscross pattern using a torque wrench to 40, 60 and 70 Nm.
7. Connect the gas lines to the reactor.
8. Switch the extractor on.
9. Check that all connections are properly tightened.
10. Check that the **inlet** valve is closed.
11. Open the gas supply and set the pressure to the starting pressure.
12. Check that the **outlet** valve is closed.
13. Slowly open the **inlet** valve and monitor the reactor pressure.
14. Slowly close the inlet valve when the desired pressure is obtained.
15. Check the pressure gauge to ensure that no gas leak is present.
16. Inspect all seals for integrity.
(Use a diluted soap solution to check all connections and bolts for leaks.)
17. Check that the **inlet** valve is closed.
18. Slowly open the **outlet** valve to purge the reactor to atmospheric pressure.
19. Close the **outlet** valve.
20. Slowly open the **inlet** valve to pressurise reactor to starting pressure.
21. Close the **inlet** valve when the starting pressure is reached.
22. Attach the heating jackets to the reactor.
23. Ensure that all connecting wires are away from surfaces that will be heated.
24. Switch on the heating jacket.
25. Continuously monitor the reactor temperature and pressure until the desired conditions are reached.
26. Switch off the heating jackets.
27. Allow the reactor to cool to below 30°C.
28. Vent the reactor by slowly opening the **outlet** valve.
29. Disconnect the gas lines from the reactor.
30. Loosen the bolts in a crisscross pattern.
31. Carefully remove reactor top.

32. Remove the sleeve from the reactor.
33. Transfer the products from the sleeve to appropriate containers.
34. Clean the inside of the reactor, reactor top, gasket, and sleeve.
35. Remove any debris from bolt holes.

A.2 Phenol calibration curve

The phenol calibration curve was constructed in order to determine the phenol concentration for a given peak area when produced for a given sample. Different phenol stock solutions were prepared and their corresponding areas were determined by HPLC analysis. The results of the phenol calibrations are shown in Figure A-1.

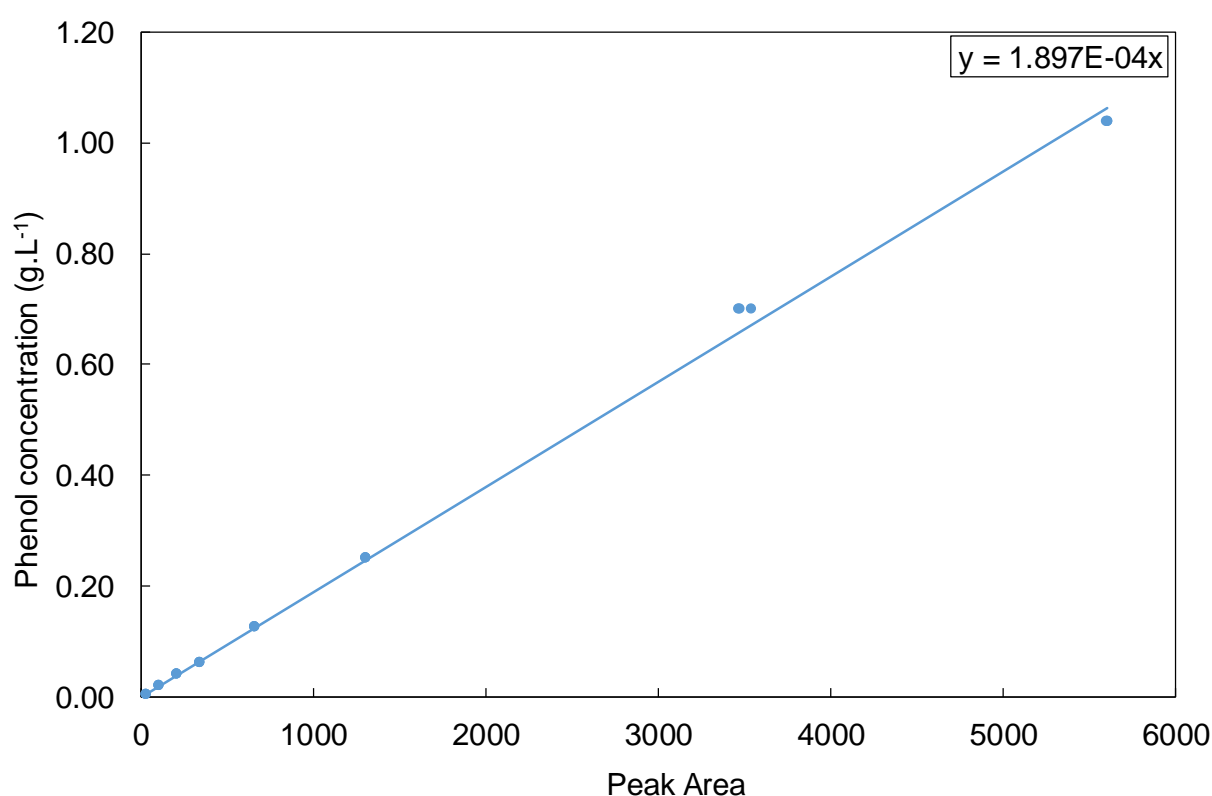


Figure A-1: The phenol calibration curve.

The final phenol calibration was calculated as shown in Equation (A-1)

$$C_{phenol} = 1.86 \times 10^{-4} (area) \quad (A-1)$$

where the phenol concentration is calculated in g.L⁻¹.

APPENDIX B

B.1 Preliminary adsorption experiments

Preliminary adsorption experiments were performed at a pH of 8 and an initial phenol concentration of 1000 ppm to determine the adsorption capabilities of the biochar towards phenol. The biochar was able to remove 143.61 ppm phenol within the first 1620 minutes or 27 hours of the experiment. The experiment was performed at a temperature of $25^{\circ}\text{C} \pm 2^{\circ}\text{C}$, a rotary speed of 150 rpm and a biochar dosage of 10 g.L^{-1} . It was therefore decided to choose a maximum initial phenol concentration of 150 ppm, as that was the maximum concentration of phenol the biochar could remove. The lower initial phenol concentration of 10 ppm was chosen, as it was close to the total phenol concentration in the collected industrial wastewater.

B.2 Raw adsorption data

The raw data generated during the different adsorption experiments for each sampling period is given in this section. The raw data generated during the phenol adsorbent dosage experiments at an initial phenol concentration of 150 ppm is given in Table B-1. The concentration was calculated from the area determined by HPLC analysis as shown in Equation A-1.

Table B-1: Raw data obtained from changing the adsorbent dosage

Adsorbent dosage (g.L^{-1})	Time (min)	Area	Concentration (ppm)
2	0	786.25	146.24
	30	770.16	143.25
	60	770.14	143.25
	90	750.74	139.64
	120	757	140.80
	180	757.29	140.86
	240	748.98	139.31
	360	751.54	139.79
	1440	742.52	138.11
4	0	786.25	146.24
	30	747.43	139.02
	60	748.27	139.18
	90	747.09	138.96
	120	743.49	138.29
	180	743.78	138.34
	240	741.88	137.99
	360	741.92	138.00
	1440	729.11	135.61

6	0	786.25	146.24
	30	747.34	139.01
	60	741.96	138.00
	90	739.67	137.58
	120	739.72	137.59
	180	739.01	137.46
	240	734.28	136.58
	360	731.21	136.01
	1440	724.74	134.80
8	0	786.25	146.24
	30	741.19	137.86
	60	736.01	136.90
	90	739.71	137.59
	120	730.56	135.88
	180	727.51	135.32
	240	724.32	134.72
	360	722.18	134.33
	1440	714.34	132.87
10	0	786.25	146.24
	30	740.88	137.80
	60	734.04	136.53
	90	728.85	135.57
	120	727.79	135.37
	180	723.29	134.53
	240	720.71	134.05
	360	714.85	132.96
	1440	704.07	130.96
12	0	786.25	146.24
	30	735.04	136.72
	60	726.91	135.21
	90	724.51	134.76
	120	726.29	135.09
	180	714.75	132.94
	240	710.3	132.12
	360	706.39	131.39
	1440	689.56	128.26

The raw data generated when the initial phenol concentration was varied between 10 ppm – 150 ppm is given in Table B-2. The concentration was calculated from the area determined by HPLC analysis as shown in Equation A-1.

Table B-2: Raw data obtained from the changing the initial phenol concentration

Initial phenol concentration (ppm)	Time (min)	Area	Concentration (ppm)
10	0	61.62	11.46
	30	50.745	9.44
	60	50.24	9.34
	90	50.15	9.33
	120	50	9.30
	180	48.985	9.11
	240	52.225	9.71
	360	49.215	9.15
	1440	50.73	9.44
30	0	147.925	27.51
	30	134.17	24.96
	60	134.09	24.94
	90	133.46	24.82
	120	132.01	24.55
	180	133.455	24.82
	240	131.78	24.51
	360	131.36	24.43
	1440	129.475	24.08
60	0	304.405	56.62
	30	282.355	52.52
	60	278.86	51.87
	90	276.435	51.42
	120	272.97	50.77
	180	269.245	50.08
	240	272.47	50.68
	360	268.395	49.92
	1440	265.165	49.32
90	0	462.58	86.04
	30	423.66	78.80
	60	419.995	78.12
	90	425.52	79.15
	120	417.055	77.57
	180	414.48	77.09
	240	410.455	76.34
	360	416.395	77.45
	1440	399.165	74.24
120	0	614.445	114.29
	30	568.45	105.73
	60	562.39	104.60
	90	568.28	105.70
	120	552.7	102.80
	180	552.025	102.68
	240	561.035	104.35

	360	542.695	100.94
	1440	534.105	99.34
150	0	786.25	146.24
	30	735.04	136.72
	60	726.91	135.21
	90	724.51	134.76
	120	726.29	135.09
	180	714.75	132.94
	240	710.3	132.12
	360	706.39	131.39
	1440	689.56	128.26

The raw data generated during the binary adsorption experiment of phenol (10 ppm) and calcium (600 ppm) is tabulated in Table B-3.

Table B-3: Raw data of the binary adsorption of phenol and calcium

Time (min)	Area	Concentration (ppm)
0	51.24	9.53
30	49.67	9.24
60	49.75	9.25
90	49.79	9.26
120	49.66	9.24
180	50.27	9.35
240	50.43	9.38
360	50.37	9.37
1440	50.25	9.35

Lastly, the adsorption data obtained during the wastewater experiments with both the produced biochar and activated carbon is given in Table B-4.

Table B-4: Raw data obtained during the wastewater adsorption experiment

Time (min)	COD (ppm)	
	Biochar	Activated carbon
0	2720	2720
30	603	<100
60	2301	1833
90	2232	1758
120	2271	1773
180	2289	1770
240	2271	1800
360	2280	1884
1440	2448	1814

B.3 Experimental error calculations

The experimental error for the proximate analysis and the adsorption experiments were calculated as shown in Equation B-4. Firstly, the average of the data points, \bar{x} was calculated as seen in Equation B-1.

$$\bar{x} = \frac{1}{n} \sum_{j=1}^n x_j \quad (\text{B-1})$$

where n is the sample size and x_j is the value of each data point. The variation of the data points from the average, the standard deviation, was then calculated by using the calculated average as shown in Equation B-2.

$$\sigma = \sqrt{\frac{\sum (x_j - \bar{x})^2}{n - 1}} \quad (\text{B-2})$$

The calculated standard deviation was then used to determine the confidence level by considering a 95% level of confidence, as shown in Equation B-3.

$$\text{Confidence level} = 1.96 \left(\frac{\sigma}{n^{0.5}} \right) \quad (\text{B-3})$$

Lastly, the experimental error was determined as shown in Equation B-4.

$$\text{Experimental error (\%)} = \frac{\text{Confidence level}}{\bar{x}} \times 100 \quad (\text{B-4})$$

By considering the experimental error calculation steps discussed, the experimental error based on the proximate analysis of paper sludge is given in Table B-5.

Table B-5: Experimental error calculated for the proximate analysis of paper sludge.

	Moisture (g.g ⁻¹)	Volatile matter (g.g ⁻¹)	Ash content (g.g ⁻¹)	Fixed carbon (g.g ⁻¹)
Sample 1	0.56	0.32	0.091	0.034
Sample 2	0.54	0.32	0.11	0.031
Sample 3	0.53	0.33	0.10	0.042
Sample 4	0.56	0.31	0.093	0.034
Average	0.55	0.32	0.10	0.04
Standard deviation	0.016	0.007	0.007	0.005
Experimental error (%)	2.86	2.23	7.04	12.82

The experimental error for the adsorption experiments were calculated in a similar manner and is given in Table B-6.

Table B-6: Experimental error calculated for the adsorption experiments.

	Removal efficiency (%)
Sample 1	21.66
Sample 2	24.91
Sample 3	22.64
Sample 4	20.88
Sample 5	20.80
Average	22.18
Standard deviation	1.70
Experimental error (%)	6.71

This certificate declares that the dissertation with the title **Co-adsorption of phenol and calcium from an industrial wastewater stream** by Karina van der Merwe was edited by:

Ann-Lize Grewar

BA in Language and Literature Studies

BA Hons in Translation Studies

SATI-membership number 1002647

SATI Accreditation: APSInterp Afr-Eng

Chairperson of SATI North-West Chapter

Professional Editor's Guild membership number BOS008

Language Director at Language Matters PTY(Ltd)

annlizeboshoff@gmail.com / 072 758 5797



Signed on 11/11/2019

Ann-Lize Grewar
Language Practitioner
B.A. Language and Literature Studies
B.A. Hons. Translation Studies

Contact us:
info@languagematters.co.za
www.languagematters.co.za



Ann-Lize Grewar
Taalpraktisyn
B.A. Taal- en Literatuurstudies
B.A. Hons. Vertaalkunde

Kontak ons:
info@languagematters.co.za
www.languagematters.co.za